AFCRL-68-0097
MARCH 1968
SPECIAL REPORTS, NO. 72

AIR FORCE CAMBRIDGE RESEARCH LABORATORIES

L. G. HANSCOM FIELD, BEDFORD, MASSACHUSETTS

Proceedings, AFCRL Tethered Balloon Workshop, 1967

Editor
THOMAS W. KELLY

OFFICE OF AEROSPACE RESEARCH
United States Air Force

BLANK PAGES IN THIS DOCUMENT WERE NOT FILMED

AFCRL-68-0097
MARCH 1968
SPECIAL REPORTS, NO. 72

AEROSPACE INSTRUMENTATION LABORATORY PROJECT 6665

AIR FORCE CAMBRIDGE RESEARCH LABORATORIES

L. G. HANSCOM FIELD, BEDFORD, MASSACHUSETTS

Proceedings, AFCRL Tethered Balloon Workshop, 1967

Editor
THOMAS W. KELLY

OFFICE OF AEROSPACE RESEARCH

United States Air Force

Abstract

The AFCRL Tethered Balloon Workshop was held in October 1967 for the purpose of exchanging information on the current tethered ballooning. This was the first such meeting held exclusively for reporting on this rapidly expanding technology. In addition to informal meetings, nineteen prepared talks were presented, all of which are contained herein. Subjects include: tethered balloon motion, balloon design, fiberglas tether cables, tethered balloon instrumentation, a tethered balloon winch, and several operational programs that used tethered balloon systems.

Contents

PROCEEDINGS, AFCRL TETHERED BALLOON WORKSHOP, 1967

1. Equations of Motion of a Tethered Kite Balloon

J.H. Smalley
National Center for Atmospheric Research
Boulder, Colorado

Abstract

The classical equations of motion of a tethered balloon are presented -- without derivation. Comparison is made with the similar equations for an airplane. A very brief discussion is given of how the equations might be utilized and of some possible benefits which might arise.

1. INTRODUCTION

Bairstow, Relf, and Jones (1915) published a report titled "The Stability of Kite Balloons: Mathematical Investigation." This report gave the complete equations of motion of a "rigid" kite balloon, including the effects of the kite wire -- assuming a catenary for the wire profile curve. They showed that the rigid-balloon equations are separable into longitudinal and lateral groups. Furthermore, the characteristic equation of each group is of sixth degree as contrasted with a characteristic equation of fourth degree for the corresponding case of a rigid, heavier-than-air craft.

(Received for publication 16 February 1968)

At that time it was extremely difficult to carry the analysis much further. Today, however, the techniques of dynamic analysis have been considerably advanced, and powerful computing machinery is available. Therefore, it seems appropriate to take a fresh look at the study of the dynamic stability of tethered balloons.

Because the original paper is not readily available, its results will be briefly reproduced here and some comments added.

2. SYMBOLS AND DEFINITIONS

a, b, c	position* of the top of the cable with respect to the center of gravity (b assumed zero)
f, g, h	position* of the center of buoyancy with respect to the center of gravity (g assumed zero)
g	acceleration of gravity
k	horizontal component of catenary cable tension
m	mass of balloon components
m_1, m_2, m_3	components* of effective balloon mass (e.g., m_1 = m + "added" mass in x direction)
p, q, r	rotational velocities* of the body axes with respect to the inertial axes
u, v, w	perturbation velocities* of the body axes with respect to the inertial axes
w	weight per unit length of the kite wire (used in expressions for cable derivatives)
x, y, z	axes* fixed in body of kite balloon, origin at center of gravity
	also
x, y, z	perturbation displacements* of body axes with respect to the inertial axes
A, B, C	moments of inertia* of balloon (including "added" inertia)
D, E, F	products of inertia of balloon (D and F assumed zero)
F	buoyant force
L, M, N	external moments* applied to balloon
U, V, W	incident steady-state wind velocities* (V and W assumed zero)
X, Y, Z	external forces* applied at center of gravity of balloon
α, β, γ	rotational displacements* of the body axes with respect to the inertial axes
ξ, η, ζ	axis system* fixed to the earth
λ	differential operator with respect to time (≡ d/dt)

*Longitudinal, lateral, and vertical, respectively

3. EQUATIONS OF MOTION

An axis system (ξ, η, ζ) is established with its origin at the lower end of the kite wire. The system is assumed fixed with respect to the earth except for a translational velocity $-U$ along the ξ axis. Body axes (x, y, z) are fixed in the kite balloon with their origin at the center of gravity. Initially they are parallel to the ξ, η, ζ system.

The stiffness and extensibility of the wire and the wind forces on it are neglected, resulting in a catenary for the wire profile curve. The components of wire tension are derived and applied at the center of gravity. The following direction cosines are used (small perturbations are assumed throughout) when transferring forces from the top of the cable to the center of gravity.

	x	y	z
ξ	1	$-\gamma$	β
η	γ	1	$-\alpha$
ζ	$-\beta$	α	1

Use is made of

$$d\xi = x + \beta c$$
$$d\eta = y - \alpha c + \gamma a$$
$$d\zeta = z - \beta a$$

for perturbations of the position of the top of the wire. The derivatives which arise from the use of the kite wire are listed in Table 1.

"The derivatives given ... [in Table 1] ... have, of course, a simple physical significance. The item in the row starting with $m_2 Y$ and in the column headed by α means that if the kite balloon is rotated about the axis of x while everything else is unaltered, the force along the axis of y is increased by an amount

$$\left(\frac{ck}{\xi} - k \sinh \frac{w}{k}\left(\xi + \xi_0\right)\right) \alpha ,$$

as long as α is small. The numbers in the column headed "o" relate to the equilibrium values of the forces."

The equations of motion are derived in the usual manner (Durand, 1934). The assumed symmetry of the system and assumed small perturbations allow the six equations corresponding to the six degrees of freedom to be separated into two groups.

The longitudinal group of equations is given in Table 2 and the lateral group in Table 3. Note that the derivatives with respect to α, β, γ, x, y, and z arise from the influence of the wire, and the derivatives with respect to u, v, w, p, q, and r arise from the influence of wind.

4. DISCUSSION

The assumption that the wire profile is a catenary is known to be grossly in error, especially for long wires. Such an assumption need not be made for steady-state conditions. Nevertheless, the derivatives resulting from this assumption may still be very useful for studies of the kite motion. The assumption that the curve is a catenary has the advantage of limiting the problem to six degrees of freedom. The problem is complicated by treating the wire as a chain of lumped masses, but a computer makes it tractable. In general, wind drag on the wire cannot be ignored.

The authors make an important distinction between the mass of the balloon components and the effective mass. Furthermore, the effective mass is different along different axes. The additional mass due to acceleration of the surrounding air is a significant fraction of the mass of air displaced, and kite balloons displace a mass of air greater than the mass of their components. A body of literature has been developed on the subject of additional mass (Imlay, 1961).

No effort was made in the report to evaluate the aerodynamic stability derivatives except that those which are zero due to symmetry have been omitted. Methods of estimating stability derivatives for airplanes are almost too numerous to mention--which probably indicates the difficulty of arriving at a completely satisfactory method. A summary up to 1955 is given by Thomas (1955). A great deal of this effort for airplanes should be directly applicable to the kite balloon. One considerable simplification for the kite balloon problem is that compressibility effects should never have to be considered.

Although theoretical and empirical methods of estimating stability derivatives for airplanes are applicable to the kite balloon, for best estimates it will be necessary to conduct wind tunnel tests of the particular configuration contemplated. For example, experience has shown that there is considerable upwash along the sides of a lifting balloon hull--a circumstance not found in airplanes. This, of course, has a strong influence on the horizontal tails. Scaling from model tests to full size will present problems. For this reason, and to verify dynamic stability studies, the full-size balloon will have to be instrumented in the manner of flight-test airplanes.

The importance, together with usefulness, of dynamic stability studies for airplanes has been amply demonstrated. For the best performance such studies are required for the kite balloon. To quote from the authors, "Actual observation of the motions of a kite balloon will be made in order to estimate finally how nearly

the mathematical analysis indicates the type of resulting motion. Once this is established, the analysis can be safely used to indicate improved methods of steadying the motion of captive kite balloons."

References

Bairstow, L., Relf, E.F., and Jones, R. (1915) The Stability of Kite Balloons: Mathematical Investigations, Aeronautical Research Council, Great Britain, Reports and Memoranda, No. 208.

Durand, W.F. (1934) Aerodynamic Theory, Vol. V, division NV.

Imlay, F. (1961) The Complete Expressions for Added Mass of a Rigid Body Moving in an Ideal Fluid, David Taylor Model Basin Report 1528 (AD 263,966).

Thomas, H.H.B.M. (1955) Notes on Stability and Control Derivatives at Subsonic and Transonic Speeds, Royal Aircraft Establishment Tech Note Aero. 2405 (AD 107,100).

Table 1. Derivatives Due to Use of Kite Wire

	o	x	y	z	α	β	γ
m_1 X	$-k$	$-\nu$	o	$-\mu$	o	$\mu a - \nu c + k \sinh \frac{w}{k}\left(\xi + \xi_o\right)$	o
m_2 Y	o	o	$-\frac{k}{\xi}$	o	$\frac{ck}{\xi} - k \sinh \frac{w}{k}\left(\xi + \xi_o\right)$	o	$k\left(1 - \frac{a}{\xi}\right)$
m_3 Z	$-k \sinh \frac{w}{k}\left(\xi + \xi_o\right)$	$-\left(\nu\mu_1 + \nu_1\right)$	o	$-\mu\mu_1$	o	$k + \mu\mu_1 a - c\left(\nu\mu_1 + \nu_1\right)$	o
AL	o	o	$\frac{ck}{\xi}$	o	$-\frac{c^2 k}{\xi} + ck \sinh \frac{w}{k}\left(\xi + \xi_o\right)$	o	$-ck\left(1 - \frac{a}{\xi}\right)$
EM	$-ck + ak \sinh \frac{w}{k}\left(\xi + \xi_o\right)$	$-c\nu + a\left(\nu\mu_1 + \nu_1\right)$	o	$-c\mu + a\mu\mu_1$	o	$ck \sinh \frac{w}{k}\left(\xi + \xi_o\right) + ac\mu - c^2\nu - ak - a^2 \mu\mu_1 + ac\left(\nu\mu_1 + \nu_1\right)$	o
CN	o	o	$-\frac{ak}{\xi}$	o	$\frac{ack}{\xi} - ak \sinh \frac{w}{k}\left(\xi + \xi_o\right)$	o	$ak\left(1 - \frac{a}{\xi}\right)$

where

$$\mu = (1/\delta)\,\xi$$

$$\nu = (1/\delta)\,\frac{k}{w} \sinh \frac{w}{k}\,\xi$$

$$\delta = \frac{2k}{w^2}\left(1 - \cosh \frac{w}{k}\,\xi\right) + \frac{\xi}{w} \sinh \frac{w}{k}$$

$$\mu_1 = \frac{\xi}{\xi} \cosh \frac{w}{k}\left(\xi + \xi_o\right) \cosh \frac{w}{k}\,\xi_o - \frac{k}{w\xi} \sinh \frac{w}{k}\,\xi$$

$$\nu_1 = w \cosh \frac{w}{k}\left(\xi + \xi_o\right)\left(1 - \frac{k}{w\xi} \cosh \frac{w}{k}\left(\xi + \xi_o\right)\right)$$

Table 2. Longitudinal Group of Equations

$$\left(-\lambda^2 + \lambda X_u + X_x\right)x + \left(\lambda X_w + X_z\right)z + \left(\lambda X_q + X_\beta + UX_w + \frac{mg - F}{m_1}\right)\beta = 0$$

$$\left(\lambda Z_u + Z_x\right)x + \left(-\lambda^2 + \lambda Z_w + Z_z\right)z + \left(\lambda\left(Z_q + U\right) + Z_\beta + UZ_w\right)\beta = 0$$

$$\left(\lambda M_u + M_x\right)x + \left(\lambda M_w + M_z\right)z + \left(-\lambda^2 - \lambda M_q + M_\beta + UM_w - \frac{Fh}{B}\right)\beta = 0$$

Table 3. Lateral Group of Equations

$$\left(-\lambda^2 + \lambda Y_v + Y_y\right)y + \left(\lambda Y_p + Y_\alpha - \frac{mg-F}{m_2}\right)\alpha - \left(\lambda\left(Y_r - U\right) + Y_\gamma - UY_v\right)\gamma = 0$$

$$\left(\lambda L_v + L_y\right)y + \left(-\lambda^2 + \lambda L_p + L_\alpha - \frac{Fh}{A}\right)\alpha + \left(\lambda^2\frac{E}{A} + \lambda L_r + L_\gamma - UL_v\right)\gamma = 0$$

$$\left(\lambda N_v + N_y\right)y + \left(\lambda^2\frac{E}{C} + \lambda N_p + N_\alpha + \frac{Ff}{C}\right)\alpha + \left(-\lambda^2 + \lambda N_r + N_\gamma - UN_v\right)\gamma = 0$$

II. Dual-Diagnostic Balloon Arrays for the AJAX Event

Dewey Struble
Sea–Space Systems Inc.
Torrance, California

Abstract

Two tethered balloon arrays were provided to support 300-lb instrumentation packages above the surface on the AJAX nuclear event at the Nevada Test Site, Mercury, Nevada. The Sea-Space Systems' superpressure balloons successfully lofted LRL instruments and complied with stringent telemetry positioning and boresighting requirements. Although designed for 26 mph wind speeds, the balloons withstood winds gusting to 32 mph. A positioning accuracy during operational periods of less than 10-ft spherical error was achieved.

Operational flexibility was provided by inflating the balloons in the bottom of an old nuclear crater and then moving the inflated balloons to the operational area. A specially equipped launch truck enabled the balloons to be inflated on board with a taut bubble, thereby increasing wind capacity. The move to the site having been completed, the balloons were erected directly from the truck.

Positioning accuracy presented a definite technical problem in array rigging since a very "hard" system was required to maintain spherical positioning to 10 ft and yaw to 5° over an extended unattended period. This was achieved by using fiberglas cables with an extensive balloon attachment array. The fiberglas tether cables exhibited low elongation under load. Disadvantages of the cable were the cost and large diameter reels required for handling. The 1/4-in. cable had a guaranteed breaking strength of 7800 lb with an elongation of 0.63 percent at 3000 lb.

The SSS balloon employed an extensible liner inside of a nylon strength shell wherein the liners were reused several times. An emergency deflate valve was located at the top of the balloon through a mechanically actuated dump valve to release all gas.

The Model SP-N1 superpressure balloon system had the following characteristics:

Volume:	20,799 ft^3
Diameter:	36.4 ft
Gross lift:	1,248 lb
Electronic payload:	300 lb

The balloon was laid out and constrained on a special inflation track attached to the top of the launch truck. At the site, the balloon, together with payload, was released from the truck on a vertical tether cable and vertical tether loads were gradually transferred to the triple fiberglas array. This inflation and launch technique provided considerable operational flexibility.

A crew of six men was employed to operate three vehicles and one aircraft.

3. DESIGN CONSIDERATIONS

Meeting the technical specifications of the Lawrence Radiation Laboratory for the AJAX Event required a balloon system with only modest payload and altitude requirements. However, the positioning accuracy for the telemetry antenna presented a definite technical problem in array rigging. A very "hard" system was required to obtain a 10-ft spherical error compared with a more normal "spongy" rigging system. For example, the use of Dacron tether lines, the best conventional material, would result in a spherical error of over 30 ft under a wind speed spectrum of 0 to 20 mph. In addition, the wind capacity specified (20 mph) necessitated a superpressure balloon design to avoid both a spongy response and high drag loads.

It should be noted that the specifications delineated by LRL for AJAX seemed straightforward when proposed by the Project Group, but became an unusual balloon design problem when the wind capacity required was increased to 20 mph and the allowable positioning of the payload was held to within a 10-ft sphere. If a conventional system had been used and had been allowed "to grow" in size, a very large and complicated design could have evolved. The SSS approach was to keep the balloon system as lightweight as possible in order to keep over-all system size down, and, therefore, reduce the problems from wind drag. A specific design was evolved to meet the specific and unique LRL specifications.

In addition, the over-all design requirements and field operating conditions were approached on a systems basis, resulting in a completely integrated design to solve the AJAX diagnostic array requirements. This meant that balloon inflation, LRL payload mating and field erecting problems were all considered in the initial as well as the final layout. Thus, balloon inflation remote from the crowded GZ

area and a compatible field transportation technique were important in providing a satisfactory diagnostic balloon array useful within the field construction constraints and evolutions constantly under way at the Nevada Test Site.

2. BALLOON HARDWARE

The balloon system hardware provided for the AJAX event used several new techniques. The balloon itself used new materials in construction and novel rigging techniques. The tether cables were made of continuous fiberglas filaments epoxyed axially together under equal tension. Figure 1 shows the balloon array in the field.

Figure 1. SSS Dual Tethered Balloon Array Used in the AJAX Nuclear Event

The SSS Model SP-N1 balloon employed an extensible polyurethane liner inside of a nylon strength shell. This method had the advantage of being much less expensive than conventional approaches because of the potential of reusing the liners. Although the stringent schedule prevented a thorough test of the liner approach, one liner was inflated several times with good success. This gives data on the validity of the liner technique for tethered superpressure balloons.

3. RIGGING

The critical design requirement in achieving the telemetry objectives of the AJAX balloonborne instrumentation was the stringent positioning-pointing accuracy.

The specified pointing accuracy for the telemetry antenna was ±5° in yaw and ±8° in pitch. This accuracy was to be maintained over a wind speed range of 0 to 20 mph. Meeting these requirements necessitated use of fiberglas tether cables with an extremely low elongation under load. For example, the 1/4-in. fiberglas cable used had an elongation of 0.63 percent at 3,000 lb and 1.7 percent at 9,600 lb (break). However, the choice of fiberglas cable had certain disadvantages, such as cost and the large diameter reels required to handle the cable. Seven foot diameter reels were used to avoid excessive bending of the cables.

If for any reason deflation was required, an emergency deflate valve at the top of the balloon was provided. This system was used to deflate all balloons during recovery operations.

Table 1. Superpressure Balloons for AJAX

System	
Model SP-N1 superpressure balloon with fabric strength shell and extensible Merfilm U liner fiberglas tether cables	
Specifications	
Volume	20,799 ft³
Oblate diameter	36.4 ft
Total lofted balloon system and payload weight	481 lb
Performance	
Gross lift	1248 lb
Operational wind velocity	20 mph
Blowdown velocity	28 mph
Safety Factors	
Balloon-design at 20 mph	3.0
Cable at blowdown (30° to upwind cable)	4.3

4. BALLOON OPERATIONS

Operational flexibility was provided by inflating the balloon at an old nuclear crater, and then moving the inflated balloon to the balloon surface zeros. A specially equipped launch truck enabled the balloons to be inflated with a taut bubble, thereby increasing wind capacity at launch, and then to be moved as desired for launch and recovery evolutions.

Inflation of each unit was done with the balloon tethered to a launch platform constructed over a two-ton truck. All inflations were made in the bottom of an abandoned crater. Figure 2 shows this setup. At the start of inflation, the balloon was laid out on a special inflation track attached to the top of the truck. The balloon-payload mating lines were attached to the payload frame prior to inflation.

Figure 2. SSS Inflating an SP-N1 Balloon in the U9ad Crater

The top of the balloon was reeved under a roller arm attached to a moving cart. This technique enabled a taut bubble to be maintained continuously during inflation, thereby increasing system wind capacity during the critical inflation phase. When the balloon was fully erect and the lift force taken by the payload mating lines, the roller arm was removed.

When the balloon was fully inflated and the rigging lines secured, the truck was driven out of the crater to the balloon surface zero. The distance to the balloon surface zero points was approximately 1/2 mile from the inflation site.

Six concrete anchors were used to position and secure the balloon arrays. These blocks were 5 ft × 5 ft × 5 ft and weighed 16,000 lb each. Cable calculations were based on ground termination at the 5-ft height. Figure 3 gives the array elevation layout.

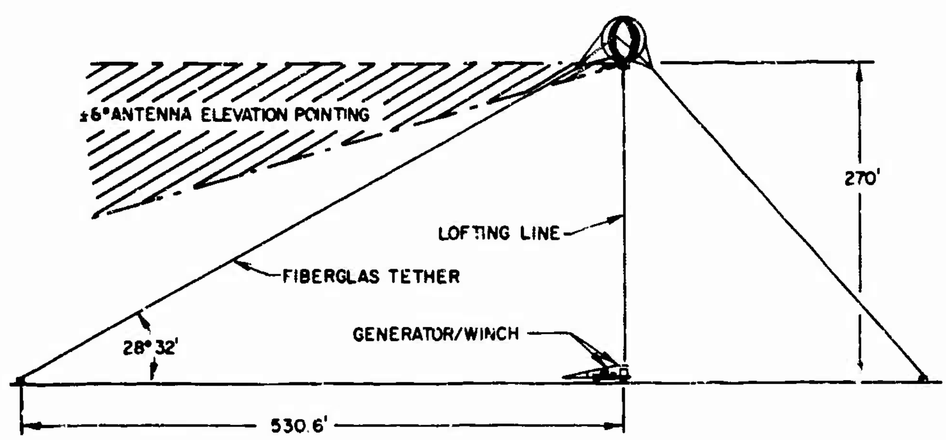

Figure 3. NIP Tethered Balloon: Array 1

5. SYSTEM POTENTIAL

The superpressure balloon technology used on the AJAX arrays demonstrates the methods for more sophisticated tethered balloon systems of the future. The balloon system characteristics presented herein can be modified to represent an extension of the AJAX experience for more demanding future requirements. Design experience and hardware are available to implement these capabilities on relatively short notice from Sea-Space Systems.

III. DASA Requirements for Tethered Balloon Systems

Jock Kelso
Hq, Defense Atomic Support Agency
Washington, D.C.

Abstract

In performing its mission of studying the effects of nuclear and high explosive detonations in the atmosphere and near the earth's surface, the Defense Atomic Support Agency has successfully employed steel towers, free balloons, and low-altitude tethered balloons to position detonation sources and effects sensing instrumentation at desired altitudes and locations. In the event that nuclear testing in the atmosphere is resumed, high-altitude tethered balloons would present a more attractive carrier and positioning vehicle. A high-altitude tethered balloon capability would ensure maximum control of a nuclear device at all times and precise positioning of a detonation source for missile interaction experiments would present an almost ideal test environment.

This will be a two-part presentation. I will cover general requirements as foreseen by the Defense Atomic Support Agency (DASA) and Dr. Marion Balcerzak of the General American Research Division (GARD) will discuss a particular application of current interest.

Tethered balloons are of interest to DASA for two purposes, namely, to carry detonation sources such as nuclear devices or high explosives to the various altitudes

above the ground and to position instrumentation near a nuclear or chemical explosion either at altitude or near the surface.

In this latter role, you have already heard from Mr. Dewey Struble of Sea Space Systems and will hear more later from Mr. H.G. Laursen of Sandia Corporation. Of course, under the current Nuclear Test Ban Treaty these measurements are made only on contained underground events. As I will discuss later, we have used free flight balloons in the past to carry both nuclear and chemical explosive sources to the altitude together with instrumentation.

During the PLUMBOB test series at the Nevada Test Site in 1957 and the HARDTACK Phase II Tests in 1958, a number of nuclear events were carried out at low altitude using tethered balloon systems to position the nuclear devices for the first time. Spherical tethered balloons were flown at altitudes between 500 and 1,500 ft by a three guy-cable suspension system to individual winches. The height of each test was determined by the necessity of avoiding fall-out and local radioactive contamination. Consequently, the larger the size of the weapon, or yield, the higher the required height of burst.

Originally, a 100-ft tower was used in 1945 for TRINITY. Subsequent tests during Operations RANGER, BUSTER, JANGLE, TUMBLER and SNAPPER at the Nevada Test Site were almost exclusively air drops. However, it was not always desirable to employ aircraft delivery. In addition, precise diagnostics were required so that a fixed position was necessary for both weapon development and measurement of effects. Consequently, over the years tower heights increased successively to 200, 300, 500 and finally 700 ft, as the yields increased. The cost of steel towers also went up. Elevator systems were required to transport personnel and equipment to the working platforms. Although these elevators were dismantled before the test, the towers were destroyed by the detonation and much of the investment was lost. In fact, the detonation would usually vaporize part of the tower and scatter contaminated fragments over the desert.

It was found uneconomical to build a large number of very high towers, so that consideration was given in 1957 to using tethered balloons as device carriers. Tethered balloons also eliminated the radioactivity hazard and reduced the cost considerably, since the winches could be used again. Also, on some high explosive tests carried out at the Tonopah Test Range, and some nuclear safety tests (Operation ROLLER COASTER) to be described by Mr. Laursen, gages were suspended from balloon cables to make measurements in air above the surface. Aerodynamic balloons were used for a similar purpose in the Pacific at Eniwetok to make blast measurements at altitude for a shallow underwater detonation UMBRELLA in 1958.

Tethered balloons were again used at the Nevada Test Site in 1962 to carry nuclear devices. By this time aerodynamic balloons had been developed by Mr. Laursen which could carry 5000 lb to 1500 ft and 2500 lb to 5000 ft. The

British used tethered balloons to carry nuclear devices aloft in some of their tests at Maralinga, Australia, in 1957 and at Christmas Island, in 1958.

Use of free flight balloons to carry nuclear devices or high explosives has been discussed at previous Balloon Symposiums. In 1958, a free flight balloon was used to carry a nuclear device to an altitude of 86,000 ft in the Pacific (see Figure 1 - VHA System). An aircraft carrier was used as a launch platform. This technique presents an optimum launch condition by neutralizing the wind and permits arming and firing in flight. However, elaborate safety precautions have to be taken to minimize the chance of losing control of the balloon. In addition, since the wind speed aloft may exceed that of the aircraft carrier, command and control responsibility may have to be transferred to orbiting aircraft. Also, the launch window may be limited by the approach of darkness. This program was known as VHA.

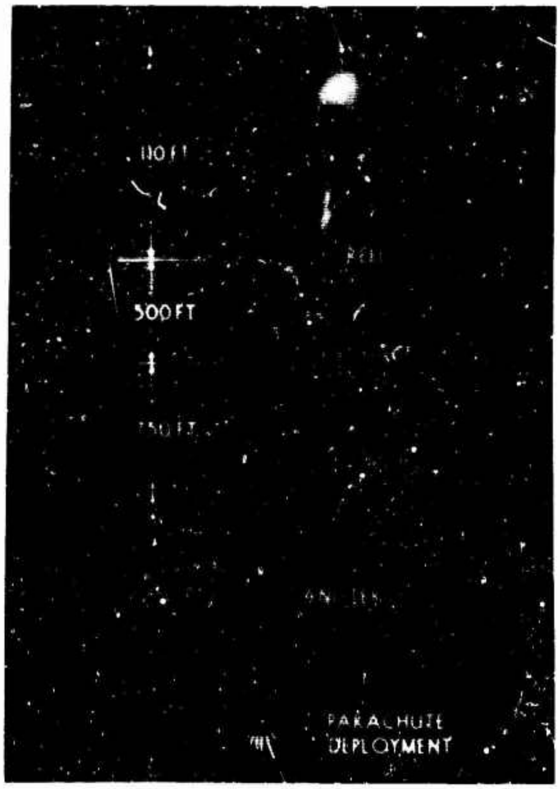

Figure 1. VHA System Flight Configuration

In preparation for another nuclear test series in the Pacific, a follow-on system known as VHB was developed. A polyethylene balloon having a deployed volume of approximately 5.25×10^6 ft^3 was used to carry the design payload to a float altitude of 115,000 ft (see Figure 2 - VHB). This same balloon and three additional balloon designs were used in Operation BANSHEE to carry a high explosive charge of 500 lb of pentolite to float altitudes of 38,000, 80,000, 100,000, and 115,000 ft (see Figure 3 - BANSHEE). Also, during FISHBOWL in 1962, free balloons were utilized in the Southwest Pacific to make radiation measurements. In order to have a greater flexibility, a sea launch capability was developed by the Air Force Cambridge Research Laboratories which could utilize a smaller ship than an aircraft carrier (see Figure 4 - "C" Launch System).

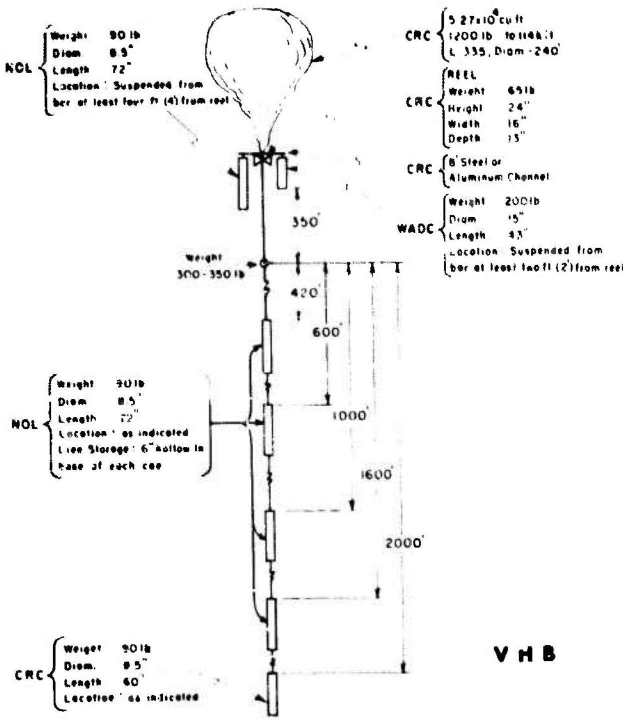

Figure 2. VHB System Flight Configuration

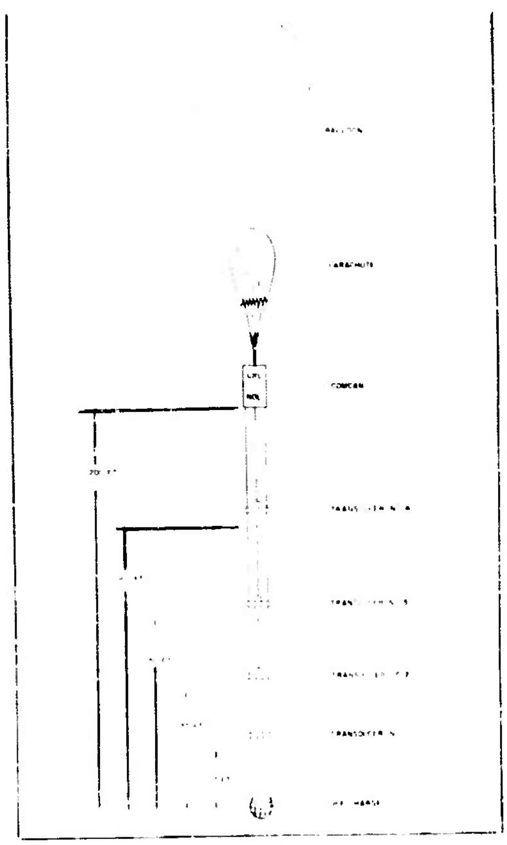

Figure 3. BANSHEE System Flight Configuration

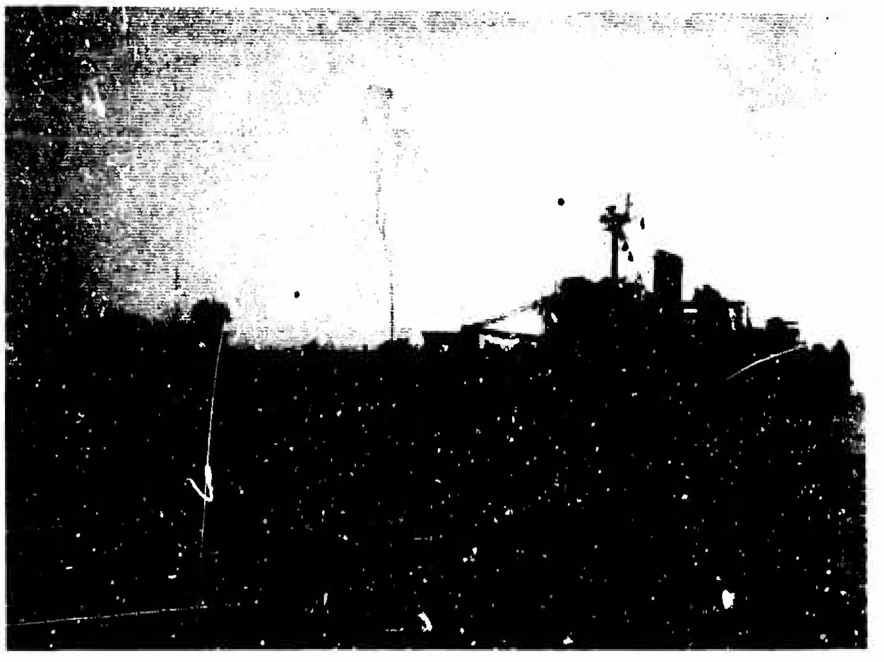

Figure 4. "C" Launch System LST Balloon Launch Platform

With regard to future requirements, in the event that nuclear testing in the atmosphere is resumed, tethered nuclear balloons are more attractive than free floating balloons for high-altitude nuclear detonations, since they ensure control of the nuclear device at all times. Presumably, they could be launched from a ship. However, it would be preferable to tether a balloon from Johnston Island. This would simplify the ground measurement problem since instrumentation is available at Johnston Island, as well as minimize the support required from the Naval Forces. This would give a capability for precisely positioning a nuclear explosion which then might lead to missile interaction experiments. Once developed, high-altitude tethered balloons could also be used at the Nevada Test Site or the White Sands Missile Range. A low altitude capability already exists.

A similar pattern of development appears in the SLEDGE program. Due to restrictions to nuclear testing in the atmosphere, it was necessary to develop a blast simulation technique using explosive gases for various applications at the surface. When these were contained by a large balloon, it was possible to use a lifting gas such as methane or hydrogen so that the buoyant system would rise to proper altitude. At present, free balloons are being considered for this purpose. However, a tethered system would be more attractive for such experiments for the same reasons as described in the foregoing. Dr. Balcerzak will now describe the SLEDGE program.

IV. Tethered Balloon Requirements for SLEDGE

M.J. Balcerzak
General American Transportation Corporation
Niles, Illinois

Abstract

The development of the high-altitude SLEDGE (Simulating Large Explosion Detonable Gas Experiments) technique has continued during the past year.* The over-all objective is to provide a blast and shock environment that simulates the environment produced by 10 to 20 tons of TNT at altitudes up to 100,000 ft. Although the high altitude SLEDGE tests presently contemplated call for free-flight balloons, there is a developing need for a tethered capability. The advantage of a tethered detonable gas balloon system are evident.

1. A tethered detonable gas balloon presents a relatively fixed point in space around which missiles and aircraft may be deployed to determine their blast vulnerability.
2. A tethered detonable gas balloon eliminates the need of a tower and its associated degrading effects when used to support TNT for height-of-burst explosion experiments.
3. A tethered detonable-gas-balloon capability can be used to static launch high-altitude SLEDGE balloons by facilitating instrumentation and payload train deployment.

---

*This work is being supported by the Defense Atomic Support Agency (DASA) and the Advanced Research Projects Agency (ARPA), Washington, D.C., under Contract DA-49-146-XZ-573.

To review briefly, the SLEDGE technique has been under development for approximately two years. All of the actual field tests have been conducted on or near the ground. The largest detonable gas explosion accomplished was a 125-ft diameter hemispherical envelope filled with approximately 20 tons of propane-oxygen gas mixture (see Figures 1, 2, and 3). Two tests with 110-ft diameter spherical balloons which were to be filled with approximately 20 tons of methane-oxygen gas mixtures were terminated prematurely, the first by a structural failure of the balloon and the second by a preignition of the detonable gas mixture. Static electricity is suspected as the cause of the latter abort (see Figures 4, 5, 6, and 7).

It had been planned to raise the spherical balloons to a height where the center of the balloons would have been 85-ft above ground level. A straightforward tethering scheme, which used nylon tether lines, sandbags and line cutters, was designed and tested. The tethering system consisted of 8 vertical and 8 diagonal tethers and was planned to raise the 110-ft balloon (net lift was calculated to be approximately 5500 lb) to the required height of burst in two stages (see Figure 9). A 32-ft diameter spherical balloon was used to test the deployment and tethering system (see Figure 8). There was every confidence that the system would have successfully raised the balloon to the desired height. Unfortunately, this system was not used because of the test aborts.

In order to increase the over-all tethering system reliability, a three-winch system was subsequently designed by GARD. It was to be capable of raising the detonable gas balloons to 200 ft (see Figure 10). Because of difficulties in obtaining a balloon material that satisfied the strength and antistatic specifications of SLEDGE, further work on large scale detonable gas explosion tests was suspended and the tethering system was neither fabricated nor tested. A suitable material is currently under development. It is hoped that as soon as it is available, the SLEDGE test program will continue.

Current SLEDGE activities include model testing in the U.S. Army Ballistic Research Laboratories, High Altitude Simulating Blast Sphere located on the Aberdeen Proving Grounds, Maryland. This facility has a 30-ft internal diameter and can simulate pressure altitudes up to 200,000 ft. Over seventy 10-ft diameter detonable-gas-filled balloons have been tested in the Blast Sphere.

The purpose of the tests is threefold:

1. To determine the detonation limits of various candidate detonable gas mixtures as a function of altitude, oxygen to fuel mole ratios, and ignition energies.

2. To determine air blast effects generated by the detonable gas explosions and to correlate experimental data with GARD predicted blast data.

3. To determine the applicability of a tandem (that is, bar-bell) balloon concept for SLEDGE. The mixing rates of various candidate detonable

gas mixtures were to be observed when injected into opposite ends of the tandem balloon (fuel gas on top, oxygen on bottom) and allowed to mix by diffusion and/or any other mechanical pumping process.

Preliminary results indicate that detonations can be successfully achieved up to an altitude of 90,000 ft. As expected, the ignition energy has a marked effect on detonation initiation. It was found by experiment that 72.4 grains of PETN equivalent were required to achieve detonation at 90,000 ft. At lower altitudes, lesser ignition energy is required but for increased reliability the 72.4 grain igniters are recommended for all altitudes.

The air blast data correlates very well with predicted data. There appears to be some degradation of the correlation at altitudes above 60,000 ft. This is consistent with tests in which TNT was actually detonated at reduced pressures.

The detonable gas mixing process using the tandem balloon concept wherein the fuel gas is injected in the top of the balloon and the oxygen in the bottom appears to be a problem area. Diffusion alone seems to be the principal mechanism for mixing the gases. Although considerable movement of the balloon material was observed during the tests as the Blast Sphere pressure was reduced, this material motion apparently had little, if any, effect on the mixing process. Since a certain amount of time is required for mixing to be accomplished by diffusion, and since the mixing times observed to date have been excessive from a practical system point of view, the gases will have to be mixed on the ground before launch. Any additional mixing which takes place during the ascent to altitudes would increase the reliability of having a homogeneous detonable gas mixture in the balloon prior to ignition.

Although the high-altitude SLEDGE tests presently contemplated call for free-flight balloons, there is a developing need for a tethered capability. The advantages of a tethered detonable gas balloon system are evident.

1. A tethered detonable gas balloon presents a relatively fixed point in space around which missiles and aircraft may be deployed to determine their blast vulnerability.

2. A tethered detonable gas balloon eliminates the need of a tower and its associated degrading effects when used to support TNT for height-of-burst explosion experiments. The height-of-burst requirements are usually from ground level up to 1000 and 2000 ft. For this application a detonable gas balloon would require a 3 tethered system to maintain accurate positioning over a ground zero point.

3. A tethered detonable-gas-balloon capability can be used to static launch high-altitude SLEDGE balloons by facilitating instrumentation and payload train deployment.

In conclusion, a tethered capability for the detonable gas balloon up to 10,000 ft (50,000 ft is the long-range goal) would greatly enhance its applicability in weapons effects testing.

Figure 1. 125-ft Diameter Hemisphere During Filling Operation

Figure 2. Fully Inflated Hemisphere as Seen From Technical Observation Point

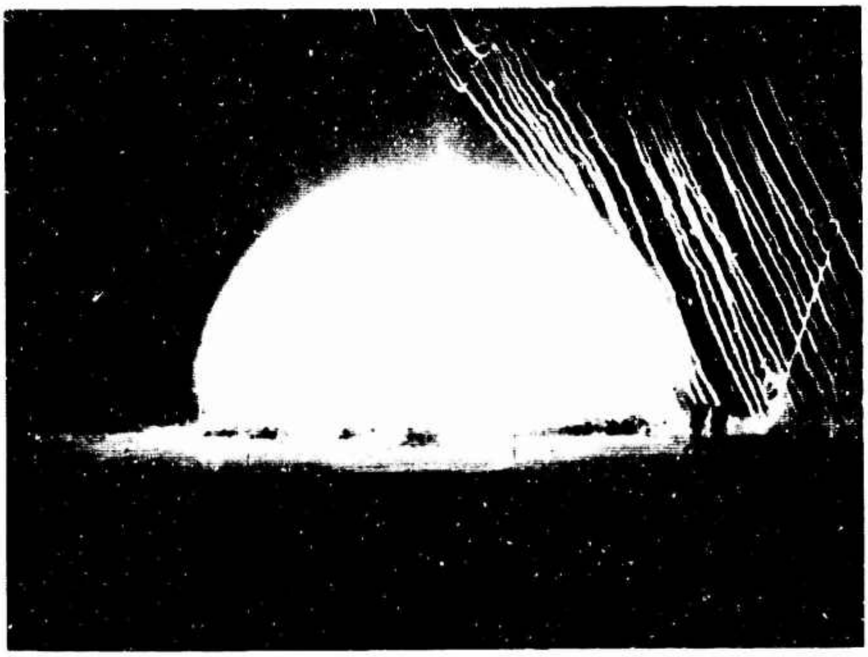

Figure 3. Detonation of 125-ft Diameter Hemispherical Envelope Filled With Oxygen and Propane (O_2/C_3H_8 = 3.5, by volume) 22 July 1966

Figure 4. 110-ft Diameter Spherical Balloon During Initial Stages of Inflation

Figure 5. Inflated Balloon Showing Position of Ballonet After Approximately 60 Percent of Oxygen Fill

Figure 6. 110-ft Balloon Shortly Before Structural Failure

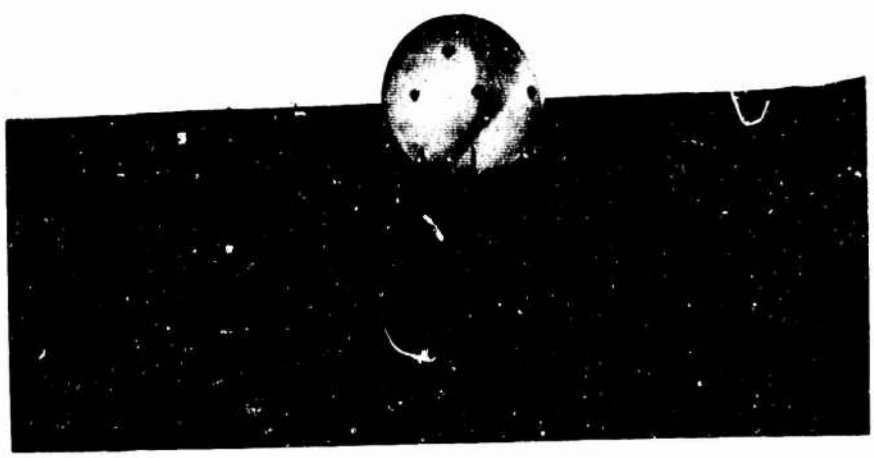

Figure 7. 110-ft Balloon Immediately Before Premature Detonation. Note position of ballonet

Figure 8. Tethering Test of 32-ft Balloon Filled with Helium and Air

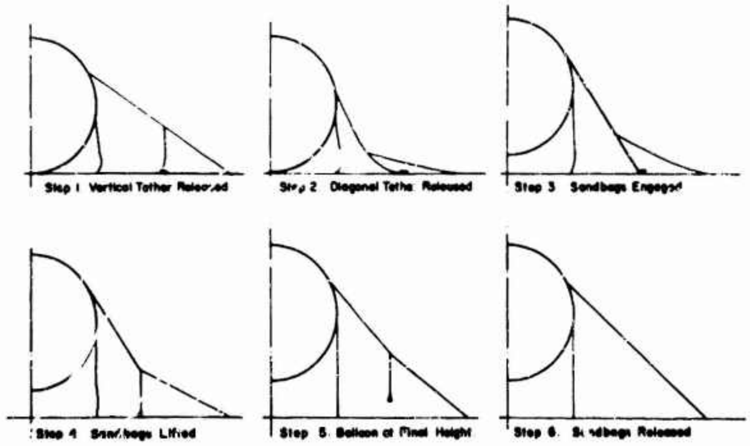

Figure 9. 110-ft Balloon Deployment Sequence

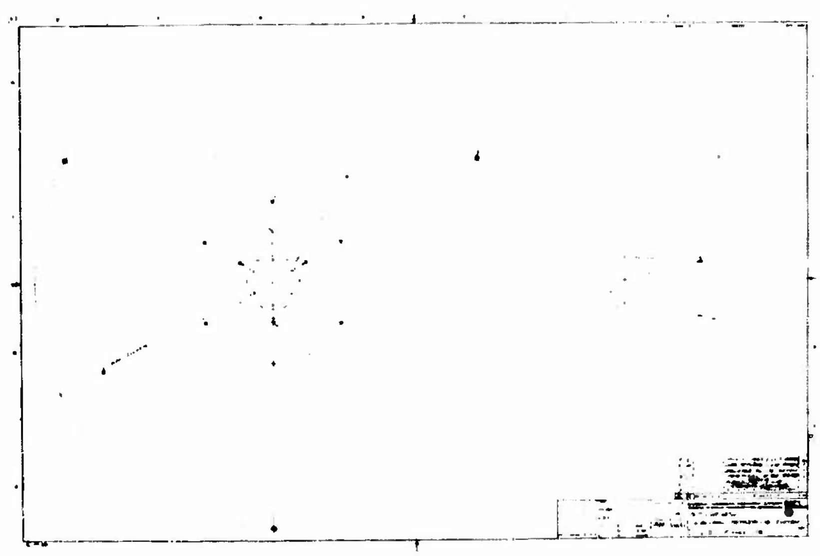

Figure 10. Balloon Tethering System

V. Estimating the Probability of Subcritical Upper-Air Wind Speeds and Their Duration

Irving I. Gringorten
Air Force Cambridge Research Laboratories
Bedford, Massachusetts

Abstract

The question to be answered is, "What is the probability that wind speed aloft, at given geographic location, altitude, and time of year, will not exceed a critical threshold speed for 12 hours, 48 hours, two weeks or other interval?" More specifically, "If the speed is measured, and known, at time zero, what is the conditional probability that the threshold speed will not be exceeded in a subsequent time interval?" The answers to these questions could be found by sorting a large sample of observations. But present practice is to measure wind speed aloft every 12 hours or, at some stations, every six hours. The empirical answer would not apply to continuous speeds. Moreover, meteorological records are too short, especially to provide stable values of conditional frequencies.

It has been found that the wind speeds, like many other meteorological variates, fit into a stationary Markov process. Consequently, it has been profitable to develop a model of duration based on the Markov process, which yields the required estimates and answers to questions on the exceeding of threshold values.

1. INTRODUCTION

Tethered balloon research has posed several problems in climatology concerning wind speeds, such as the following:

1. Given a critical or threshold wind speed, what is the likelihood of duration of subcritical wind speeds for one day, two days, or 31 days?

2. Given a 10 percent risk, what is the wind speed that will not be exceeded in two days, at this level of risk?

3. Suppose that the wind at flying altitude has been measured at an initial time t_o. What is the conditional probability of a 10-day duration of the wind speed below the critical speed?

4. If a balloon must be kept aloft for 31 days, with replacement when one is lost, what is the longest fraction of a month that the wind speed will remain below the threshold, for which a balloon and its instrumentation should be planned to stay aloft?

The approach to these problems would be a direct sampling of wind to obtain desired frequencies, if the data were sufficiently abundant. But upper winds are measured normally at 12-hourly intervals at relatively few weather stations. The historical records usually are short and the machine manipulation would be excessive and expensive. Hence, a sampling procedure, to yield frequencies of one-day, two-day, or 31-day maximum speeds, the durations of subcritical speeds, and so forth, would, at best, result in shaky estimates.

As an alternative to direct sampling, a stochastic model was sought that would require only the basic frequency distribution of 12-hourly wind speeds as input to yield estimates of maxima and minima.

2. THE MODEL

In recent years the Markov process has found great favor and application in meteorology. Its success on the wind speeds warrants its description in this paper, ignoring the diurnal cycle. When the model is fitted to monthly data, the annual cycle can be ignored as well. The primary assumption is: "The conditional probability distribution for the state at any future instant, given the present state, is unaffected by any additional knowledge of the past history of the system" (Kendall and Buckland, 1957).

To apply the simple Markov model to the wind speed, the frequency distribution of the wind speed, V, at given location, level and month, is plotted on normal probability paper (for example, Figure 1) which automatically transforms V into the normal Gaussian variate with mean zero and variance 1.0 symbolized in this paper as $y(N|O, 1)$. For example, in Figure 1 the speed $V = 30$ knots occurs with cumulative frequency 79 percent and corresponds to $y = 0.80$.

It is y that is assumed to vary in a stationary Markov process whose hourly values $y_o, y_1, \ldots y_i$ are given by

$$y_o = \eta_o, \ \ldots \ y_i = \rho \cdot y_{i-1} + \sqrt{(1-\rho^2)} \cdot \eta_i \qquad i \geq 1 \qquad (1)$$

where $\eta(N|O,1)$ is also normally distributed, but all η are random and independent of one another; ρ is the hour-to-hour correlation, assumed constant.

For two observations y_i and y_j that are $|j-i|$ hours apart, their correlation ρ_{ij} is

$$\rho_{ij} = \rho^{|j-i|} . \qquad (2)$$

If the two observations are less than one hour apart then Eq. (2) gives a greater correlation, asymptotically approaching 1.0 as the time interval approaches zero.

In terms of the simple Markov model, the problems reduce to the following:

1. To find the probability distribution of the m-hour maximum, y_{max}, where m can vary arbitrarily from a fraction of an hour to 768 hours or 32 days. There will be a one-to-one correspondence of y_{max} to V_{max} (Figure 1). Once the device is constructed to obtain y_{max}, given m, then the same device can be used to find the duration m, given y_{max}.

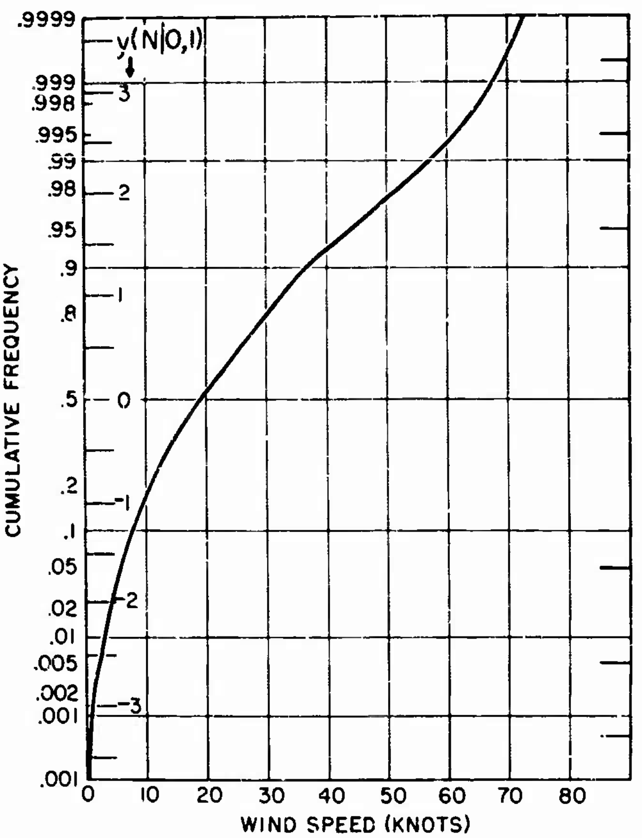

Figure 1. The Cumulative Frequency of Wind Speed at 10,000 ft over Miami, Florida in January, Based on 1956-1960 Data. The chart transforms wind speed V into the normalized variate y (N|O, 1)

2. To find the conditional probability distribution of y_{max} in the m hours following the initial value y_o.

3. To find the probability distribution of the lowest m-hour maximum in 32 days, or the probability that there will be m hours in the month during which y (or V) will not exceed the threshold value.

After making inquiries among several theoretical statisticians, this author resorted to a Monte Carlo simulation technique, in the belief that a purely mathematical

solution is not possible. Some 500 sets of random normal numbers were generated by computer (IBM 7044), 768 numbers in each set, which were transformed into a Markov chain of serially correlated values (Eq. 1) to simulate one month of hourly values. The frequency distribution of the maximum in m hours, m varying from 1 to 768 hours, was obtained and entered into charts (Gringorten, 1966).

For the problem of the tethered balloon, the simulation of hourly observations was not enough. Consequently, the Monte Carlo technique was again applied to simulate a nearly continuous variation of y. At Miami, Florida, January, 700 mb the 12-hourly observations were found to have a correlation of 0.865, which, in the Markov process, corresponds to an hour-to-hour correlation of 0.988, and further corresponds to a correlation between values 1/64-hour apart equal to 0.999812. The generation of $(64 \times 768) + 1$ random normal numbers, serially correlated by Eq. (1), repeated 500 times and sorted to give m-hour maxima, produced the results as shown in Figure 2. (Further details and theory of this procedure have been submitted for publication, the date having not yet been determined.)

Example: Figure 1 for the 700-mb winds at Miami, Florida in January, gave wind speeds (knots) corresponding to

$$y = -1.5, \ldots, 4.0$$

as shown by the bracketed figures on the edges of Figure 2. Consequently the probabilities of m-hour maximum of wind speed can be estimated directly from Figure 2.

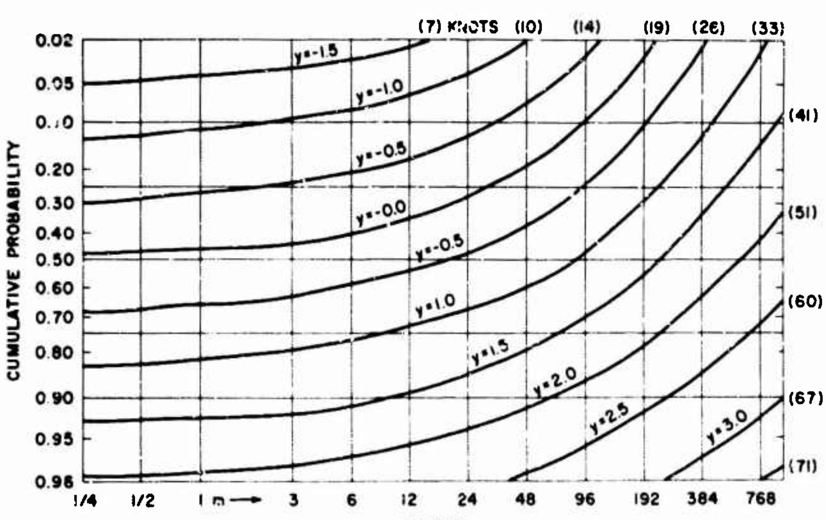

Figure 2. The Cumulative Probability Distribution of the m-Hour Maximum of y(N|O, 1), When the Hour-to-hour Correlation ρ = 0.988 in a Stationary Markov Process. The figures in brackets are for wind speeds in knots (Figure 1)

For example, there is a 50 percent chance that the wind will not exceed 26 knots for any 16 consecutive hours. There is a 98 percent certainty that it will not exceed 60 knots for 40 continuous hours. There is a 2 percent chance that it will not exceed 32 knots in a full month (744 hours), and so on.

An extensive study of the hour-to-hour correlation of wind speeds has not been made yet. Consequently the serial correlation obtained for Miami (0.988) is accepted as an interim value. Figure 2 becomes a working tool for the estimates of probabilities of m-hour maxima. It needs to be used with a distribution of basic values (Figure 1) of wind speed.

3. THE MODEL WITH KNOWN INITIAL WIND SPEED

The Monte Carlo exercise was repeated for initial values of $y_o = 1.0, \ldots, -4.0$ (Figures 3a through 3f).

Example: With the use of a threshold value of wind speed V = 40 knots, the lines y = 1.4 from Figures 3a through 3f were collected (Figure 4) to show probability of m-hour maximum for initial values V = 33 knots, ..., calm. Figure 4 shows that, if the initial wind speed is 33 knots then the probability of exceeding 40 knots in 48 hours is 52 percent. But if the initial speed is less than 10 knots then the probability of exceeding 40 knots in 48 hours is negligible (less than 2 percent). When the initial speed is calm, then it is 88 percent certain that the wind speed will not exceed 40 knots for eight days (192 hours).

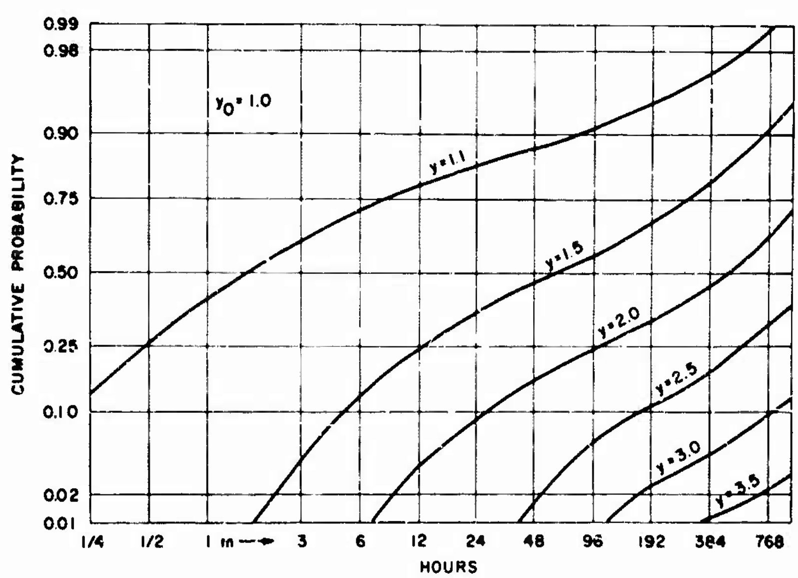

Figure 3a. The Conditional Probability Distribution of the m-Hour Maximum of Continuous y(N|O, 1) When the Hour-to-hour Correlation $\rho = 0.988$ in a Stationary Markov Process. Initial value $y_o = 1.0$

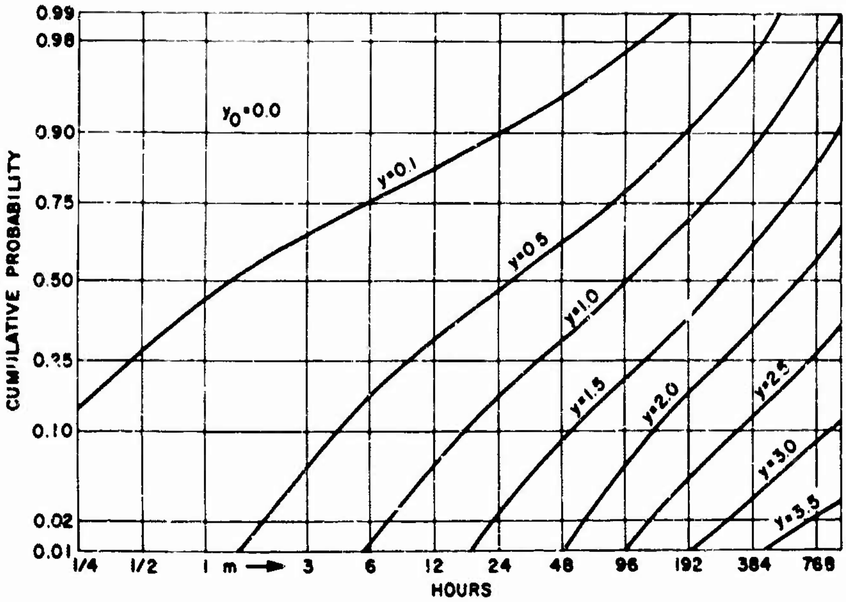

Figure 3b. Initial Value y_o = 0.0

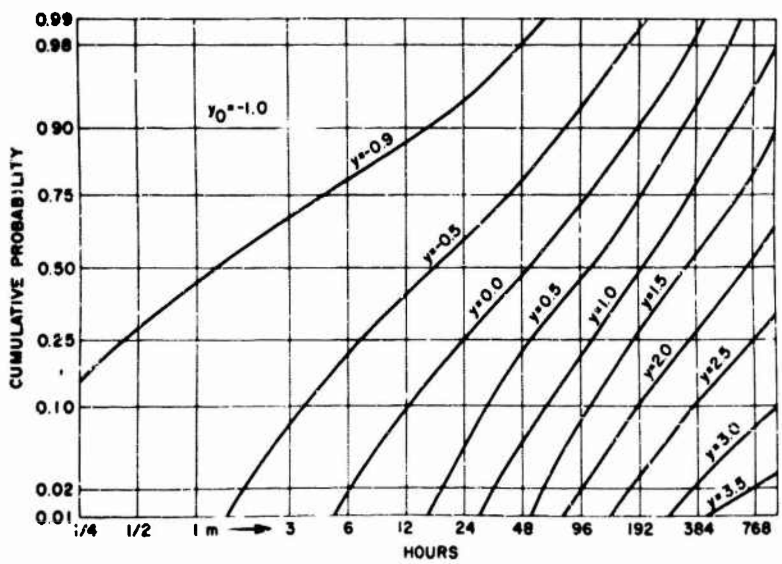

Figure 3c. Initial Value y_o = -1.0

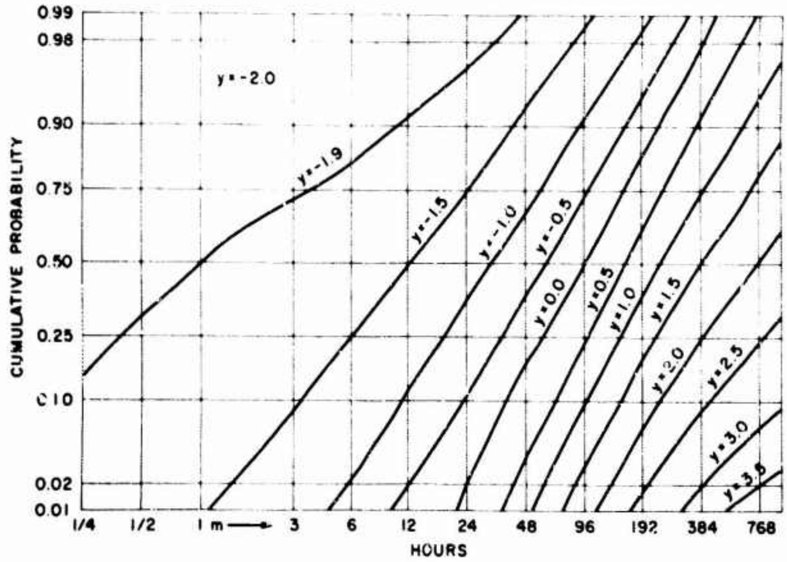

Figure 3d. Initial Value $y_o = -2.0$

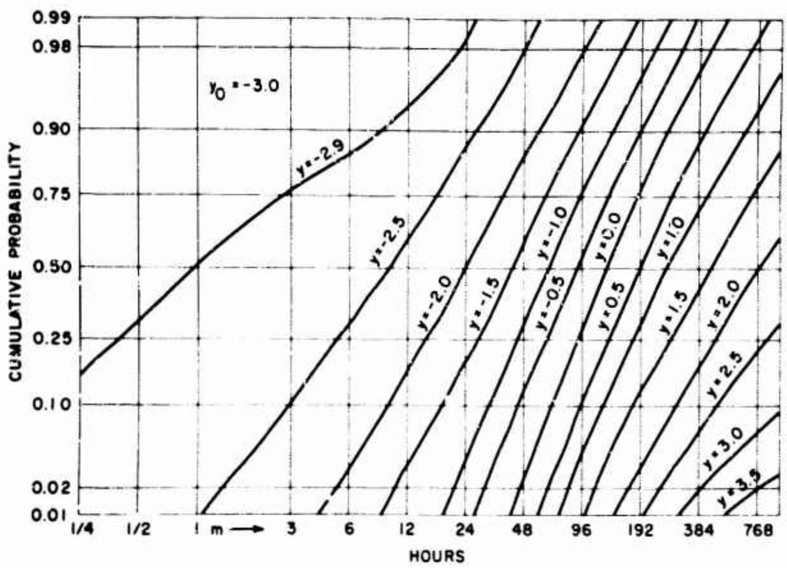

Figure 3e. Initial Value $y_o = -3.0$

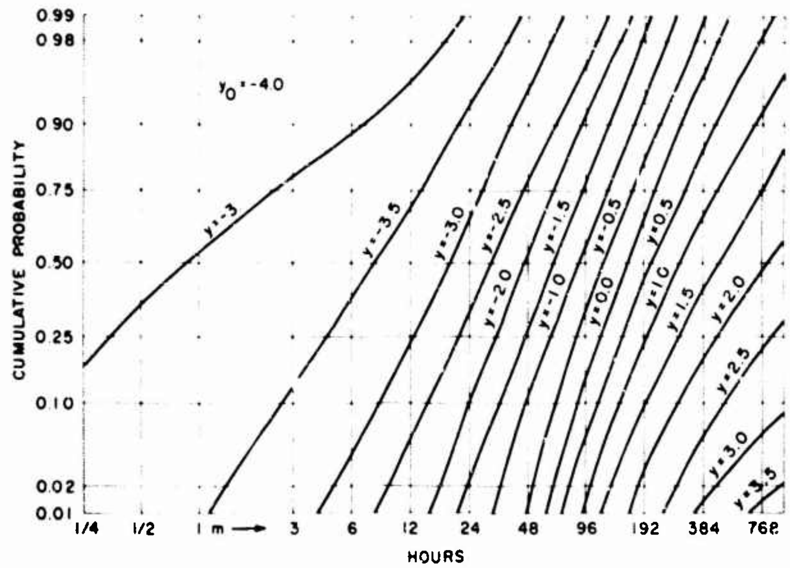

Figure 3f. Initial Value y_0 = -4.0

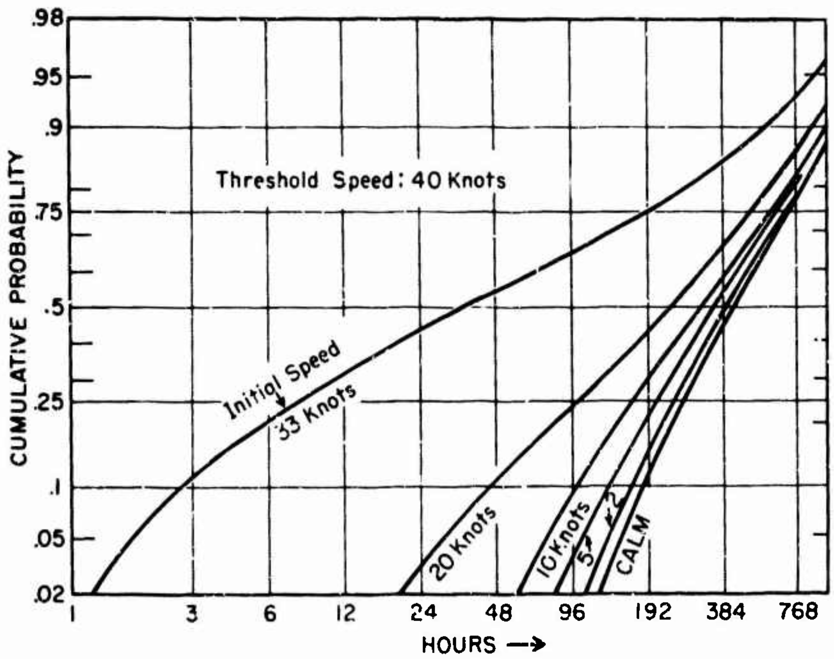

Figure 4. Chart for Estimating the Conditional Probability That the Continuous Wind Speed at 10,000 ft Over Miami, Florida, in January, Will Exceed 40 Knots in m Hours, m Ranging from 1 to 768 Hours, Initial Speed from Calm to 33 Knots

4. ON THE LONGEST DURATION OF SUBCRITICAL WIND SPEEDS IN ONE MONTH

In the published paper (1966) there are results of the Monte Carlo simulation giving the probability distribution of the lowest m-hour maximum in 32 days. Figure 5 shows isopleths of y-values, the hour-to-hour correlation being 0.988 (see above). Using Figure 1, for the example of January, 700 mb at Miami, Florida, one observes that the wind speed V corresponding to each y was determined and the value is shown in brackets around the periphery of the figure.

As an example of the use of the figure, if 40 knots is the threshold wind speed, Figure 5 shows that there is a 50 percent likelihood that the maximum duration of subcritical winds will be close to 21 days within the 32 days. There is a 25 percent chance that the duration will be for the full month, and a 98 percent certainty that the longest period will be at least nine days.

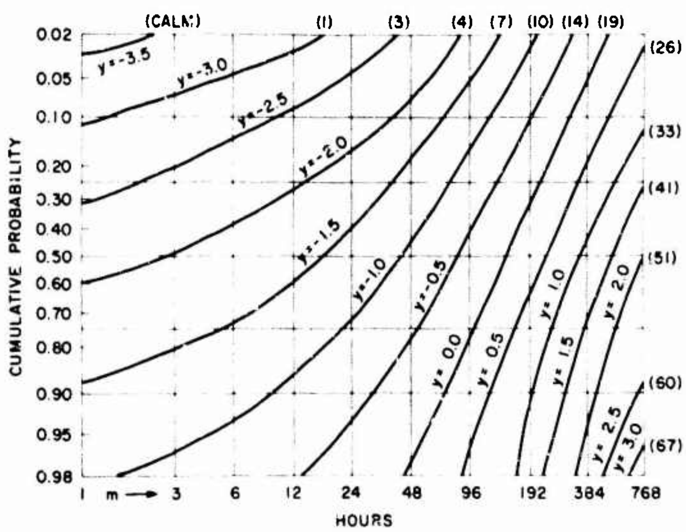

Figure 5. The Cumulative Probability Distribution of the Lowest m-Hour Maximum in 768 Hours (32 days) of y(N|O, 1). The figures in brackets on the periphery are in knots, to give maximum wind speeds over Miami, Florida in January at 10,000 ft

5. DISCUSSION

To accept the model, several assumptions must be tenable. The simple Markov process must be assumed to fit the stochastic variation of the wind speed, and the hour-to-hour correlation of the transformed variate must be a constant.

Since, at this writing, this correlation (0.988) was obtained only from Florida data, it is not known whether such a single value, or indeed the Markov process itself, will prove satisfactory for other locations, time of year, and elevations above sea level. There will need to be further testing. The diurnal cycle had been ignored, but, aloft, this assumption is readily acceptable.

There is another assumption that must be made, but which is instinctively acceptable. Winds that are observed by rawinsonde every 12 hours have a frequency distribution that should be representative of all winds, whether they be sampled daily, hourly, or every two minutes.

Still another complication is atmospheric turbulence. The winds, as given in the meteorological records, have been averaged over 1000-ft layers, or are equivalent to two-minute averages. Thus, gusts have been smoothed out. The probabilities of exceeding threshold values are therefore underestimated, whenever turbulence is present in the atmosphere. A rough estimate is that gustiness occurs 7 percent of the time (Anderson, 1956). The levels of most frequency turbulence are 24, 280 ft, 36, 090 ft, and 47, 250 ft. Three levels of relative minimum turbulence are 20, 340 ft, 31, 170 ft, and 35, 340 ft. There is a definite decrease of turbulence above 50, 000 ft. The probability of turbulence is increased to 10 percent when wind speed is greater than 31 knots, to 13 percent when wind speed is greater than 68 knots. When gusts do occur they have roughly a root mean square value of nine knots with a one percent probability of 21 knots (Endlich and McLean, 1965; AFCRL, 1967).

6. SUMMARY

Figures 2, 3, and 5 are presented as working tools for the estimation of probabilities of duration of subcritical wind speeds. As input, they require a parent distribution of wind speeds (for example, Figure 1). Figure 2 makes possible probability estimates of the maximum speed that will not be exceeded for a given length of time or, conversely, the probability estimate of the duration of subcritical speeds. Figures 3a through 3f do the same when the initial speed is known. Figure 5 provides estimates of the maximum wind speed of given duration, or the longest duration of a given threshold within an operational period of one month.

References

AFCRL (CREW) Conference (1967) Standard Wind Profile (and Associated Gust) Design Criteria for Cape Kennedy and Vandenberg, a working level Air Force meeting of Aerospace, Inc., NASA, Kaman Avidyne, AFFDL, and AFCRL personnel.

Anderson, A.D. (1956) Free-Atmosphere Turbulence, Naval Research Laboratory Report 4735.

Endlich, R.M., and McLean, G.S. (1965) Empirical relationships between gust intensity in clear-air turbulence and certain meteorological quantities, J. Appl. Meteorol. 4:222-227.

Gringorten, I.I. (1966) A stochastic model of the frequency and duration of weather events, J. Appl. Meteorol. 5:606-624.

Kendall, M.G., and Buckland, W.R. (1957) A Dictionary of Statistical Terms, Oliver and Boyd, London, 493 pp.

VI. High-Altitude Tethered Balloon Design

William F. Conley
Goodyear Aerospace Corporation
Akron, Ohio

Abstract

This paper was prepared for presentation at a meeting on tethered balloons held at AFCRL, Hanscom Field, Bedford, Massachusetts. Included is a brief description of balloon and cable design procedure and a more detailed description of system solutions by the use of graphical superposition.

1. INTRODUCTION

Initial indications are that high-altitude tethered balloons (50,000 to 100,000 ft) can be built and flown if certain problems can be overcome. We may find that the balloon will have many uses now provided by satellites, aircraft, and free balloons. Balloons are launched and operated by the use of "mother nature's" gravity which produces buoyant lift. How inexpensive this is compared to the tremendous rocket power required of our satellites. A tethered balloon may be returned easily to the ground whereas a free balloon is difficult to recover. Production cost of a balloon is minute compared to that of an aircraft or rocket. Consider all this, plus a nearly stationary platform, which is not possible with the satellite, aircraft, or free balloon.

Presentation of three topics will provide an insight into the work accomplished under a project monitored this week by our hosts, the Air Force Cambridge Research Laboratories. They are:

1. Balloon Design Curves
2. Cable Design Curves
3. Compatible Balloon Cable Systems (Examples)

Note that the solutions obtained as presented in this paper provide only for static equilibrium at float altitude. Launch and retrieval problems have not been considered.

2. PROBLEM APPROACH

Before the foregoing topics are presented, a brief look at the approach to the problem is advisable. Examination of all of the unknown parameters as provided in Table 1 might lead us to believe that a trial and error solution is the only possible approach. That is, after specifying user inputs of float altitude, wind profile, and so forth, we might begin the solution by selecting a balloon volume, then design the balloon to determine its weight and aerodynamic characteristics. A cable design might now proceed which will provide a cable stressed to an allowable limit and provide a particular profile. Perhaps this solution would result in a cable that would tend to become horizontal at a level above the ground. In such a case, a larger balloon would be chosen and the process repeated until a desired condition is met.

Needless to say, such a solution does not lend itself to examination of a large number of float altitudes, wind profiles, balloon and cable types. A method of superposition was thus developed which provides all possible balloon-cable solutions at a glance. The coordinates of these superposed graphs are net lift $\left(L_n\right)$ and net lift-net drag ratio $\left(L_n/D_n\right)$. These factors of lift and drag are the only parameters common to both the balloon and cable which allow a separate solution of each component and later joining to determine compatible systems.

Prior to developing the balloon and cable relation for net lift and net drag values, a note about environment is necessary. Environmental factors of density and wind profile are the items of major concern in the design of a balloon-cable system. Volumetric expansion, the occurrence of which is attributed to changes in the density of the atmosphere, has been encountered in the design of free balloons. Therefore, no new consideration need be given to these factors at this time. Wind profile, however, has not previously been encountered for high altitude systems. This item, therefore, presents certain problems not yet tested.

Table 1. Unknown Parameters for Balloon-Cable System Determination

Typical User Inputs

1. Float Altitude
2. Payload Weight
3. Operating Time
4. Wind Profile
5. Total Downwind Displacement Permissible

Quantities Unknown by Designer

A. Balloon

1. Balloon Type
2. Balloon Volume
3. Angle of Attack
4. Stresses in Balloon
5. Balloon Weight
6. Component Design
7. Component Weight
8. Balloon Expansion Capability
9. Dilation or Ballonet System
10. Power Requirement
11. Drag on Balloon
12. Lift on Balloon

B. Cable

1. Cable Type
2. Cable Tension
3. Cable Diameter
4. Cable Weight
5. Cable Length (to include blowdown dist.)
6. Drag on Cable
7. Lift on Cable
8. Vertical Angle Formed by Cable

C. Winch Equipment

D. Ground Handling Equipment

Much research has been conducted by AFCRL to establish realistic wind profiles at three locations of interest. Typical plots of wind velocity versus altitude for summer and winter conditions in area 1 are provided in Figure 1.

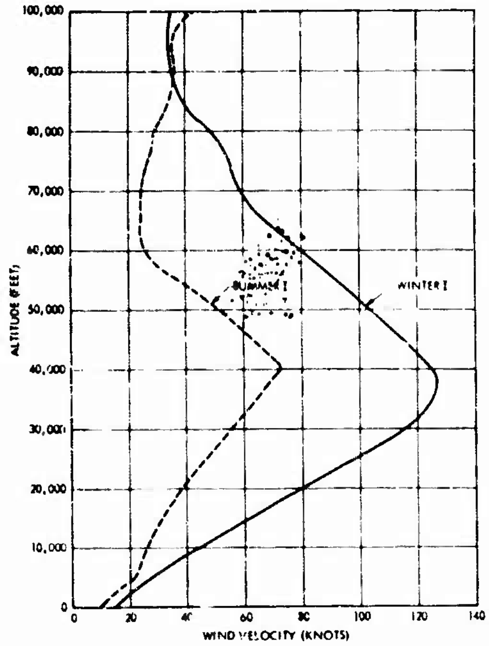

Figure 1. Variation of Wind Velocity with Altitude at Geographic Location I

3. BALLOON CURVES

A multitude of balloon types exist; thus it is impractical to examine all possibilities. Five balloon types were examined which provide a range of characteristics typical of most designs now in existence.

Those selected for examination include:

1. Natural balloon
2. Streamlined balloons
   a. Class C
   b. Mark II Modified
   c. Vee
   d. Ram Air Class C

A brief description of each balloon type is given here, with Figures 2 and 3 providing a pictorial description. Since L_n and D_n are the factors of interest, computer programs were established to estimate weight of the balloon components and aerodynamic characteristics of the balloons.

1. Natural Balloon

The shape of a natural balloon is that formed by enclosing a buoyant gas within a loose bag connected to a payload or cable. The load may be reacted at the top and/or the bottom. Circumferential stress is eliminated by allowing excess material to occur in a circumferential direction at every point along the gore. Additional work has been accomplished for a top loaded cylinder balloon to establish weight, size, shape, reefing control, superpressure control, and so forth.

Evidence thus far collected indicates that a simple design approaching that of a cylinder type balloon provides the optimum design as concerns stress and weight. Volume change control and superpressure capability seem best to be provided by means of a top loaded balloon. Testing of a 15-foot diameter model to demonstrate these factors for altitudes up to 100,000 ft is planned. Figure 4 depicts the shape change and corresponding volume change developed by top loading.

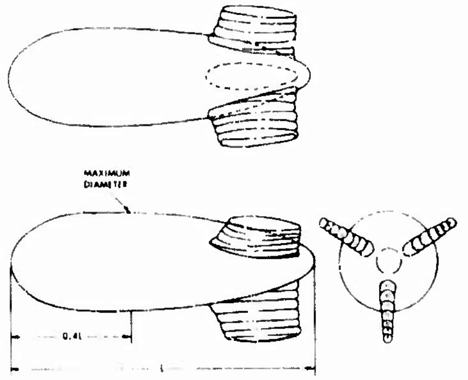

Figure 2a. Class C and Ram Air C Configuration

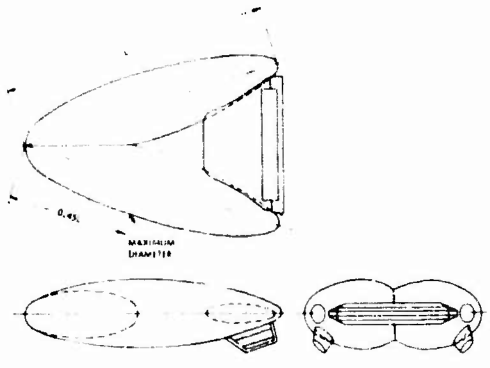

Figure 2b. Vee-Balloon Configuration

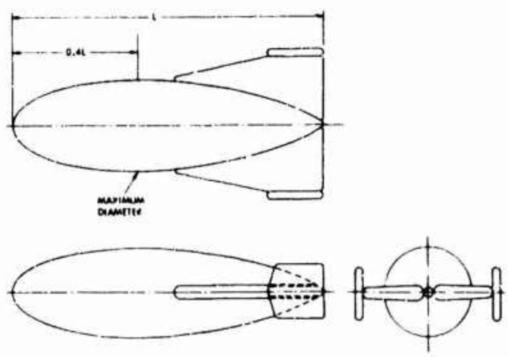

Figure 3a. Modified Mark II Balloon Configuration

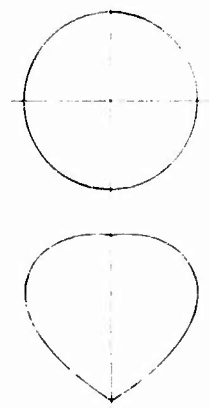

Figure 3b. Superpressure, Natural Shape Balloon Configuration

Values of L_n and D_n necessary to plot the design curves are based on the following equation:

$$L_n = L_b + L_a - P - W$$

where

L_b = buoyant lift of the gas

L_a = aerodynamic lift of the wind

P = payload weight

W = balloon weight.

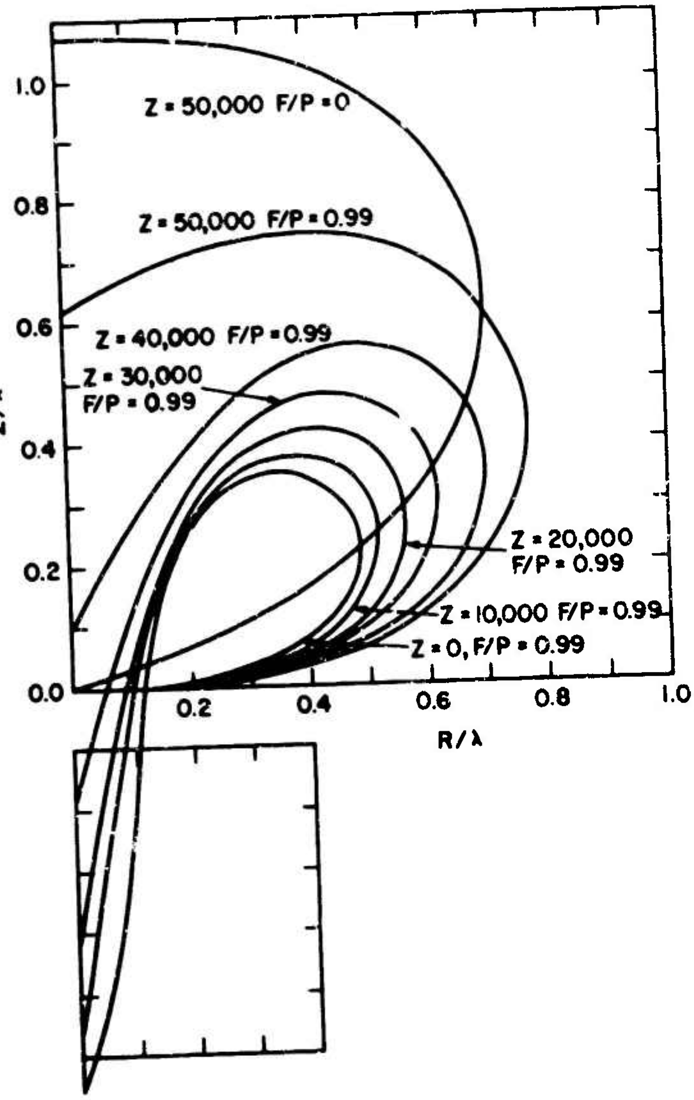

Figure 4. Natural Balloon - Size and Shape as Altitude Varies

Aerodynamic characteristics are based on the assumption that the balloon is spherical in shape. Thus aerodynamic lift is zero. Drag, on the other hand, is easily computed. Wind tunnel data recently obtained for aerodynamic characteristics of a balloon with zero top load will be incorporated in future work.

A balloon design curve is provided in Figure 5. Here a float altitude of 100,000 ft is shown. Note that two wind conditions are used in the design, namely, Summer I and Winter I. The curve is obtained by determining L_n and D_n for various balloon volumes which are marked on the curves.

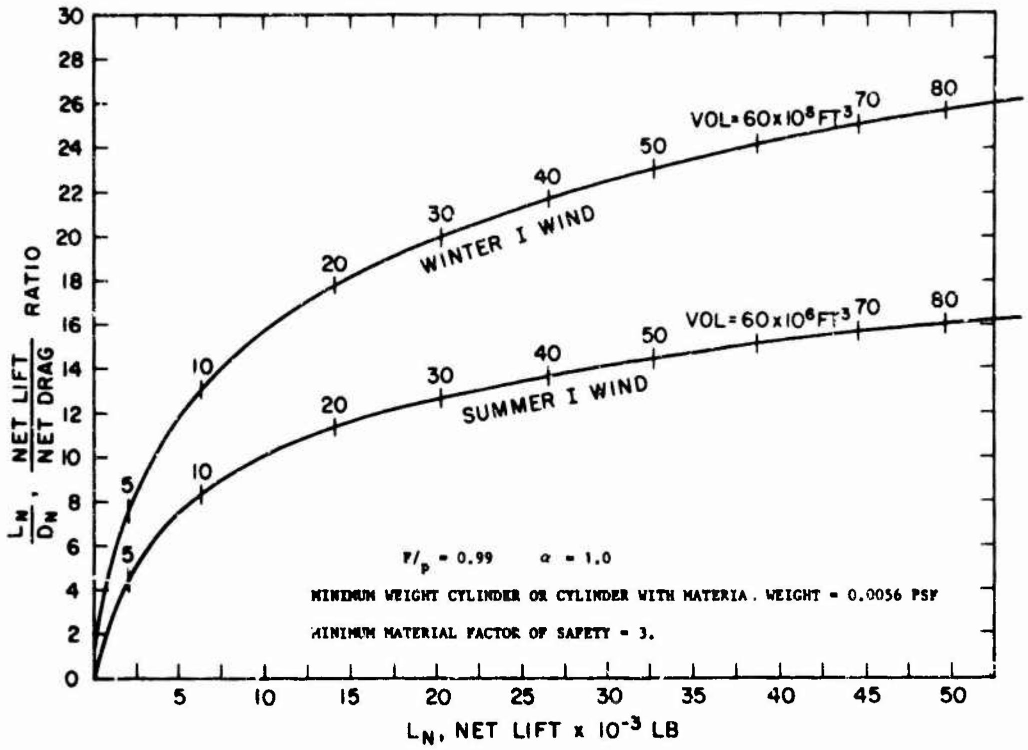

Figure 5. Net Lift and Drag Characteristics of Superpressure, Natural Shape Balloon for Altitude of 100,000 ft and payload of 500 lb

2. Streamlined Balloons

Design procedure and weight estimates for tethered streamlined balloons greater than approximately one quarter million cu ft have not previously been established. Therefore, a simplified design procedure was developed for the parametric computer study utilized in this program.

The basic design feature specifies a catenary curtain attached throughout the length of the hull. Such an attachment will allow transference of the buoyant and aerodynamic load at any section directly to the cable. With a properly designed catenary, the bending moment occurring at any section can be reduced in magnitude to a value where other stress factors are more important to the design of the material strength and weight. Other design factors are presented in the reference, including features for the other streamlined balloons. Results of a typical computer printout of component and equipment sizes and weights is provided in Table 2. Significant here is the fact that only six parameters are input and a total of 61 items are printed out which reflect design assumptions stated in the reference.

Table 2. Computer Printout Data for a Class C Balloon Configuration

COMPUTER INPUT DATA:

Payload = 500 lb	Altitude = 50,000 ft
Velocity = 85 ft/sec	Angle of Attack = 5°
Volume = 1,000,000 ft^3	Operating Time = 48 hr

Lift and Drag Coefficients = f (angle of attack)

Hull unit fabric weight (lb/ft^2)	0.022
Stagnation pressure (lb/ft^2)	1.3184
Design stress, includes safety factor of 3 (lb/ft)	466
Hull length (ft)	262
Projection area of 1 horiz tail (ft^2)	3000
Wetted area of 1 horiz tail (ft^2)	7031
Thickness of vert. tail, avg (ft)	5.75
Total volume of balloon (ft^3)	1,051,800
Wetted area of spherical ballonet (ft^2)	44,806
Volume lost by leakage (ft^3/day)	489
Volume flow thru blower (ft^3)	1,973,800
Aerodynamic stress by tether tension (lb/ft)	16.36
Weight of hull fabric (lb)	1199
Weight of intersect attachments (lb)	0
Weight of internal partitions of horiz tail (lb)	129.6
Weight of internal partitions of vert. tail (lb)	129.6
Weight of exit valve (lb)	72.3
Weight of ballonet seams and attachments (lb)	31.1
Weight of suspension system (lb)	574
Buoyant lift (lb)	10,610
Balloon weight (lb)	3292
Unit lift (lb/ft^3)	0.01009
Internal design pressure (lb/ft^2)	1.516
Max hull diameter (ft)	99.2
Projected vert. tail (ft^2)	3,000
Wetted area of 1 vert. tail (ft^2)	7,031
Volume of 1 horiz tail (ft^3)	17,253
Ballonet volume (ft^3)	890,730
Intersect area (ft^2)	0
Volume req'd for temp change (ft^3/day)	105,180
Blower operating time at altitude (min/day)	13.4
Buoyant stress by tether tension (lb/ft)	39
Weight of hull seams (lb)	120
Weight of 1 horiz tail (lb)	152
Weight of 1 vert. tail (lb)	152
Weight of blower (lb)	127
Weight of check valve (lb)	63
Weight of misc equip, battery and blower (lb)	22
Weight of handling lines and catenary (lb)	134
Net lift (lb)	9507
Drag (lb)	928
Wetted hull(s) area (ft)	55,500
Location of max diameter (ft)	104.8
Thickness of horiz tail, avg (ft)	5.75
Volume of 1 vert. tail (ft^3)	17,253
Diameter of spherical ballonet (ft^3)	119
Volume flow rate of blower (ft^3/min)	15,790
Volume to replace each day (ft^3/day)	211,300
Max stress due to inflation (lb/ft)	100
Intersect weight (lb)	0
Weight of attachments of 1 horiz tail (lb)	15.2
Weight of attachments of 1 vert. tail (lb)	15.2
Weight of batteries (lb)	44.6
Weight of ballonet (lb)	311
Aerodynamic lift (lb)	2689
Lift coefficient	0.204
Drag coefficient	0.0704

3. Balloon Curve Plots

Utilizing the information presented above, one observes that curves of L_n versus L_n/D_n may be plotted for specified design parameters. Examples of such curves are provided in Figure 6. Note that each point shown on the curves represents a new design point; that is, new stresses, weights, and so forth, are necessary to establish each point on the curves.

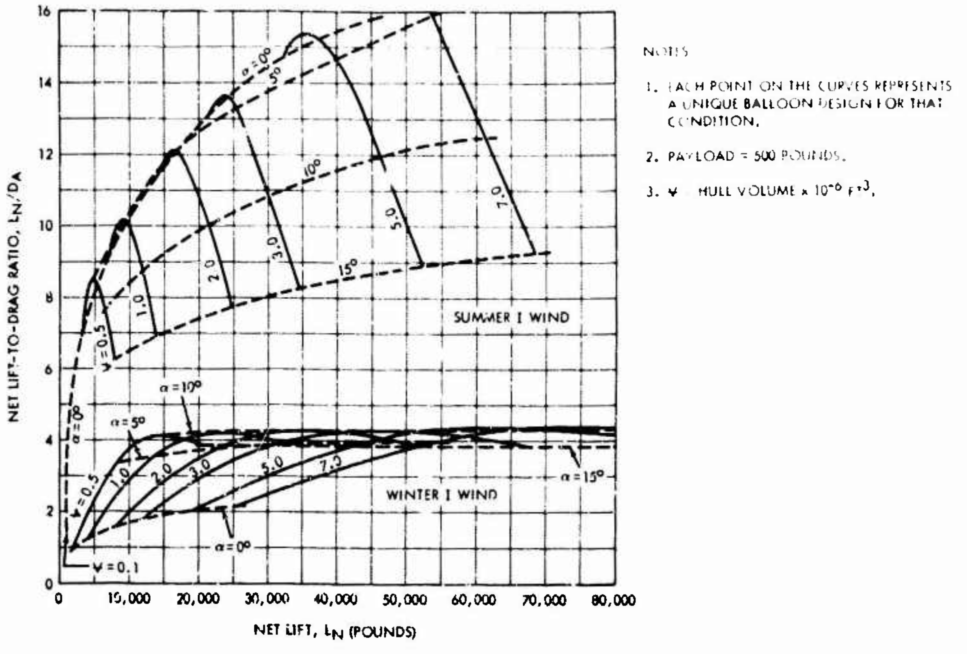

Figure 6. Net Lift and Drag Characteristics of Class C Balloon for Altitude of 50,000 ft

4. CABLE CURVES

Unit material weight and strength of cable materials are two important factors necessary to determine static system performance once a balloon has been selected.

A cable solution by use of the computer is obtained by applying a static equilibrium solution to successive incremental segments of the cable. Figure 7 provides a free body diagram for which a value of L_n/D_n is assumed at the top end of the cable and a cable tension and corresponding diameter are determined based on a specified safety factor. This weight and diameter are assumed constant for the first segment length. Wind and gravity forces are applied to this portion and a compatible set of equilibrium forces is computed for the bottom end of the segment.

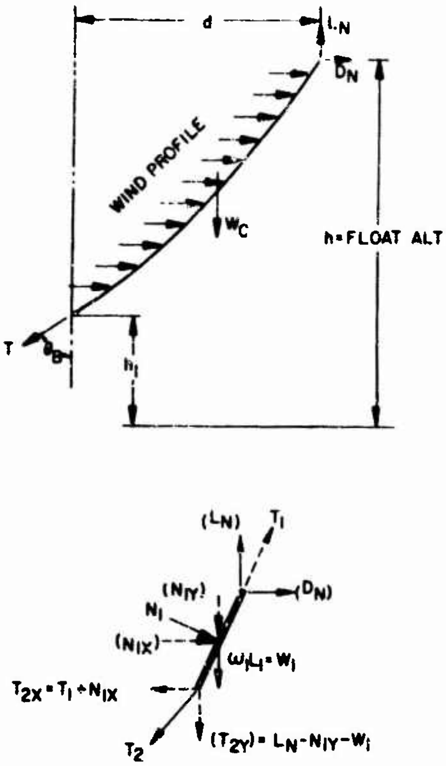

Figure 7. Cable Free Body Diagrams

At this point, a new c ble weight and diameter are selected consistent with the factor of safety. This process is continued until the cable reaches the ground or becomes horizontal. The cable obtained is essentially the ideal tapered cable that will accomplish the task. Since a practical cable can only approach this solution, the method establishes a bound on the problem in the form of a minimum weight.

From the solution presented, several factors are obtained including angle at the base of the cable θ_b, altitude at low point of cable h, downwind displacement d, total cable weight W_c, and tension at the base of the cable T_b.

Families of curves of the foregoing parameters may be plotted after several computer solutions are made. An example of these plots is provided in Figure 8 for a particular wind and float altitude condition (Summer I wind at 50,000 ft).

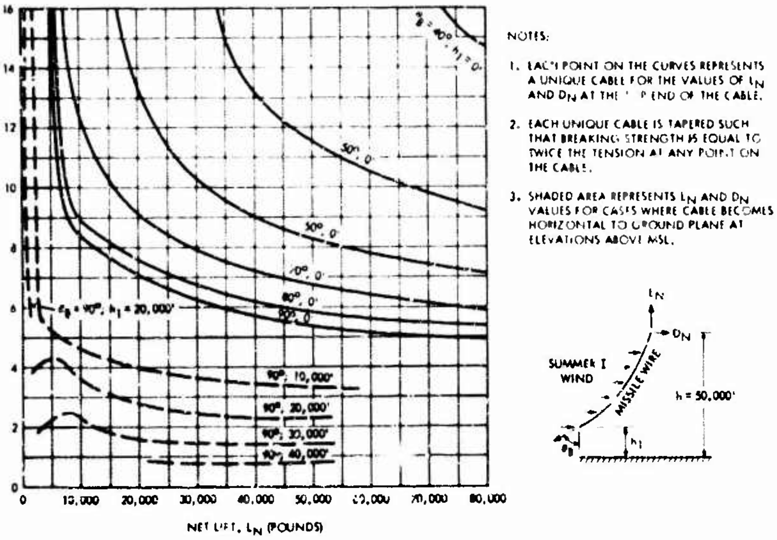

Figure 8. Angle at Bottom End of Cable for Missile Wire at 50,000 ft in Summer I Wind

5. COMPATIBLE BALLOON–CABLE SYSTEMS (EXAMPLES)

Solutions for particular tethered balloon systems are obtained by selecting the proper set of curves consistent with user requirements.

As a first example, a single balloon system is designed for the following requirements:

<u>General</u>

Float altitude	=	50,000 ft
Wind profile	=	Summer I wind
System type	=	Single balloon

<u>Cable</u>

Material type	=	Glastran cable
Factor of safety	=	2.0
Cross-section variation	=	Tapered
Selection criterion	=	Angle at base = 70 degrees

<u>Balloon</u>

Balloon type	=	Natural
Component design	=	As per reference
Angle of attack	=	Not applicable

An overlay of the proper curves as provided in Figures 9 and 10 indicates that a solution exists when a natural balloon of 1.9×10^6 cu ft is provided. A matching point from Figure 11 indicates the total cable weight is 10,000 lb, and Figure 12 provides a blowdown distance of 47,000 ft.

A second example is provided to show the method for designing a multiple balloon system. The requirements here are:

<u>General</u>

Float altitude	=	100,000 ft
Wind profile	=	Winter I wind
System type	=	Minimum number of balloons possible

<u>Cable</u>

Material type	=	Glastran cable
Factor of safety	=	2.0
Cross-section variation	=	Tapered
Selection criterion	=	Not specified

<u>Balloon</u>

Balloon type	=	Natural at float altitude
	=	Class C at other altitudes
Component design	=	As per reference
Angle of attack	=	Natural balloon - not applicable
		Class C = 5 degrees

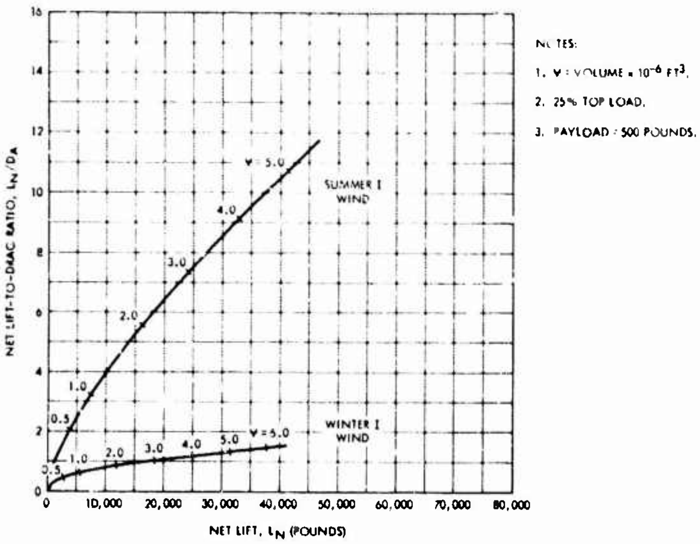

Figure 9. Net Lift and Drag Characteristics of Superpressure, Natural Shape Balloon for Altitude of 50,000 ft

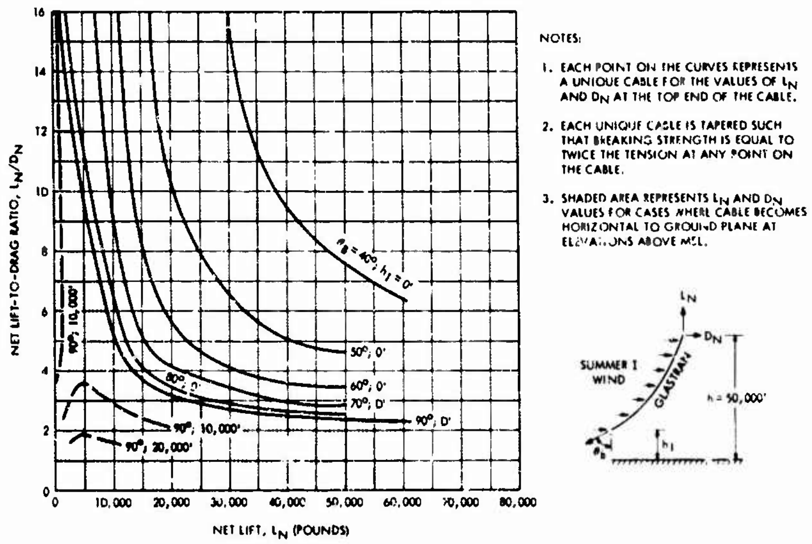

Figure 10. Angle at Bottom End of Cable for Glastran at 50,000 ft in Summer I Wind

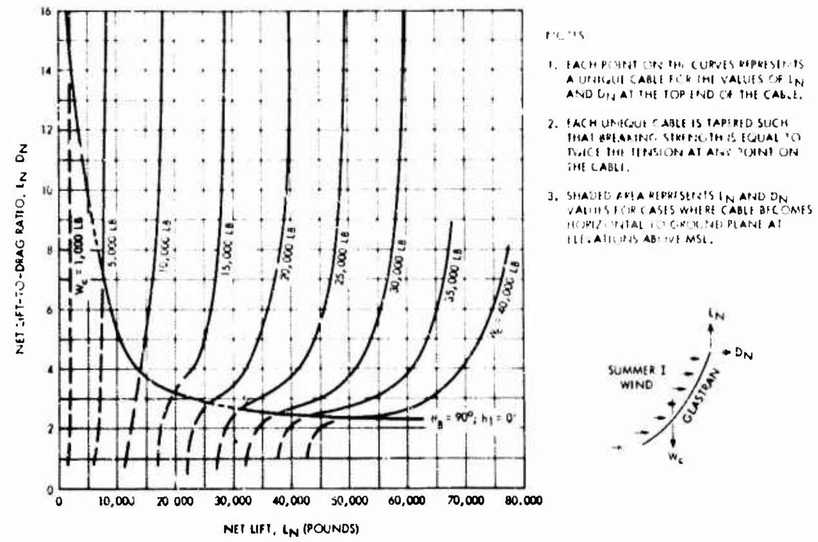

Figure 11. Cable Weight for Glastran at 50,000 ft in Summer I Wind

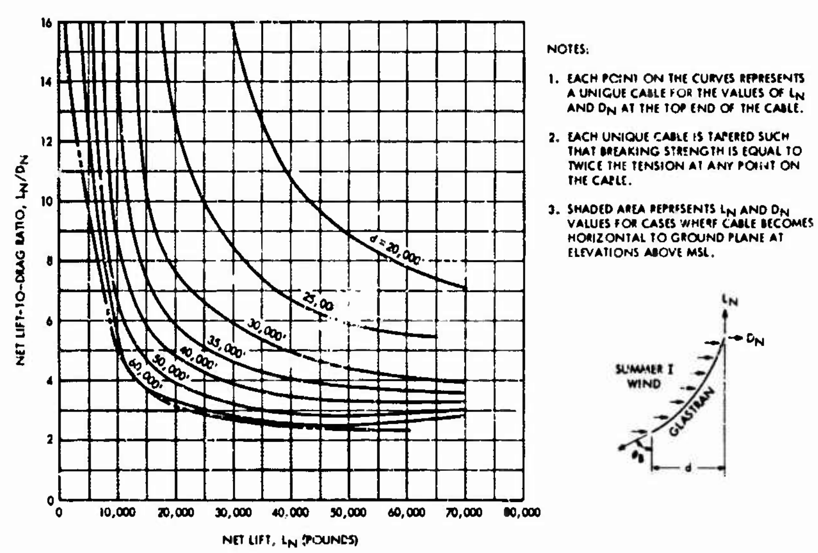

Figure 12. Blowdown Distance for Glastran at 50,000 ft in Summer I Wind

An overlay of Figures 5 and 13 will show that a 79×10^6 cu ft natural balloon at float altitude provides a cable which becomes horizontal at an altitude of 20,000 ft. A single balloon this large may be considered undesirable, although its volume on the ground will be less than 1,000,000 cu ft. Two balloons can be designed roughly one-half this size and placed in tandem at 90,000 and 100,000 ft, if desired. A matching point obtained from Figure 14 indicates that the cable tension at this lower altitude is 12,000 lb. Since the cable is horizontal at this point, the tension represents the total drag of the cable and balloon above. By placement of another balloon at this 20,000 ft altitude, additional lift is provided. The combined drag of the upper cable and the lower balloon is then added vectorially to the lift of this lower balloon to provide a resultant vector enabling a segment of cable to reach the ground. Figures 15 and 16 are provided for the following factors:

<u>General</u>

Float altitude	=	20,000 ft
Wind profile	=	Winter I
System type	=	Second balloon of a multiple balloon system

<u>Cable</u>

Material type	=	Glastran cable
Factor of safety	=	2.0
Cross-section variation	=	Tapered
Selection criterion	=	Cable to become horizontal at the ground (if possible)

<u>Balloon</u>

Balloon type	=	Class C
Component design	=	As per reference
Angle of attack	=	5 degrees

To provide a direct solution to this problem, the axes of Figures 15 and 16 are selected to be L_n or D_n. An overlay of the graphs with the cable curve shifted downward by a drag amount equal to the cable tension will provide an intersection indicating that a Class C balloon volume of 600,000 cu ft will provide the desired solution.

6. SUMMARY

The preceding presentation has depicted three items. First, computerized parametric balloon solutions can be established without regard for cable problems. Second, cable profile solutions can be established in a similar fashion. Finally, proper coordinate axes can be selected for the balloon and cable plots which make possible solutions that exist.

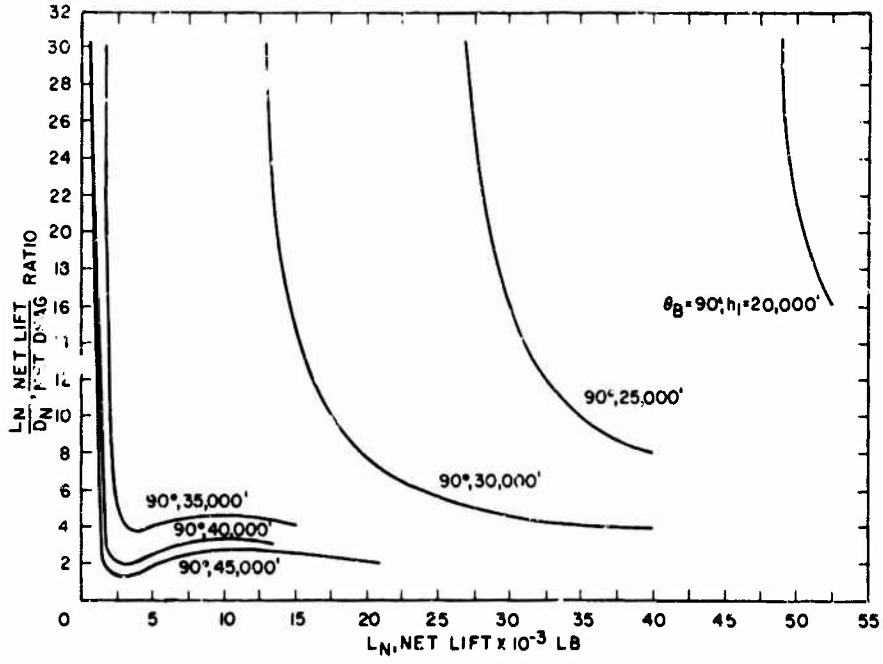

Figure 13. Cable Profile Plot for Base Cable Angle of Glastran Cable at 100,000 ft in Winter I Wind

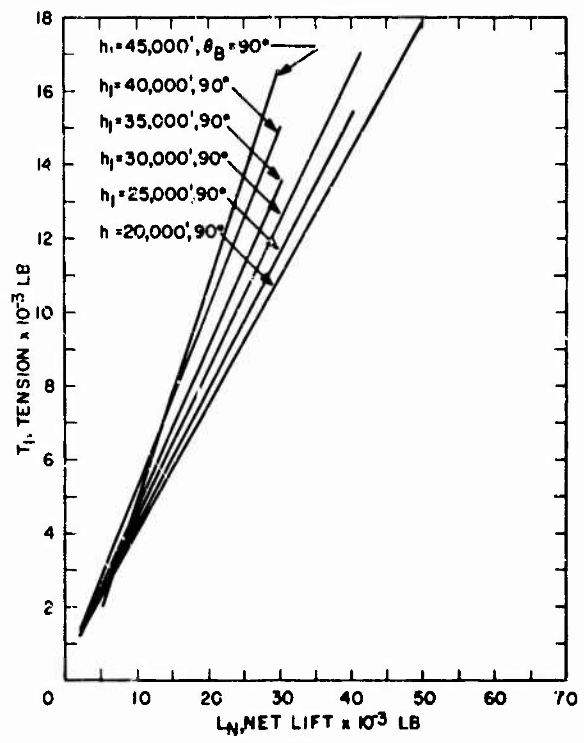

Figure 14. Tension at Base of Glastran Cable for 100,000 ft Float Attitude in Winter I Wind

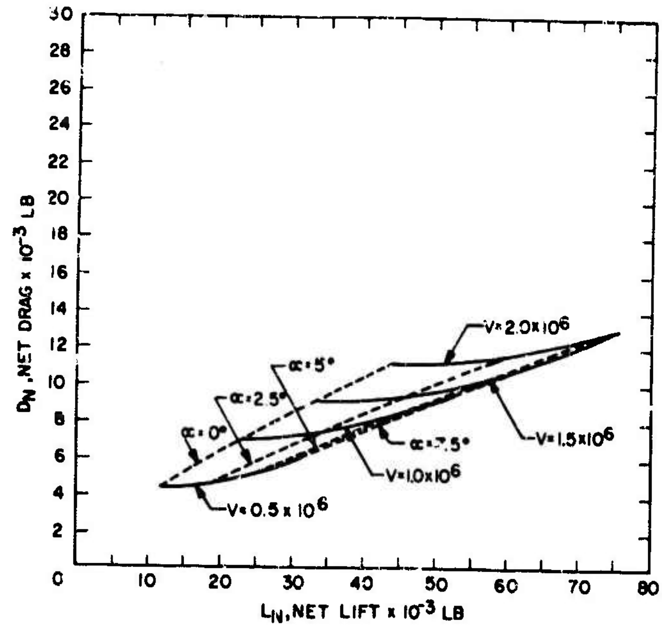

Figure 15. L_N vs D_N Class C Balloon at 20,000 ft Altitude, Winter I Wind

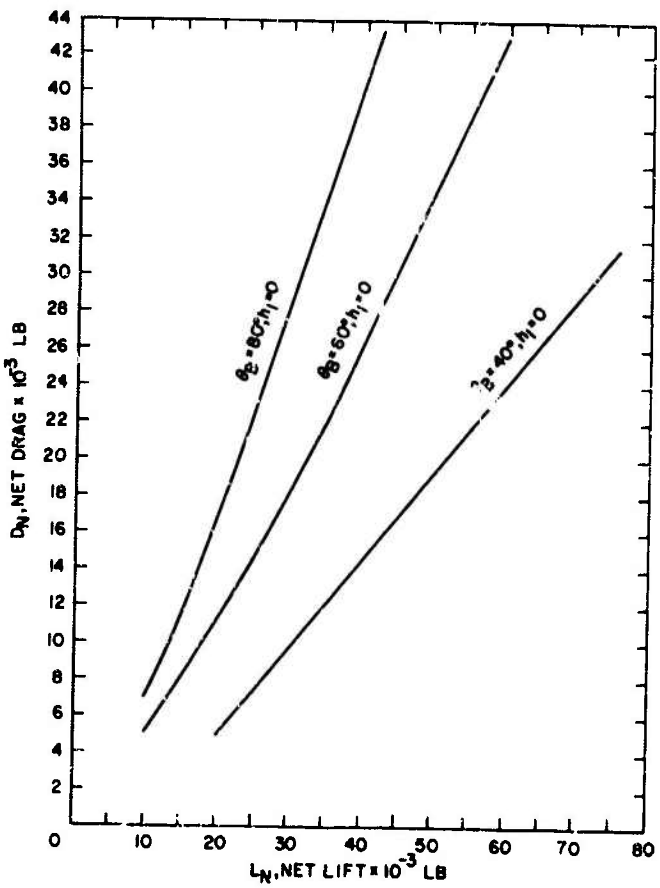

Figure 16. Cable Profile Plot for Base Cable Angle (θ_B) for Glastran Cable at 20,000 ft Altitude in Winter I Wind

Acknowledgments

Many figures included in this report are direct copies of those presented in the reference.

References

Menke, J.A. (1967) High-Altitude Tethered Balloon System Study, Task Report No. 1, Goodyear Aerospace Corporation, GER-13260, Contract F19628-67-C-0145.

VII. Balloon Operations on Operation Roller Coaster

H.G. Laursen
Sandia Corporation
Albuquerque, New Mexico

Abstract

Balloons having 7,000 lb of net lift were used to support a mobile array of ninety motor-driven samplers and 720 sticky cylinders and plates. The array covered an area of 1,800 ft wide by 1,500 ft high. A detailed discussion of the difficulties encountered is given.

Six out of eight attempts to fly the complex instrument arrays were successful.

1. INTRODUCTION

The design of the Roller Coaster experiment placed much emphasis on thorough measurements of the nature and distribution of particulate material in the cloud generated by each test event. Tethered balloons were used to support arrays of particle samplers for obtaining these measurements. The details of the balloons and arrays, as well as the operational problems encountered, will be discussed.

British balloons were used to support a number of single cable-supported instruments. I shall not discuss them due to the limited time.

Figure 1 and Table 1 give the details of the instrument curtains.

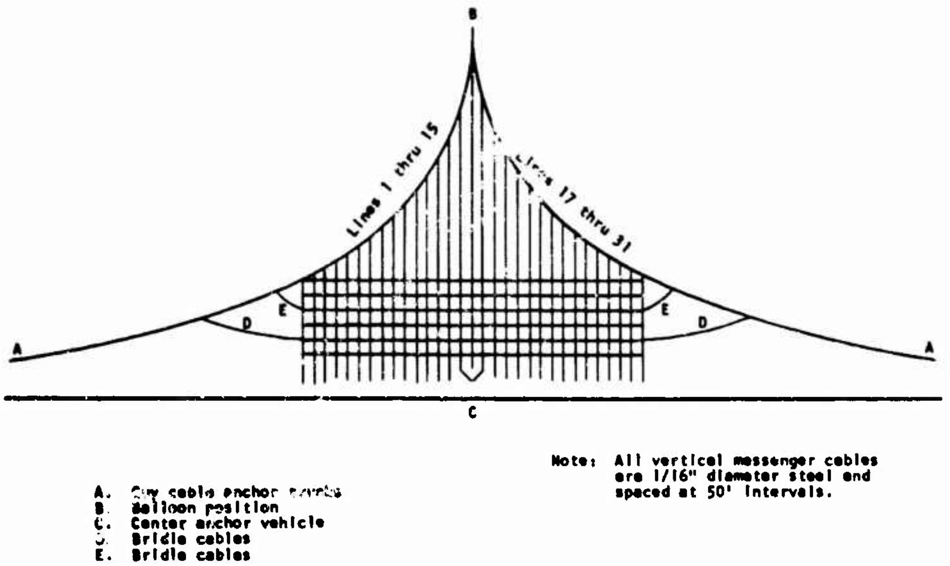

Figure 1. Balloon Curtain Array

Table 1. Description of Instrument Curtains

	Double Tracks Event	Clean Slate Event
Balloon altitude	1,775 ft	2,774 ft
Main cable		
Diameter	5/8 in	7/16 in
Breaking strength	41,600 lb	20,400 lb
Guy cable		
Diameter	5/16 in	3/16 in
Length	4,237 ft	6,600 ft
Breaking strength	10,540 lb	4,200 lb
Distance-semitrailer to each guy truck	3,750 ft	5,700 ft
Bridle cables		
Diameter	1/8 in	Not used
Breaking strength	2,000 lb	Not used

Note: For details of messenger cable sizes and dimensions, see Figure 3.

2. METHOD OF CALCULATING DIMENSIONS OF THE ARRAY

The lengths of the guy cables, the main cable, and the top sections of all the vertical wires were determined by the method of successive approximation. The approximate load on each vertical line was calculated first. Next, a value for the horizontal tension in the guy, H, and the distance from the guy truck to the first sampler string, X, were arbitrarily selected. These values, along with the height of the first sampler string, Y, and the weight per foot of the cable, W, defined the catenary up to the point of attachment of the vertical messenger for the first string of samplers. At the first vertical sampler messenger, the weight of that vertical string was added to the vertical component of the tension, V, already in the cable and the new parameters thus determined were used to calculate the next section of the guy cable. This was continued up each section of the cable until the balloon was reached. The values of V and the altitude were then examined to see if they were within the lifting capability of the balloon. If they were not, new values of H and X were selected and the process repeated.

Table 2. Balloon Description

Diameter	52 ft
Length	138 ft
Volume	Greater than 185,000 cu ft
Balloon weight	Approximately 2,700 lb
Coefficient of lift	Cl varied between 0.50 and 0.65
Coefficient of drag	CD = 0.24
Maximum net lift at 5,000 ft MSL	7,000 lb
Fineness ratio	3.0 to 1 (design)
Approximate cost	$40,000

The power required to operate the ballonet blower, fin blower, pressure relief valves and deflation valve was supplied by a 28 volt, 50 ampere-hour, Ni-Cad battery bank.

3. ELECTRICAL HARNESS CONSIDERATIONS

The criteria used in determining the wire size for furnishing power to the samplers were these:

1. The wire should be as light as possible.

2. The voltage at the end sampler of a string should be a minimum of 110 volts, and the first sampler should have a maximum of 125 volts.
3. The current in any wire should not be above the rated carrying capacity of the wire.

The wires were heavier than needed, since the actual current taken by each sampler was only 1.1 amperes instead of the 2.0 amperes quoted by the supplier. See Figure 2 for the wiring diagram.

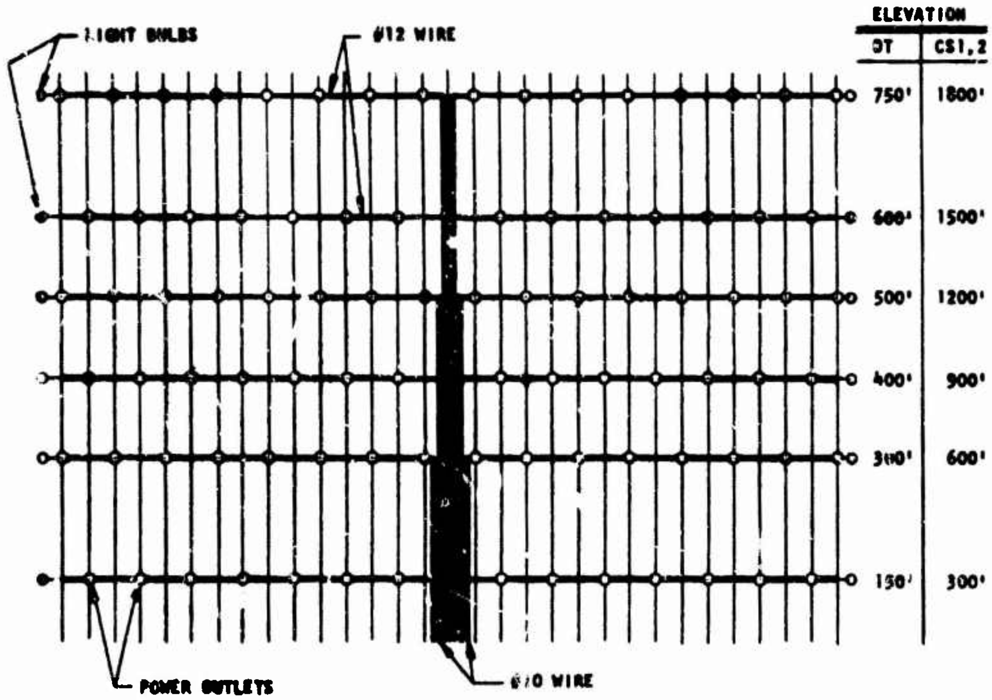

Figure 2. Balloon Curtain Wiring, Project 2.7, Roller Coaster

4. ARRAY MOBILITY

The mobility of the arrays was made possible by attaching the two guy and the main cable to vehicles. A $2\frac{1}{2}$ ton, 6 × 6 truck was used on the guy lines. Load cells were attached to the guy lines at each anchor truck so the tension in each guy line could be monitored at all times. The guy cable vehicles moved on a road at a radius of 4,200 ft from ground zero as the semitrailer holding the balloon moved on a road at a radius of 2,500 ft from ground zero. The semitrailer holding the

main balloon mooring cable had a 12-ton concrete block mounted on it, along with a 25- and a 35-kW gasoline generator. The auto-transformers used to adjust the voltage to each set of samplers were also mounted on the trailer, together with the load cell for reading the tension in the main mooring cable.

5. ARRAY ASSEMBLY

The following description of activity in putting up the array for DOUBLE TRACKS is typical of the steps followed on all test events.

The balloon was normally allowed to fly at an altitude of 1,000 to 1,700 ft during the day. As the winds dropped in the evening, a caterpillar tractor was hooked to the main cable and the balloon pulled down to within 50 ft of the main anchor vehicle so the Ni-Cad batteries that supply the blowers could be recharged and any necessary helium could be added. The two guy cables were also attached to the balloon at this time.

As soon as helium addition and battery charging had been completed, usually 1 to $1\frac{1}{2}$ hours, the balloon was allowed to rise at a speed of 20 to 30 ft per minute. Two men were assigned to each of the 30 vertical lines. They kept the line lifting smoothly and attached sticky cylinders at previously marked intervals of $37\frac{1}{2}$ ft (below the 750-ft horizontal cable) and hooked on and plugged in the motor-driven samplers at the 750, 600, 500, 400, 300, and 150-ft levels. As each of the six separate electrical circuits left the ground, voltage was applied to determine if power was being received at the light bulb at the end of each horizontal pair of wires. A schematic drawing of the sampler array is shown in Figure 3.

To permit the array to spread out on the ground and be lifted in an orderly fashion, the balloon trailer was moved forward toward the bottom of the array as the balloon was allowed to rise. Approximately 3 hours was required to complete array instrument placement and have the balloon at full altitude and ready to move. The array was then moved to 2,500 ft from ground zero. The main anchor tractor-trailer was then driven around the arc, with the guy anchor trucks keeping the guy tensions at 1,500 lb while they followed an arc road at 4,200 ft from ground zero. The main anchor trailer was then positioned so that its center was directly down wind from ground zero, the power turned on to all samplers, and the crew evacuated to the CP. Table 3 gives a summary of events.

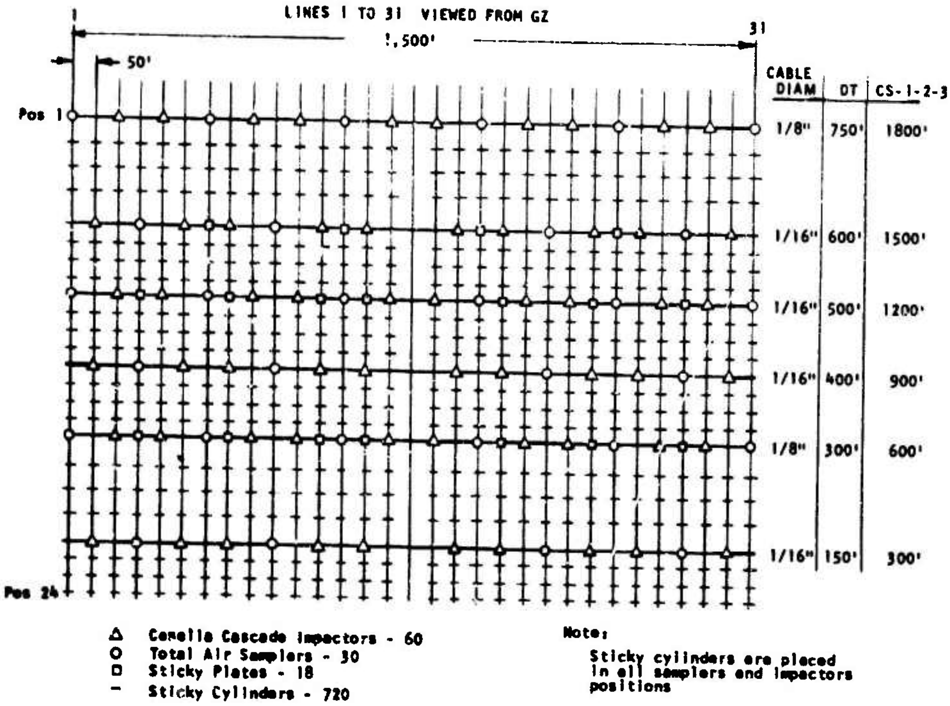

Figure 3. Schematic Representation of Sampler Array for First (close-in) Balloon Curtain

Table 3. Summary of Array Activities

Date	Activity	Difficulty	Results
10 April	Balloon inflation	High winds arose	Fins left uninflated
11 April	Fins patched-harness and fin lines adjusted	High winds arose	Balloon moved out to dry lake on 50 ft cable
12 April	Topping-off tube broke loose and fin torn up	Failure of 2000 lb nylon line and high winds	Balloon deflated and sent back to factory for repair
18 April	Balloon inflated and transported to site	High winds	Couldn't transfer cables and raise to 1000 ft. Balloon left at 50 ft
18 April	Generator refueling	Fire	Gasoline tank exploded and ruptured bottom fin
18 April	Transported to deflation area	High winds	Balloon struck rough ground and destroyed by the wind
24 April	Balloon inflated, raised to altitude and transported	High winds in mountain pass	Main cable broke. Balloon destroyed. Man and equipment thrown off of semitrailer
30 April	Balloon inflated, raised to altitude and transported to site	None	Stronger main cable used
2 May	Dry run of instrument array	Electrical wires shorted to main cable	Array modified so it was not tied to main cable
8 May	Balloon flying at 1700 ft on standby	Winds in excess of 50 knots	Balloon became unstable. Dived toward ground and tore apart
8 May	Balloon inflation	Explosive net line cutter failed	Balloon punctured in 6 to 8 places by rolling cutter. Balloon deflated and repaired
11 May	Repaired balloon inflated	Ballonet ruptured	Helium had to be added each time the array was erected
12 May	Dry run conducted	None	Everything worked satisfactorily for the first time
15 May	Double Tracks fired at 0255	None	All ninety motor-driven samplers ran and all sticky cylinders and plates recovered except for a few close to the ground

Table 3. Summary of Array Activities (Contd.)

Date	Activity	Difficulty	Results
15 May	Balloon deflated	None	Ballonet repaired
20 May	Balloon inflated	Ballonet ruptured again	Dilution of helium, again. On D-1, 40,000 cu ft of helium had to be added to balloon and fins to get the required 7,000 lb of net lift
21 May	Clean Slate No. 1 attempted	Winds not in right direction for firing	East guy broke while lowering the array
25 May	Clean Slate No. 1 fired at 0415	None	Instruments recovered and balloon deflated on Antelope Lake bed so ballonet and fins could be patched
30 May	Balloon inflation	None	Balloon which had been repaired at factory used
31 May	Clean Slate No. 2 fired at 0345	West guy line broke while raising the array	Lost 16 sticky cylinders and plates - 45 minutes for cable repairs. Array moved 4 miles to Clean Slate No. 3 and was recovered there
2 June	Balloon flying on standby at 1500 ft altitude	50 knot winds and leaking helium relief valve	Balloon destroyed
5 June	Smaller balloon inflated	None	Was to be used for a lighter, farther out array
7 June	Balloon flying on standby	30 to 40 knot winds and fouled ballonet relief valve	Extensive damage to balloon and equipment
7 June	Clean Slate No. 3 attempt	Favorable weather conditions did not develop	Balloon left flying on standby
8 June	Balloon flying on standby	Helium relief valve limit switch failed and winds	Last balloon destroyed

6. SUMMARY OF HAZARDS AND FAILURES

6.1 Personnel Hazards

Five accidents exposed people to injury during the balloon operations. Fortunately, only minor injuries resulted.

1. A man was thrown from a semitrailer by lines attached to a balloon which broke its mooring cable while being transported in high winds.
2. A man was lifted approximately 5 ft into the air when a loop of cable formed a knot around his hand during the erection of a large cloud sampling array.
3. A guy cable broke and struck a man with sufficient force to dent his hard hat.
4. A guy cable broke and caused a partially erected instrument curtain to shift horizontally along the ground. One man was thrown to the ground and dragged several feet by elements of the curtain that wrapped around his legs.
5. A 50-ft-long, 7/16 diameter leader twisted upon itself when tension was released, and a man had two fingers caught in the twisted cable. His gloves protected the fingers from being more than severely bruised.

6.2 Hardware Failures

1. Mooring cable failed in high winds.
2. Guy cables failed twice.
3. Inflation check valve came unscrewed and fell out of balloon filler tubes twice.
4. Batteries discharged before recharging could be accomplished.
5. An explosive cutter failed to free the inflation net during two inflations.
6. Electric powered valves failed to operate properly. Twice, electromechanical hardware failed, and foreign material was caught in the valve once.
7. Mooring lines for securing the topping-off tube failed.

The guy lines were a constant problem. They were hazardous to traffic, personnel, and instruments in the area, and were damaged by the traffic much too frequently. Because of the large area traversed by the guy lines, it was not practical to barricade the area.

7. SUMMARY OF RESULTS

Out of eight attempts to fly large balloons supporting complex instrument arrays, six were successful and two failed. Five balloons were destroyed and two damaged in these attempts.

VIII. The Use of a Tethered 15,000 Pound Gross Lift Natural Shaped Balloon for Remote Logging Operations

Russell A. Pohl
Raven Industries, Inc.
Sioux Falls, South Dakota

Abstract

The logging industry is plagued with the problem of economic recovery of timber in remote sites. These sites, of low or loss economics, are for the most part, canyons, ravines, and hilly terrain in which road construction costs range from \$15,000 to \$75,000 per mile. Logistic costs of this magnitude prohibit logging of such areas on an economical basis. In addition to the costs involved in road construction, the damage incurred to the terrain by the roads results in erosion and stream-river pollution.

Numerous studies resulted in the technical and economic feasibility of the use of a tethered balloon to transport logs in low or loss economic sites. Based on these studies and other engineering evaluations, a natural shaped balloon was designed, fabricated, and tested. A full scale field test, using a tethered balloon with a payload capacity of 12,000 lb, is presently in operation at a logging site in Oregon.

The basic technique involves the use of a tethered balloon as an above terrain technique for cut-to-landing site log transport. The balloon is tethered on a cabling arrangement which provides a "track" and power for transportation of logs from the cutting site to a landing site. The cable is a continuous loop design with a dual tree-stump anchor point usually located near the top of the hill and the power source at the landing site. Since the cable is continuous, and the balloon is coupled to the cable at a fixed point, the balloon can be shuttled back and forth between the cut and landing site where the yarder is located. A vertical cable attached to the balloon bottom end-fitting is used as the load train for the logs.

The system presently in use utilizes a 250,000 cu ft natural shaped balloon. This balloon has a diameter of 82 ft. A two side elastomer coating on a Dacron base fabric was used in the fabrication. With a balloon weight of 3,000 lb and a gross lift of approximately 15,000 lb, logs can be transported from cut-to-landing site with a net weight of 10,000 to 12,000 lb. Lighter logs are bundled together to obtain a net payload in the 5,000 to 7,000-lb range. The balloon is parked on the tether or bedded down on the ground during the night.

Full scale operations to date have demonstrated that the system can transport some 20 to 25 tons of logs per hour over cut-to-land site distances of 2,000 to 3,000 ft. Using an average of 20 tons, which is approximately equivalent to 4,000 board feet, a tethered balloon system has been demonstrated to be within the required economics of the logging industry.

1. INTRODUCTION

Standard methods of logging have resulted in the by-passing of millions of acres of timberland on the northwestern coast of the North American Continent. Present day procedures used to harvest timber are not usable in such areas as steep slopes, ravines, medium stand timber density, and terrain conditions in which the road costs are high. In addition, the building of roads in certain soils results in terrain damage, causing surface erosion and in turn producing stream-river pollution. Dragging heavy logs over the ground also contributes to this problem.

Both economics and conservation dictate the use of a timber harvesting technique which is economical, portable, and air-borne. A tethered balloon operating on a closed cable loop appears to meet the basic requirements of economics, portability, and above terrain transport of logs from the cut-to-landing site.

A natural shaped balloon with a net lift of 12,000 lb is presently in operation at a remote site in Oregon. This field test was initiated in May of 1967 and several hundred hours of logging operations under various conditions of weather and cable rigging have been evaluated. Results to date of this test site operation indicate that the use of tethered balloons to harvest logs can produce an economical timber yield in difficult access sites where road installations are both high in cost and detrimental to conservation of natural resources. The use of a tethered balloon to harvest timber has opened areas previously inaccessible or in a low-or-loss economic status with the use of presently employed logging methods. The required road construction has been reduced drastically and timber breakage has been minimized. Since the soil in the balloon logging areas is not altered by roads and the dragging of logs, the detrimental effects induced by loose soil contamination of the streams and rivers are eliminated. Balloon logging also permits practically any terrain, within limits, to be harvested regardless of the haul-in-direction; thus the cut-to-land transit can be made uphill, downhill, or crosshill. While yarding distances presently average

2,000 to 3,000 ft, the extension of these distances is both technically and economically feasible.

The use of a balloon logging system can open steep slope and inaccessible regions in the Pacific Northwest to economic logging and increase the total yield in this area by an amount in excess of a half billion board feet. It is believed that these steep-slope timber areas can yield additional stumpage worth over $5 million per year. The savings in road construction costs is estimated to be in excess of $300 million per year.

2. SYSTEM OPERATION

Balloon yarding involves the use of the balloon, tether coupled to a closed-loop power driven cable arrangement. A layout of the system is shown in Figure 1. With the balloon positioned overhead in the log cutting operation site, a choker is set on the log. Upon radio command, the yarder operator slackens the haul-back cable, thereby allowing the static lift of the balloon to elevate the log clear of the prevailing terrain (Figure 2). With the log airborne, the yarder operator winches in the main cable while playing out the haul-back cable. Thus, the log is transported

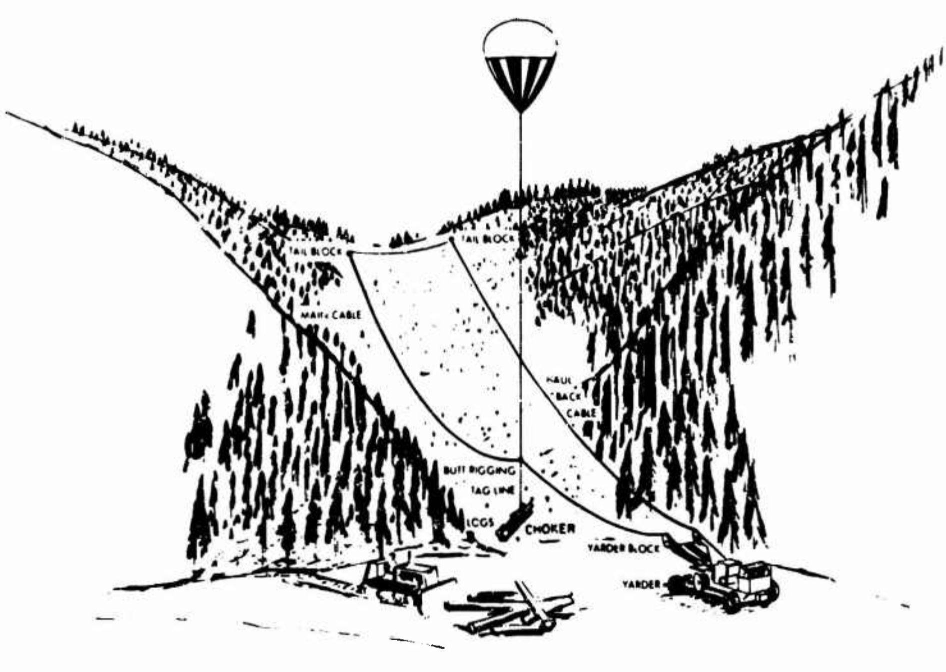

Figure 1. Balloon Yarding System Layout

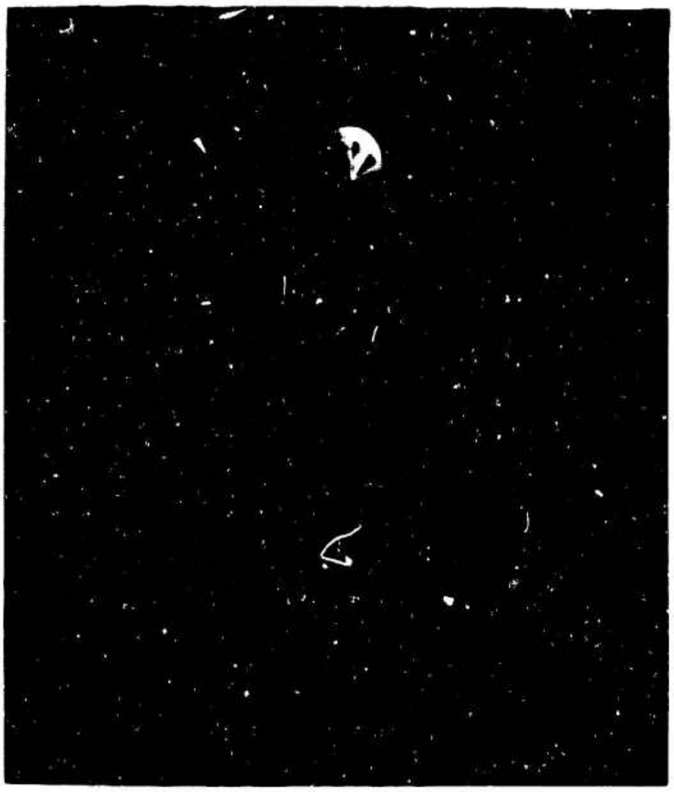

Figure 2. Balloon with Load of Logs

to the landing area (Figure 3) where a chaser unhooks the choker from the log and a landing shovel decks the log. Once the chaser unhooks the choker, the yarder back tracks the balloon travel by reversing the yarder winches and the balloon is repositioned over the log cutting area where a new transport cycle or "turn" is initiated.

The balloon is usually flown at an altitude of 500 ft above the butt rigging. This suspension consists of two 40,000-lb tensile strength cables. The log suspension or "tag line" is about 200 ft in length.

Since the lift vehicle used in this operation is a natural shaped balloon inflated with helium, log transport is primarily a function of both the static lift provided by the balloon and the horizontal force induced through the main and haul-back cables by the yarder. The operations may also be influenced by inertia forces under some conditions. With a net lift of 12,000 lb, the balloon has a single log-load capacity of 10,000 to 12,000 lb. When small logs are transported, the load will usually range between 5,000 and 7,000 lb since the chokers are difficult to couple when used in multiple pickups. An average of 20 to 25 tons of logs per hour can be transported over cut-to-landing site distances of 2,000 to 3,000 ft. Using a mean of 200 board ft per ton, the system can transport 4,000 to 5,000 board ft per hour under average weather and working conditions.

All operational limitations have not been determined on the test vehicle. However, the system has been used in ambient wind conditions of 25 mph. A mean lay-over angle of about 20° from the vertical was observed during these wind conditions.

Upon completion of a day's yarding, the balloon is left in an airborne tethered condition if the weather conditions are not extreme. In bad weather, the balloon is

Figure 3. Balloon in Log Landing Area

winched to the ground and restrained by the load line and the tie-down lines as shown in Figures 4 and 5. The maximum winds encountered during bed-down have been 50 to 60 mph. In both flight and bedding wind conditions of 25 and 50 to 60 mph respectively, no damage was incurred to the balloon. Since normal logging operations are usually suspended when wind conditions reach 30 mph, the balloon logging system appears to compete with presently used yarding equipment.

3. BALLOON DESIGN

3.1 Design Shape

The natural shaped balloon design, as shown in Figure 6, was selected on the basis of reliability, design, fabrication simplicity, costs, ease of field operation and independence from aerodynamic lift force generation. This configuration has a good volume to surface area ratio and tends to retain its shape when only partially inflated. The inherent capacity of the shape to absorb the suspended load and payload induced transient shock loads transmitted through the tether cable was another reason for selecting this shape. Since the shape is a body of revolution about the vertical axis, shock loads are distributed, in general, evenly throughout the balloon fabric. Further, the loading is, for the most part, meridional and the envelope design can be accomplished on a more predictable basis for a given set of gross load and shock load and/or aerodynamic forces. The omni-directional aerodynamic drag characteristic of this shape provides a 360° ambient wind envelope capability which is of prime importance in long duration operations. In general, a natural shape balloon, due to its design and fabrication simplicity, will cost less than half that of an aerodynamic shape when compared in the heavy payload capacity range.

Figure 4. Bedding Operation

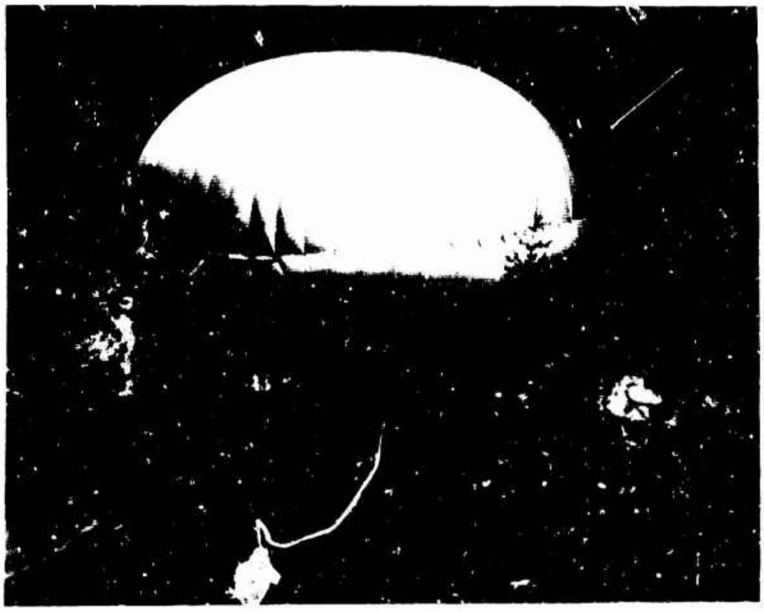

Figure 5. Balloon Fully Bedded Down

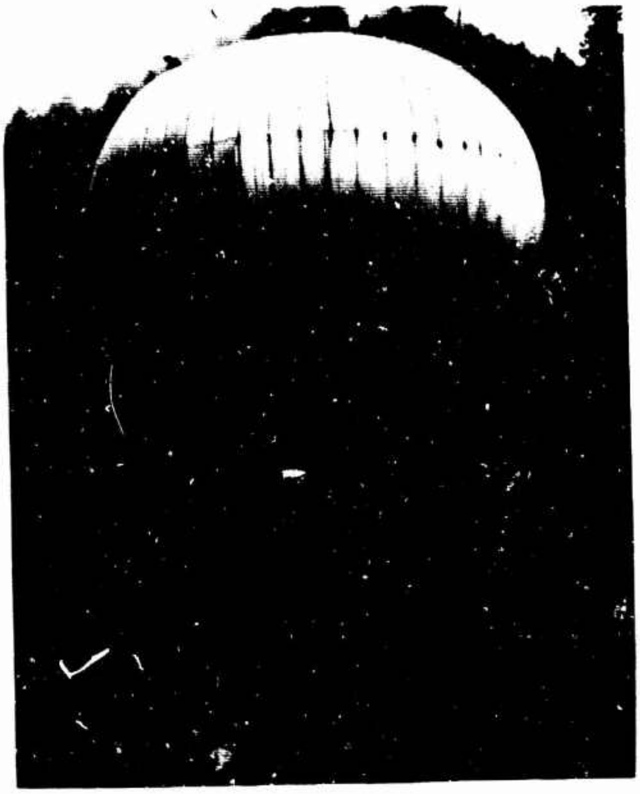

Figure 6. Natural Shaped Balloon

The balloon envelope design was based on the design parameters as listed in Table 1.

Table 1. Natural Shape Balloon Design Parameters

Volume	250,000 cu ft
Shape factor (Σ)	.00
Gore length $\left(S_{\lambda}\right)$	125.7 ft
Diameter (max)	82.0 ft
Height (inflated)	87.0 ft
Surface area	19,600 sq ft
Cone angle	100°

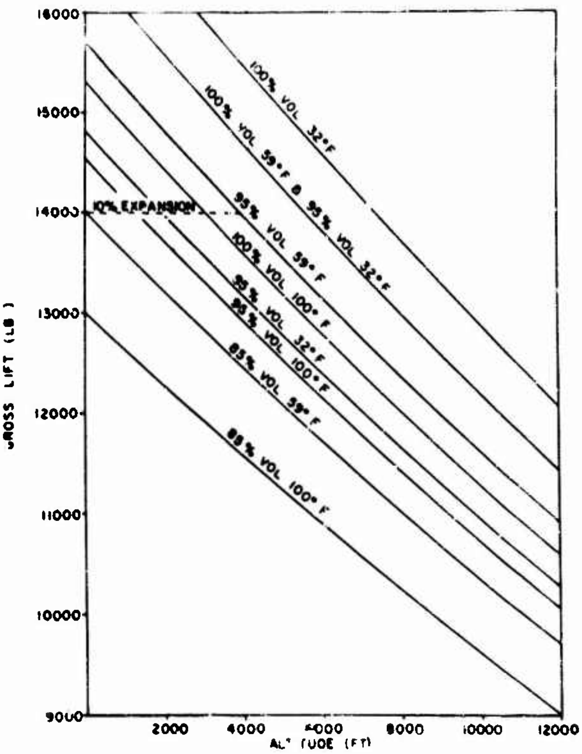

Figure 7. Lift Characteristics of a 250,000 ft^3 Natural Shaped Balloon

The gross lift characteristics of the design at various altitudes, ambient temperatures, and percentages of full inflation are shown in Figure 7.

The following ground rules and assumptions were used to provide a basis for the balloon maximum volumetric expansion.

1. Maximum field operating conditions will not exceed yarder plus tethered flight altitudes of 12,500 ft MSL. With this altitude limit the yarder area can be located at 10,000 ft MSL, tail block at 1,500 ft above yarder and balloon altitude 1,000 ft above tail block.
2. The average internal temperature (superheat) of the balloon will not exceed 20°F above ambient.

A balloon logging operation can be either uphill or downhill from a maximum yarding area elevation of 10,000 ft MSL and the balloon height may vary as follows:

$$T_o = h_y \pm h_p + h_b$$

where

T_o = Altitude variation
h_y = Yarder area elevation = 10,000 ft
h_p = Pickup area elevation (tail block) = ± 1,500 ft
h_b = Balloon altitude = 1,000 ft.

Then

$$T_o = 10,000 \pm 1,500 + 1,000 = 9,500 \text{ to } 12,500 \text{ ft}.$$

Hence the balloon altitude may vary 3,000 ft during the course of a particular logging operation with the yarder remaining at one particular site. At sea level the

volumetric allowance required is 9.3 percent, and it is 10 percent at 10,000 ft MSL. Coupling this volumetric allowance with 20°F maximum superheat which will induce a 4.25 percent volume change, the total volumetric change can be approximately 15 percent.

Volumetric expansion and contraction occurs primarily in the lower portion of the balloon below the 45-ft gore station. A skirt attached at the 45-ft gore station provides a tangent harness configuration to the balloon design. The lower portion of the skirt consists of an open mesh screening and is backed up by a truncated cone made of fabric which is attached only at the upper cone ring. The fabric cone acts as a ram air scoop, thereby reducing skirt flutter. A gore length of 48 ft was used on the skirt design; thus the skirt extends about 5 ft below the theoretical balloon nadir.

3.2 Construction

The envelope was constructed of 64 half gores tailored to provide a 250,000 cu ft volume when fully inflated to an Σ = .00 shape. A Dacron base fabric, elastomer coated on both sides, designed to meet the anticipated maximum envelope stress level, plus a 6.0 safety factor, was utilized as a single membrane envelope material. The total weight of the fabric is about 10.5 oz/yd^2. This fabric has a nominal tensile strength of 230 × 200 lb/in in the warp and fill directions.

The gores were adhesive bonded to form a gastight structurally strong joint. The curve gores were stitched together during the fabrication process to facilitate handling during in-process adhesive bonding.

Load transfer from the bottom end fitting into the balloon envelope is accomplished by steel cables. The cables are then coupled to 64 ea. 2,500-lb tensile, nylon webs which extend to the top cap of the balloon. A two-to-one coupling interface is used at the cable to webbing transfer point (that is, two webs attached to each cable). The top end fitting is a 4-ft diam endless loop steel cable which collects the upper ends of all the load webs. The area within the ring is enclosed with a floating fabric cap. Upon completion, the balloon had a weight of 3,000 lb including hardware and the bottom skirt.

4. KINEMATIC PARAMETERS

The tether dynamics of a logging balloon differ from the conventional tethered balloon, inasmuch as the payload is suspended at various positions on the tether line (main cable) instead of at or near the tether cable-balloon interface. The system loading was examined in accordance with the force diagram as shown in Figure 8.

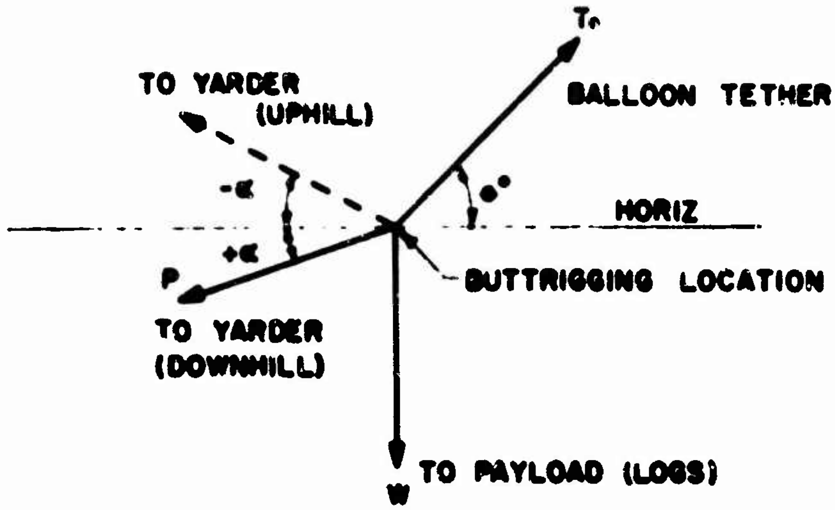

Figure 8. Force Diagram for Tethered Balloon Logging System

This analysis considers the balloon static, wind loading dynamic forces, and yarder loads. From the diagram:

$$P = T_o \frac{\cos \theta}{\cos \alpha}$$

and

$$W = T_o \frac{\sin (\theta - \alpha)}{\cos \alpha}$$

where

P = Load at butt rigging caused by balloon lift
W = Available load at choker suspension point.

The analysis was based on a balloon volume of 250,000 cu ft (Σ = .00) and an altitude of 500 ft MSL with the yarder at sea level, the tether line being a straight line couple (no catenary) and the velocity boundaries being a composite of the wind loading on the balloon and winching speed. A wetted area drag coefficient for the balloon was derived and established as C_D (n.s.) = 0.085 which is an approximate equivalent to a projected area drag coefficient of C_D = 0.34. The projected area drag coefficient for the natural shaped balloon is based on a theoretical analysis which assumes a mean value of the generated drag for sphere of like volume and a cylinder that would just contain the sphere.

$$\text{Drag}_{ns} = \frac{\text{Drag}_{sp} + \text{Drag}_{cyl}}{2}.$$

The dynamic drag evaluation considered a Reynolds number range of $10^6 < Re < 30 \times 10^6$. The results of the theoretical kinematics evaluation are shown in Figure 9. Considering a typical case in which the logging operation is being conducted on a 45° downhill slope in a 10 mph wind (wind direction from yarder toward balloon) and a winch speed of 10 mph, one observes that the log payload capacity is 9,500 lb and the winch load is 2,400 lb.

Experience in the field indicates that the theoretical analysis compares favorably with the field conditions when the additional forces involved are considered.

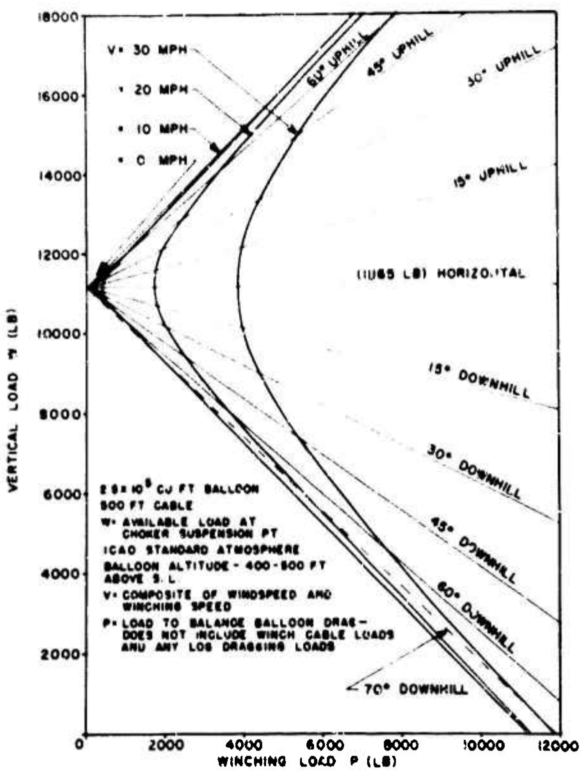

Figure 9. Kinematic Parameters for Logging Operations

5. SUMMARY

The use of a heavy load natural shaped balloon for remote area logging has been demonstrated to be feasible and practical. A static lift aerostat does perform log transit functions on a trajectory that is independent of aerodynamic lift on the balloon. The transit trajectory does not induce damage to the timber payload since the logs are not subject to dragging at the pickup site. Further, the natural shape with its inherent uniform side view projected area extends the operational limits of the system since aerodynamic lift is not required nor desired at lift-off or cut-to-landing site transport. The loading on the balloon is predictable enough to permit the design specification to be within the operational envelope.

Preliminary evaluation indicates that the timber transport costs from the cut-to-land site will be approximately \$6 to \$10 per 1,000 board ft. These transport costs are for operations in remote rough terrain areas and are not related to relatively flat area operations where conventional timber harvest equipment can be used effectively.

IX. Tethered Hot Air Balloons

James Winker
Raven Industries, Inc.
Sioux Falls, South Dakota

Abstract

In spite of the many advantages of conventional captive balloons which make them useful vehicles, there are a few drawbacks which do limit their application, particularly in short term operations. These include cost of the lifting gas, time and care required for inflation, and the problem of protecting the inflated balloon between uses. The hot air tethered balloon goes far toward solving these problems and it makes practical some applications for which tethered balloons might not otherwise be considered. Presented here are some of the factors which should be considered in a hot air tethered operation and some of the programs which have utilized hot air balloons.

1. INTRODUCTION

Much work has been done in the past few years to expand and develop the capabilities and uses of tethered balloons. Most of this effort has gone into helium balloons, and rightfully so, since this is the buoyancy medium suitable to the widest variety of captive balloon uses. There are, however, a growing number of applications for tethered balloons where the use of helium (or other light gases) entails

procurement or handling problems which relegate those applications to impracticality. This leaves a convenient niche for a balloon which can obtain its buoyancy from the surrounding atmosphere. The hot air tethered balloon is hardly a universal tool, but where convenience and low operating cost are important, it offers some very distinct advantages.

2. SYSTEM DESCRIPTION

2.1 Design

Just as with helium balloons, the hot air tethered balloon may come in a number of shapes. Presently the only operating systems are natural shaped balloons, simply because this tool has been adapted from a standard free-flight vehicle design. Three sizes of such balloons are in general use; 40, 50, and 60 ft in diameter.

The balloons are constructed of a nylon fabric which has excellent resistance to the combustion product within the balloon. This is a noncoated material which is woven tightly enough to limit gas leakage to about 1 cfm/sq ft at the normal pressure differentials. This leakage is less than the volume of the exhaust products generated during normal operation. The balloon is built to conform with certification requirements prepared by the FAA which include safety factors up to 5 for the structural elements.

The balloon material has proved to be remarkably durable. Users report operating a balloon for over 100 flights totaling several hundred hours of flying time. The limitation in envelope life is as much determined by normal wear and tear as it is on basic degradation of the material. Somewhat arbitrarily we have established a life limit at the point where fabric strength has diminished to 50 percent of the original tensile and tear values. This still exceeds the safety factor requirements for the relevant parts of the structure.

A general view of the gondola and lower part of the envelope for an S-50 balloon system is shown in Figure 1. The gondola provides space for fuel tanks, flight instruments, a pilot and passenger, and experimental equipment if required. It also provides a mounting for the propane burner which supplies the necessary heat for buoyancy. The burner has a peak output of 2.4 million Btu/hr which in thermal energy is equivalent to over 900 hp. The larger balloons are generally "twin engined" to provide a wide clearance area around the flame. The gondola is suspended from the envelope by steel cables and the entire harness assembly is surrounded by a fabric skirt. The skirt protects the flame from winds which could deflect the heat and cause damage to the envelope. Vents at the top of the skirt allow the exhaust products to bleed out at that level rather than filling the entire skirt and possibly choking the flame.

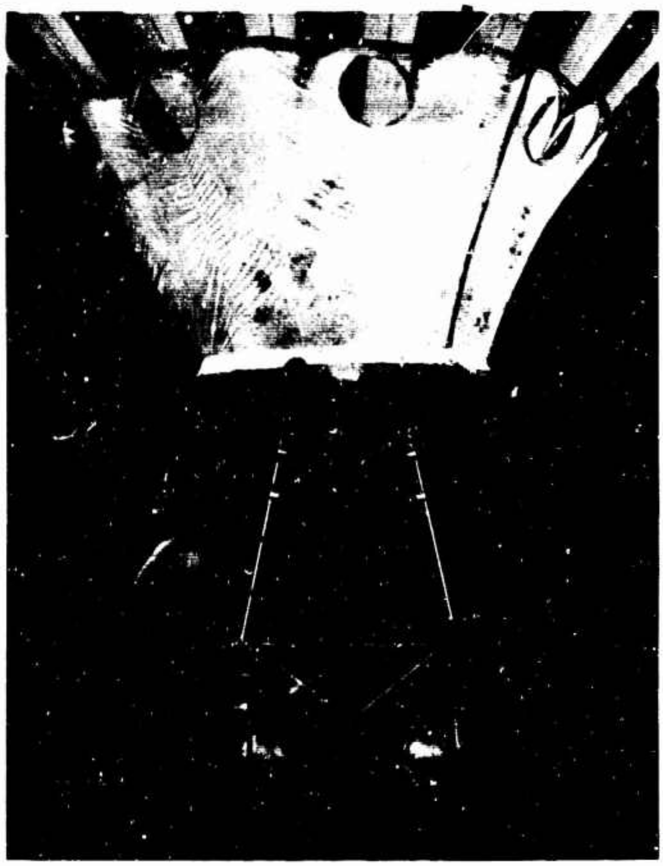

Figure 1. Typical S-50 Configuration

Buoyancy is controlled by adjusting fuel flow through a dual path. The normal buoyancy level is set by metering the flow through a needle valve. If a rapid increase in buoyancy is required, a toggle valve is operated which instantly provides maximum fuel flow. Deflation of the balloon envelope is facilitated by a large, replaceable deflation port built into the top of the balloon. When the gondola is on the ground and the flame turned off, this port is peeled open by pulling on a strap which extends down into the gondola.

For some applications, it may be a detriment instead of an advantage to carry personnel aboard the balloon during test work. A simple, unmanned gondola is available (Figure 2) which can be automatically and/or remotely operated. In this system the needle valve is again used to provide a sustaining level of heat input and is set for approximately neutral buoyancy. The burner is then modulated between this sustaining level and full output by a solenoid valve which is controlled by a thermostat located in the top of the balloon. Override of the automatic control, and fuel shutoff can be accomplished by radio command or wire link.

The balloon may be tethered at various points on the gondola or even on the envelope itself. The most practical points for tethering seem to be at about waist level or at the burner bar on manned balloons and at the base for unmanned gondolas.

2.2 Performance

The buoyancy of hot air is dependent upon ambient temperature and differential temperature between the inside and outside of the balloon. It is, of course, variable

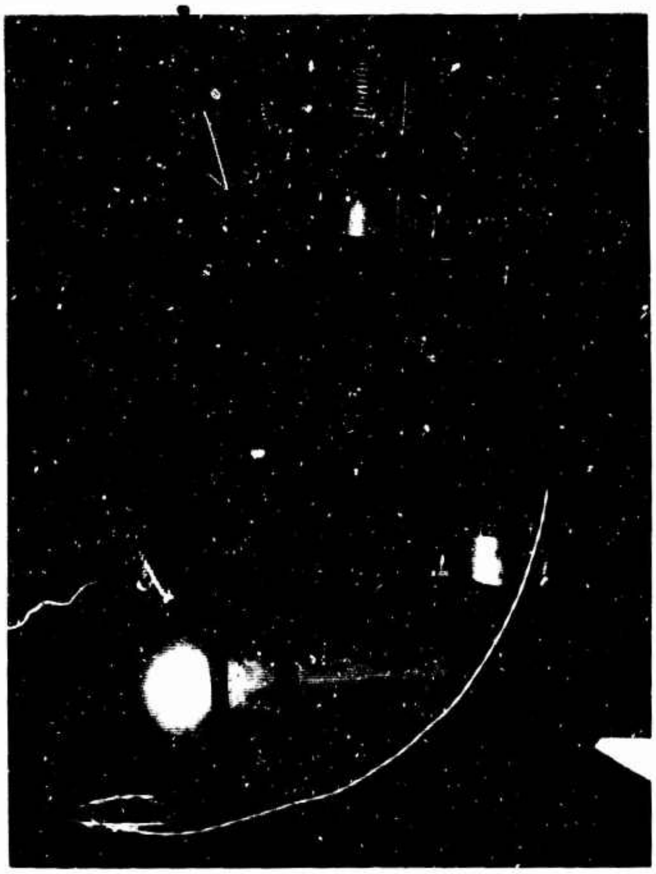

Figure 2. Unmanned Gondola

and in the normal operating range has between 25 and 35 percent of the lift of helium. This requires an envelope dimension of about 50 percent greater than a helium envelope for the same lift.

Figure 3 shows the specific lift of hot air for a range of internal temperatures at sea level standard conditions. Balloon internal temperature is limited to 250°F for sustained operation. A temperature of 300°F is permissible for short term operation and will not unduly shorten the life of the envelope. It is evident that the maximum obtainable lift factor will be less on warm days and greater on cold days because of the variation in allowable temperature differential.

Figure 4 shows the lifting capacity for the three standard balloon sizes at sea level conditions and for a range of ambient temperatures. The "dry weight" shown on the chart is meant to show typical values rather than a definite fixed weight, because there are many options for gondola configuration and fuel tankage which affect this number.

On a standard day (59°F) it may be noted that the S-50 has a gross lift of about 1300 lb. The balloon and fuel might weigh 550 lb, and allowing 250 lb for free lift, a useful payload allowance of 500 lb remains. Comparable numbers for the S-40 and S-60 are about 250 lb and 1100 lb, respectively.

The hot air tethered balloons now in operation all have open base, zero pressure envelopes. This type of balloon has an operating wind limit which is in some degree proportional to the specific lift of the hot air. At some wind velocity the dynamic pressure against the surface of the envelope will overcome the internal pressure produced by buoyancy and cause dimpling in the envelope contour. While this is not truly the limiting condition for tethered operation, it does define a point

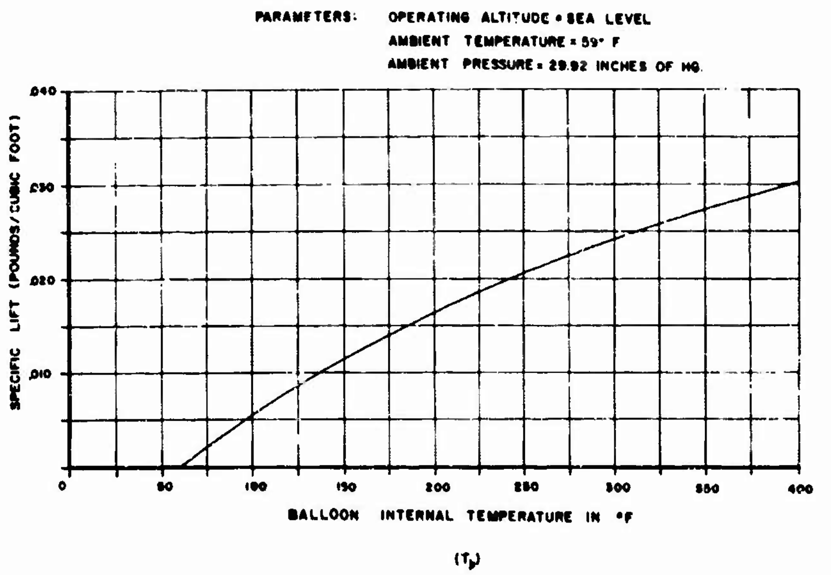

Figure 3. Specific Lift vs Balloon Internal Temperature

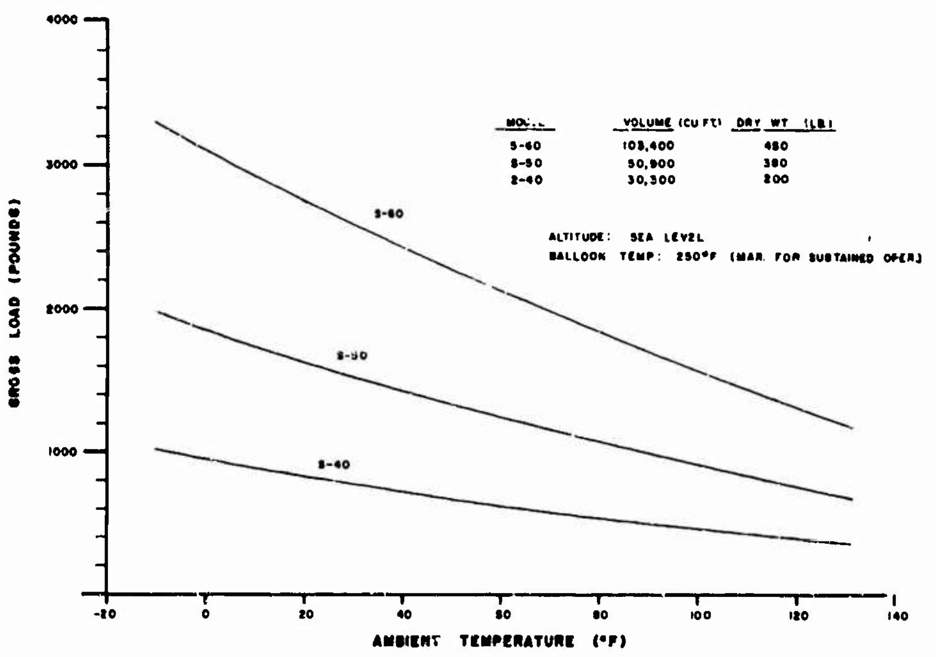

Figure 4. Maximum Authorized Operating Limits for S-40, S-50, S-60

above which instability can occur. Experience indicates that the balance of internal and external pressures at about the 25 percent Gore station determines whether or not the balloon envelope will dimple. Figure 5 compares the internal pressure at this point over a range of temperature differentials against the external dynamic pressure over a range of wind velocities. This shows that under peak temperature conditions, the wind limit to avoid dimpling is about 12 knots.

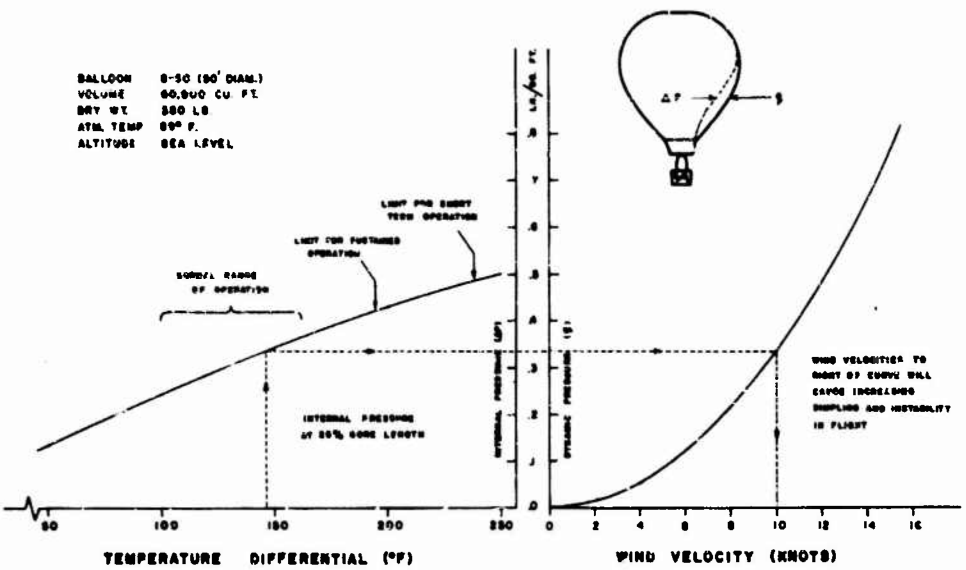

Figure 5. Envelope Dimpling Limits

Flight above the dimpling limit is entirely possible and with an experienced crew may be considered almost routine. The distortion caused by dimpling actually develops a crude airfoil shape in the envelope which adds to the lift of the system. The balloon may be flown in this manner in winds of approximately 18 to 20 knots, though at the upper limit the aerodynamic lift starts to become erratic. Figure 6 is a sketch showing the typical configuration of unpressurized balloons in high winds.

An alternate configuration for high wind operation would be a pressurized natural-shape envelope which is kept full by a blower-burner combination. Some work along this line is now in process. A higher degree of sophistication is also possible in the form of a pressurized aerodynamically shaped envelope. This is entirely feasible and can be developed whenever a customer presents the requirement.

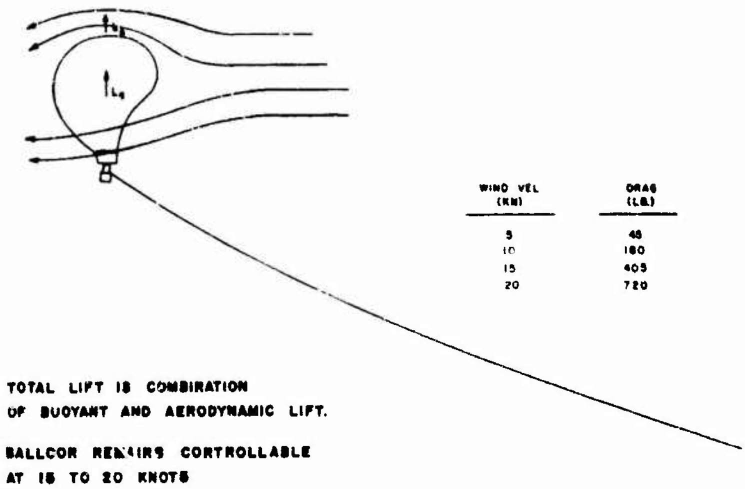

Figure 6. Action of Unpressurized Balloon in High Wind

3. APPLICATIONS

3.1 General Considerations

The relative merits of light gases and hot air determine which lifting medium is most appropriate for a given application. Light gases, such as hydrogen and helium, must be used for high altitude flight and may be preferable where long, continuous use is intended. Helium will usually have an advantage where high winds must be contended with, and for short term, high frequency uses in situations where a balloon can be stored indoors between uses. Hot air has its greatest advantage for low level operation, where per flight cost is critical, and where convenience of inflation and launching is important. Also, a major advantage is realized when the weight or logistics problems of handling compressed gas tankage limits the use of helium.

It would be very difficult to draw up a list of criteria for comparison between the two lifting media which would unequivocally show which one is more appropriate. A hypothetical case shows some of the factors which must be considered. Assume that it is necessary to lift a 400-lb payload less than 1,000 ft above sea level and have it in this position at frequent but unscheduled intervals over a period of many weeks. Further, the area is somewhat remote and not served by railroad or surfaced highways.

A helium balloon for this job might have a volume of 10,000 cu ft and a purchase price of about $6,000. The hot air balloon should have a volume of about 60,000 cu ft and it too would cost about $6,000. Operating costs for the hot air balloon will be

about \$2.00/hr for fuel used while actually in flight. Cost to fill the helium balloon would be \$500 to \$800, depending on the source and shipping distance for the gas. The weight for the balloon, payload and gas tankage would be about 5,000 lb for the helium system and 800 lb for the hot air balloon plus 10 lb of fuel per hour of operation.

To be economically competitive at all, the helium balloon would have to be kept inflated throughout the operation and would have to be capable of surviving any wind which might occur. The hot air balloon can be unpacked, inflated, perform its mission and be repacked and stored until the next use in little more time than it takes actually to perform the experiment. Adverse winds can be avoided, and yet within the wind limitation for the balloon, it is available to perform its service almost at a moment's notice. It is practical to erect it for usage times as short as just a few minutes, and with on-board fuel the balloon can remain in operation for as long as 4 to 6 hours. Greater durations can be attained if necessary by piping fuel from the ground to the balloon.

Inflation requires no elaborate preparations and can be done on open ground in winds up to about 10 knots. The time elapsed from roll out of the envelope to flight-ready status is as little as 5 to 10 min. Deflation and packing up require about the same time.

As can be readily seen, the characteristics of the two classes of lifting media are not directly comparable. Each application for which hot air might be considered must be evaluated individually to determine if hot air is indeed the preferred lifting gas.

3.2 Observation Platforms

Some of the first uses for tethered hot air balloons were simply as carriers for a human observer who needed the convenience of a high vantage point. Figure 7 shows a relatively simple application which in itself has no vital importance but offers evidence of the convenience of operation of the hot air balloon. The large balloon in the foreground is a heavy lift vehicle with a lifting capacity of 15,000 lb. In the first test inflation, a situation developed which made it important to observe visually the region around the top fitting of the balloon. On a spur of the moment basis, the hot air balloon was erected, the observation made, and the balloon returned to the ground all within an hour.

One user has purchased a balloon for a biological study program. His intent is to tether the balloon to a boat and drift offside over a herd of whales. The observer manning the balloon can then easily watch and study the life habits of these large mammals without intruding upon them in their natural environment. The United States Bureau of Fisheries has done some similar experimentation to see if schools of tuna fish can be detected from such a balloon. If this technique proves to be useful, it might very well be used commercially by tuna fishing fleets.

Figure 7. Hot Air Balloon as an Observation Platform

An S-40 balloon was purchased by Philippe Cousteau for use in conjunction with the research vessel Calypso. The research crew of the ship is involved in both underwater and surface observations and the balloon will provide assistance in a number of ways. It again will be used to observe marine life in the immediate region below the surface of the ocean. It will also be used in studies of the interaction between the sea and the atmosphere. In underwater work, it is typical for scuba divers to surface a considerable distance from the ship at the completion of their duties. Locating and recovering them is often a protracted exercise and it is expected that a spotter riding the balloon can speed this operation and cut the waiting time for the divers.

3.3 Drop Vehicles

Tethered hot air balloons have been used as platforms from which to drop test bodies. The Kaman Aircraft Corporation of Bloomington, Connecticut has used an unmanned balloon to lift and drop their Rotochute, which is a rigid-body aerodynamic decelerator. The balloon was anchored by a tripod tether arrangement and the test device was supported at the apex of the tripod. The assembly was lifted to about 3,000 ft where the body was dropped.

The Equipment Development Center of the Forestry Department has purchased a balloon for a variety of uses, one of which is to serve as a jump platform for training parachute jumpers.

3.4 Test Platforms

Two military organizations have made extensive use of tethered balloons as test platforms. The Naval Weapons Center at China Lake, California has three balloons which they use for photographic and instrumentation platforms. These are used for testing small ordnance devices or complex electronics systems. These tests must be run in a near simulation of operational conditions which means that they must not be in the proximity of a large carrier vehicle such as an aircraft. At the same time, personal attention is required to monitor the performance of the devices and to make manual adjustments during the test period. It is claimed that use of the balloon cut six months off the development time of a major missile system. One of the NWC balloons is shown in Figure 8.

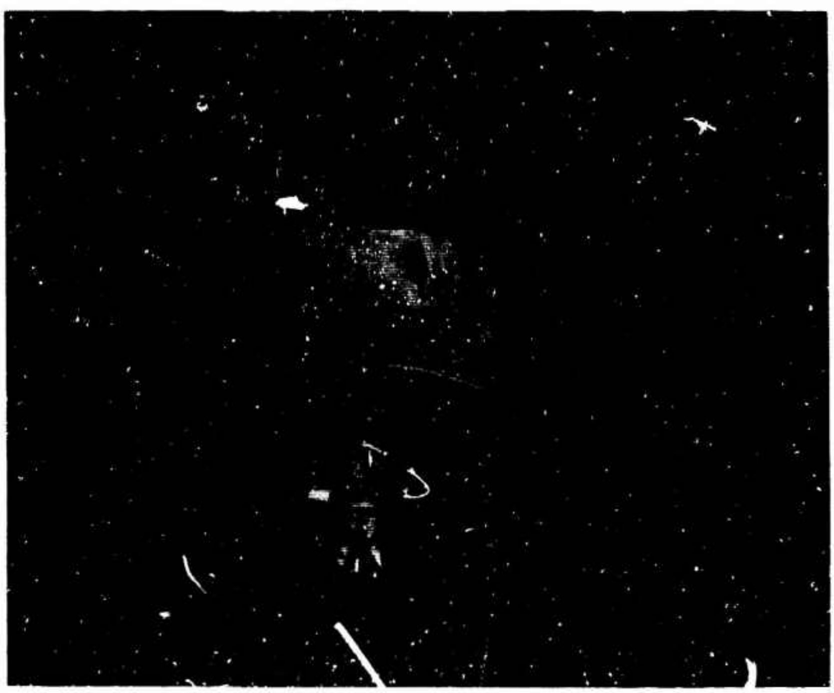

Figure 8. Naval Weapons Center Balloon

The Air Force Armament Laboratory at Eglin AFB uses a model S-60 balloon in much the same manner as the NWC balloons. They use it to test ordnance fuses and laser devices where the experiment requires that a ground objective be approached from different levels and elevations. They feel that the hot air balloon fills a gap between the capabilities of helicopters and conventional aircraft.

Another, quite different use will be attempted soon in a weather modification experiment. Mr. Charles B. Moore, of the New Mexico Institute of Mining and Technology, will use a hot air balloon to lift a large diameter, lightweight tube about 1,000 ft into the atmosphere from the top of a 10,000 ft mountain. A blower at the base of the tube will induce a flow up through the tube and out its upper extremity. Before entering the tube, the air will pass through a particle generator, which will load the air with particles having an averag diameter of 0.1μ, in a concentration of 10^8 particles/cm^3. An electrostatic precipitator will apply a charge to each particle. The effect of pushing the cloud of charged particles up into the atmosphere will be something akin to a Van de Graaff generator and it is expected that this artificial electrification process will have a pronounced influence on precipitation.

4. CONCLUSIONS

The tethered hot air balloon is a research tool which provides capabilities not fully available from any other type of airborne device. In comparison with heavier-than-air craft, it and helium balloons have similar advantages in that they offer stable, relatively fixed, inexpensive test platforms. In certain applications the hot air balloon has further advantages over helium balloons in that it offers a much simplified logistics effort, frequently at lower cost, and a much higher degree of convenience in operation.

Flight experience with hot air tethered balloons includes thousands of hours of operation with no known accidents. Performance levels which have been achieved and which should be attainable are as follows:

	Performance Achieved	Probably Attainable
Loads	up to 2,000 lb	at least 10,000 lb
Wind limit	15 - 20 knots	25 - 35 knots
Duration	6 hr	unlimited with ground fuel
Maximum altitude	3,000 ft	10,000 ft reasonable: possibly 25,000 ft

X. Some Aspects of High-Altitude Tethered Balloon Flight

L.A. Speed
Ministry of Technology
Cardington, England

Abstract

A review of tethered balloons intended for use at altitudes above 15,000 ft is made. The efforts to achieve this altitude goal since 1917 are presented along with the significant data pertinent to each balloon. The design process is analyzed to provide information concerning the effects of weight and volume on high-altitude tethered balloons. Several schemes of flying balloons in tandem are presented and discussed. The flying of tethered balloons in high winds at altitude can cause many difficulties and may render it impractical to consider. Finally, the problems of ground handling in various wind situations are addressed.

1. INTRODUCTION

In consideration of the remarkable advancement in the performance of "free" balloons over the past decade or so, an opportunity is taken to review the position regarding the performance of balloons intended for use at altitudes above 15,000 ft.

The improvement in free balloon performance can be mainly attributed to the development of new materials, although the technological advances arising from

the research and development by several organizations in the United States interested in attaining high altitudes for a variety of purposes cannot be ignored.

The launching of these balloons even in moderate winds still presents serious problems. We are presented with similar problems with tethered balloons, although no serious difficulty should be encountered in handling tethered balloons in wind speeds under 30 mph.

The main purpose of this paper is to discuss problems associated with tethered balloons designed to fly in surface winds of 30 mph and with corresponding wind speeds to attain an altitude between 15,000 and 20,000 ft. This altitude will appear low to the users of the balloons who can achieve altitudes many times greater.

One of the principal problems connected with high-altitude balloon flight is the provision to be made for expansion of the gas in the envelope on ascent — this expansion being nearly 100 percent from ground to 20,000 ft — and the retention of pressure in the envelope on descent.

Altitudes of 14,000 ft were attained in 1917 in winds up to 20 mph, the balloon being an Italian design of 70,000 ft^3 volume (Figure 1). This balloon (50,000 ft^3) was designed for observation purposes at altitudes of 5,000 ft, but by removing the observers basket, rerigging the balloon, and increasing its volume, we found that the higher altitude was possible.

Another problem associated with ballonet type balloons is the possible movement of the center of buoyancy with the envelope filled to only half its capacity, should the balloon depart from its designed angle of incidence. The surging of the gas either forward or aft upsets the balance of the balloon, sometimes with catastrophic results.

This Italian balloon having a nearly spherical gas chamber did not suffer from this defect. The weight of this balloon was 1,400 lb, producing a weight-volume ratio of 20 lb per 1,000 ft^3 of volume. This ratio is still true today for balloons designed to fly at 60 mph, made from cotton textiles, and conventionally proofed with rubber or neoprene. An improvement has been made, however, in the gas retention and weather resisting properties of these proofed fabrics. By the substitution of nylon for cotton an improvement in this ratio can be made, but although nylon is $2\frac{1}{2}$ to 3 times as strong as the equivalent weight of cotton, the resulting reduction in weight is relatively small, possibly 25 percent, with the reduction in weight-volume ratio of the balloon to 16 lb per 1,000 ft^3 of volume. By the provision of a film of Mylar as the gas retaining barrier, a further reduction in this ratio should be possible, but my limited experience with this method of gas retention has led me to believe that balloons so made need more careful handling during ground operations, that is, inflating, deflating, and packing. We have many balloons at Cardington made over 25 years ago and these balloons are still in good condition.

Nevertheless, it would appear that balloons could be produced today with a weight-volume ratio of 12 lb per 1,000 ft^3 volume. It would be interesting to obtain this ratio for balloons now being used in the United States. The only American balloon for which we have this information is the Goodyear Vee balloon, the weight-volume ratio being 25 lb per 1,000 ft^3 volume, but this is to be expected of a balloon of this design which probably has other desirable features to compensate for this high ratio.

In 1927 an attemp was made to produce a tethered balloon capable of flying at an altitude of 20,000 ft and being handled and flown in winds of 30 mph at ground level and equivalent wind speeds at altitude (see Figure 2).

This balloon Z1 was 234,000 ft^3 volume, 60 ft diameter, and weighed 3,600 lb, that is, a weight-volume ratio of $15\frac{1}{2}$ lb per 1,000 ft. This ratio would be nearer 20 lb per 1,000 ft^3 for the same volume balloon designed to fly in a 60 mph wind, owing to the stronger and therefore heavier fabric, and so forth, necessary to withstand the higher winds. Great difficulty was experienced in handling this balloon (despite the crew of 60 then considered necessary) and it was destroyed in the early stages of the performance trials, because of the external fin rigging tearing a hole in the envelope, resulting in a fire.

To minimize the movement of gas in the partially filled balloon, a surge curtain was fitted dividing the gas chamber into two equal volumes. This was porous to permit normal passage of gas, but prevent surge caused by a sudden change in balloon attitude. Another novel feature was the internal nose girder to prevent the nose of the balloon from deforming because of wind pressure (Figure 3).

During this time an expanding balloon of 270,000 ft^3 maximum volume was made, again to reach an altitude of 20,000 ft (Figure 4). This balloon was of 4-lobe cross section, the restraining rubbers working at 600 percent extension at maximum altitude. Owing to the hysteresis of the rubber, the internal envelope pressure on descent from altitude was less than that on ascent, resulting in the balloon buckling in the center. Other trouble was previously experienced with this balloon: the gas surged aft and the balloon flew with the tail vertically upwards (Figure 5). Afterwards, surge curtains were fitted dividing the balloon into 4 compartments to prevent a recurrence of this trouble. On trial, the balloon reached an altitude of 18,000 ft in winds of 22 mph.

Because of the failure of these two balloons (one by burning, the other by buckling), the operational requirement was reduced, the revised altitude being 15,000 ft, and a smaller version of Z1, designated Z2, was designed (Figure 6). The volume of this balloon was 120,000 ft^3 and weight 2,260 lb. The weight-volume ratio was 19 lb per 1,000 ft^3. This balloon flew successfully at 15,000 ft on several occasions, but only in surface wind speeds of under 25 mph.

During the development of this balloon the French had designed a 6-lobe expanding balloon to reach an altitude of 18,000 ft with maximum volume 27,000 ft^3, weight 470 lb, and a weight-volume ratio of 17.4 lb per 1,000 ft^3 (Figure 7). This balloon, intended for night use only, was colored dark green to reduce visibility, and as a consequence it was sensitive to changes of volume caused by solar radiation (superheat). On one occasion after flying at 12,000 ft altitude in bright sunshine, it descended rapidly owing to a passing cloud, and about 2,000 ft of cable was laid upon the ground before the winch could "haul in." The cloud cleared and the balloon quickly returned to its original altitude. Two balloons of this type were lost because of tether cable breakage. A change of policy ended all efforts to attain 20,000 ft altitude.

It would still appear that projects may arise where altitudes of 20,000 ft are needed and after a lapse of some 30 years the situation is now reassessed.

2. THE EFFECT OF WEIGHT ON THE VOLUME OF A HIGH ALTITUDE BALLOON

It was found that a 120,000 ft^3 volume was necessary to attain an altitude of 15,000 ft; but if the altitude is increased to 20,000 ft the volume of the balloon must be nearly doubled. The reason for this rapid increase of volume is only obvious on close analysis of the design processes.

If the gas lift of a balloon of diameter D is sufficient to lift to 15,000 ft a cable that will withstand the maximum specified winds, then the volume of the balloon must be increased to obtain greater altitude, that is, from 15,000 to 20,000 ft. The volume increases as D^3 but as the lift per cubic foot of gas decreases with altitude, the gas lift is increasing at a less rate than D^3. Simultaneously, the area of fabric increases as D^2, but for larger balloons stronger fabric is required; therefore, the weight of the fabric increases at a greater rate than D^2. The wind forces on the balloon also increase as D^2 and to withstand the increased force, the strength and therefore the weight of the cable per foot length must be increased. Finally, as the altitude increases, a greater length of cable has to be supported and so for a considerable increase in volume the gain in altitude is only small. If, however, there is some means by which the weight of cable or of balloon is reduced, it is possible to keep the increase in volume to a minimum.

The type of cable used with high-altitude kite balloons is tapered along its length to allow for the variation in tension. There is obviously a greater tension at the top than at the bottom, and the only possible means of reducing the weight is to increase the tensile strength of the cable. It has been found, however, that wire having a greater tensile strength than 150 tons in.^{2} tends to have reduced ductility with consequent increased liability to damage at the winch. (The aforementioned French

balloon flew on a cable of UTS of 220 tons $in.^2$ - two balloons were lost by cable failure at low wind speeds. It was found that the working of the cable around the winch drums reduced the strength to less than half its original value.)

Nylon may, however, be used with advantage as it is 1.5 times as strong as 150 tons $in.^2$ steel for the same weight, but as it will stretch over 20 percent in length under a load equal to one-third of its breaking load (and the maximum tension on a balloon cable is usually one-third of its ultimate), we can permit the nylon to stretch 20 percent in our calculations and with this presumption, nylon is 1.8 times the strength of the equivalent steel cable (or 0.55 heavier). Thus, flying on a nylon cable enables the static ceiling to be greatly increased. This is, however, offset to a large extent by the increased wind drag on the cable. (The diameter and therefore drag is double that of a steel cable.)

The effect of lightening the balloon and flying on a stretched cable is shown in Figure 8, catenary AB being the 1932 Z2 balloon flying at 15,000 ft on a tapered steel cable and catenary XY being a present day possibility. The altitude of the balloon is increased by 5,000 ft, but the angle of cable at ground is poor, drag of cable being three times that of balloon, 32,000 ft of cable for a 20,000 ft altitude. Catenary AB is a lighter balloon on nylon cable.

3. TANDEM FLYING

Attempts to fly balloons in tandem in 1918 were successful in light winds only (under 12 mph). See Figure 9, scheme A.

In 1941 a tandem scheme was developed where the cable of the upper balloon was attached to the top surface of the lower balloon, the limiting wind speed being about 25 mph (Figure 9, scheme B).

With use of small pressurized balloons, increased altitude was obtained by tandem scheme C.

Scheme D was ultimately developed and used successfully in wind speeds up to 40 mph with two balloons. In winds of up to 25 mph, 4 balloons were used in altitudes up to 5,000 ft. For high altitude operations, flying balloons in tandem has the advantage of giving increased lift, over the same volume of gas when contained in one envelope. Thus, 120,000 ft^3 of gas will give a buoyancy of 4,200 lb at 20,000 ft altitude; if now this 120,000 ft^3 of gas is divided into two balloons each containing 60,000 ft^3, one balloon flying at 20,000 ft and the lower at 10,000 ft, the gas lift of the upper balloon will be 2,100 lb, but because of increased lift of gas at 10,000 ft, the buoyancy of the 60,000 ft^3 of gas is increased to 2,800 lb, a net gain of 700 lb of lift. The effect of this is shown by catenary X0Z (Figure 8) "heavy" 60,000 ft^3 balloons, that is, having half the weight and lift of the original Z2 balloon, being flown in tandem, one at 20,000 ft and the lower at 10,000 ft on steel cable. A

120,000 ft^3 balloon was necessary to attain an altitude of 15,000 ft in 1932; the same altitude can now be reached by flying two 30,000 ft^3 balloons on nylon cable (catenary APC). The use of glass fiber cables with their greater strength ratio accompanied with decreased diameter will give a diametric increase in the performance of high altitude balloons.

All the above figures have been derived on the assumption that the angle of pitch of the balloon can be controlled — various pitch control devices have been tried with only moderate success. These methods rely on the moving of the attachment point of the balloon forward in higher winds. We have found generally that the weight penalty of these control systems is not balanced by the practical advantages of reduced peak cable tensions.

Winds of 60 mph for high altitude balloon flying increase many times the theoretical and practical difficulties, rendering it impracticable and nearly impossible to achieve this flying condition. The principal obstacle is the drag of the flying cable which causes the balloon to drift an unacceptable distance downwind from the tether point, but here again by the introduction of glass fiber cables this condition may be entirely altered. Streamline section flying cables have been considered to minimize this drag, but even if such a cable was possible there is no reason for supposing that it would fly in the correct attitude relative to the wind — it would probably form a spiral and result in greater drag than an equivalent area circular cable.

Other problems — not confined to high altitude balloons — arise in handling balloons in high winds. Unless the balloon can be completely screened from the wind, it has been found safer to let the balloons fly at say 1,000 ft above the ground to avoid ground eddies and allow the elasticity and catenary of the cable to act as a shock absorber. Nylon should be particularly suitable for this purpose.

Portable windscreens have been extensively experimented with, in order to shield the balloon when bedded close to the ground; these have proved useful once the balloon is on the ground, but provide another hazard — the windscreens often being more difficult to handle than the balloon.

Turntables upon which the balloon is bedded were tried some forty years ago, to accommodate changes of wind direction, but were suitable only for permanent balloon sites. The condition most favored for balloon grounding is the flying of the balloon from its point of attachment on a wire pyramid. A balloon thus moored should safely withstand 50 mph winds, depending upon the gustiness of the conditions — two 45,000 ft^3 balloons were recently lost — one broke away and the other burst by striking an obstacle on the ground in a 65 mph wind, but a similar balloon flying at 1,000 ft altitude safely rode out the gale with no apparent distress.

Figure 1. Italian Balloon (1917). Volume 70,000 ft^3

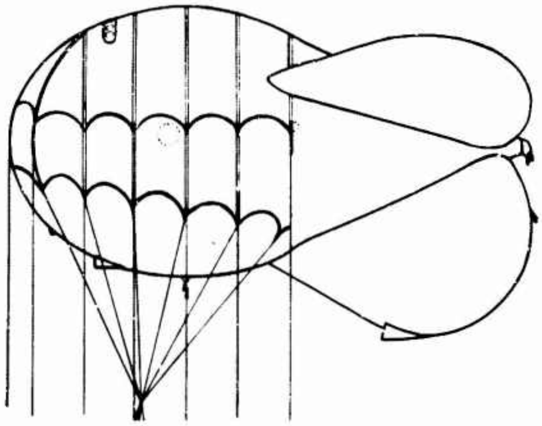

Figure 2. Balloon Designed for 30 mph at an Altitude of 20,000 ft

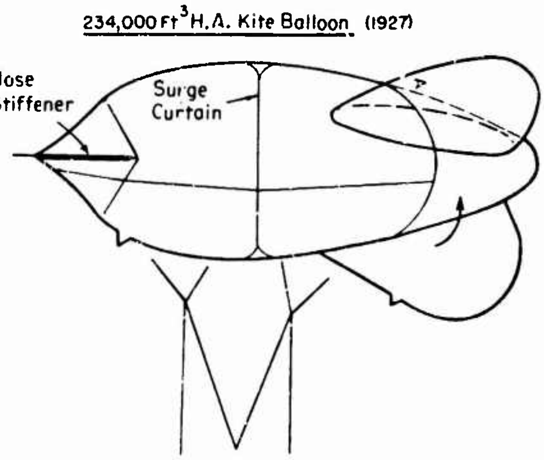

Figure 3. Balloon with Internal Nose Girder

Figure 4. Balloon with Volume of 270,000 ft^3 Designed for an Altitude of 20,000 ft

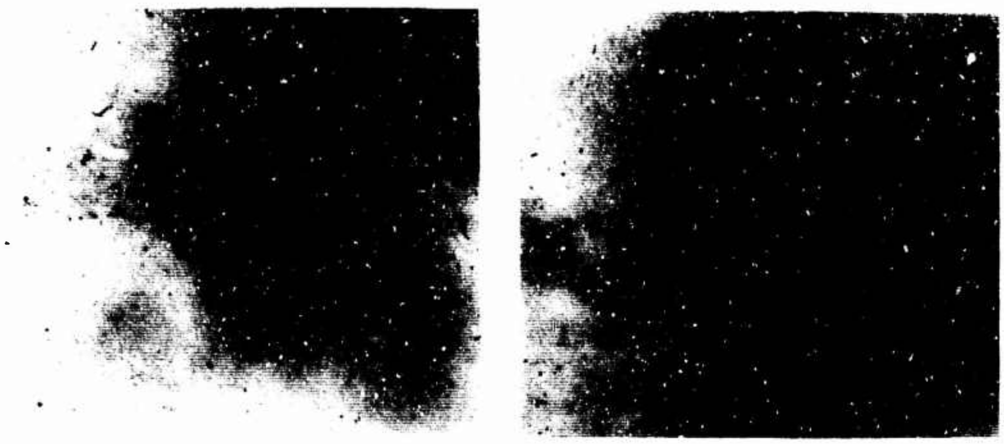

Figure 5. Destruction of Balloon Shown in Figure 4 Due to Tailward Surge of Gas

Figure 6. Z2 Balloon

Figure 7. French Designed, 6-Lobe Balloon

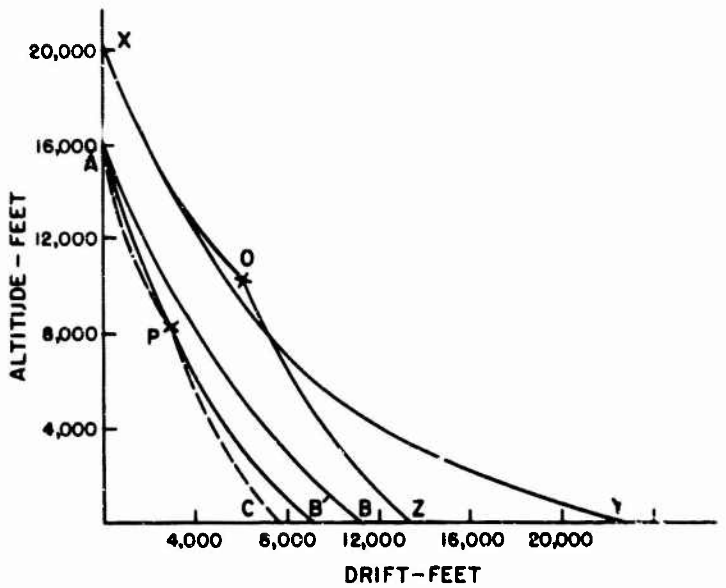

Figure 8. Downwind Drift and Altitude for Various Balloons

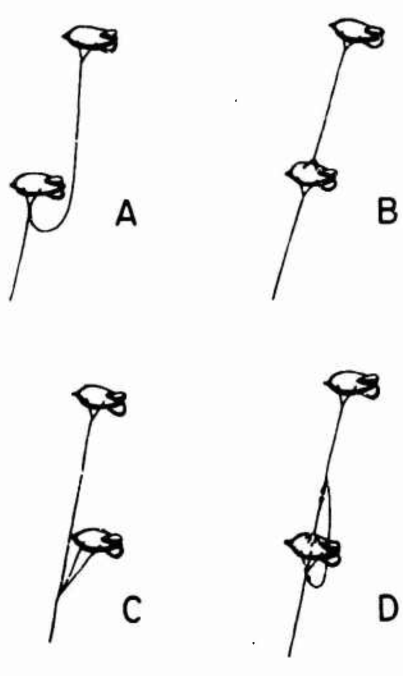

Figure 9. Tandem Balloon Schemes

XI. Barrage Balloon Skyhook

Gruver H. Martin
U.S. Naval Ordnance Laboratory
White Oak, Silver Spring, Maryland

Abstract

An experiment was conducted to determine the feasibility of using a large captive balloon to deploy an array of pressure sensors vertically above a large explosion. A British World War-II type barrage balloon was used up to an altitude of 8,600 ft above mean sea level. The payload consisted of a 5-station gage array distributed along the tether. A 5/16-in. diameter stranded fiberglas cable was used for the single tethering line.

As a result of the tests, it is concluded that a distributed payload of up to 750 lb can be deployed in a near vertical and very stable array with a barrage-type balloon up to 10,000 ft mean sea level. The system can be launched and maintained aloft under fairly adverse weather conditions and has significant advantages over other methods of gage positioning, for example, rocket emplacement, in terms of simplicity, reliability, and economy.

I. INTRODUCTION

During the first week of December 1966, the Naval Ordnance Laboratory (NOL) and its contractor, Raven Industries, Inc., conducted a test to determine the

feasibility of using a tethered balloon system as a "skyhook." For many years the Laboratory has been concerned with the dearth of experimental pressure-time data acquired at high altitudes in the region directly above large explosions. The balloon skyhook concept was designed for use on large-scale field operations either over water or over land. Large size charges weighing up to hundreds of tons would be detonated, and the balloon-supported tether line would provide a means for positioning pressure transducers at selected levels up to 10,000 ft above mean sea level.

Operations such as envisioned are usually large operations. A number of agencies utilize the operation to obtain data of special interest to them; thus inter-agency or inter-project coordination is required in such mundane things as location of equipment and time for emplacement. Working in the field imposes certain interesting constraints. Weather conditions become important and, particularly for balloon flights, conditions for launching the balloon and flying the balloon must be favorable. For a variety of reasons, "holds" in the over-all operation may be necessary: weather deteriorates, malfunctions occur, someone isn't ready. These facts of life for field operations dictate specific requirements for the balloon system. These requirements can be delineated thus:

The system should be capable of performing as a "skyhook" for the purpose of lofting and accurately placing instrumented payloads weighing up to 750 lb, excluding tether, to an altitude of 10,000 ft above mean sea level.

The system must be capable of accepting a payload which would be distributed from the surface to 10,000 ft, having sensors placed at preselected discrete locations.

The system must be capable of being launched without windbreak or shelter in winds up to 20 knots. It should withstand winds up to 40 knots, when in position, for a minimum of 72 hours with a maximum change in inclination of 20°, with respect to a vertical through the mooring point, from the time mooring is complete until the event being studied takes place.

The system must be capable of satisfactory operation on land or at sea without loss of effectiveness.

2. PRETEST PREPARATIONS

The pretest preparations included such things as the selection of a suitable test vehicle, the design and fabrication of a realistic payload and the selection and preparation of a suitable test site.

2.1 The Balloon

The balloon test vehicle selected was a World War II-type British barrage balloon, Mark 84 (see Figure 1). The inflated balloon is 112 ft long, 40 ft in diameter

with an approximate gas volume of 80,000 cu ft, a weight of 1700 lb, and a gross lift of 3900 lb at 10,000 ft. The aerodynamically shaped balloon has a ballonet which is pressurized with ram air and has air-inflatable fins and rudder. It is designed to withstand winds up to 80 knots. The balloon used in this test was manufactured in 1958 and was in excellent condition, requiring only minor repairs of damages incurred in shipping. The only refurbishment effort made was the repainting of the top portion of the gas envelope to minimize helium losses.

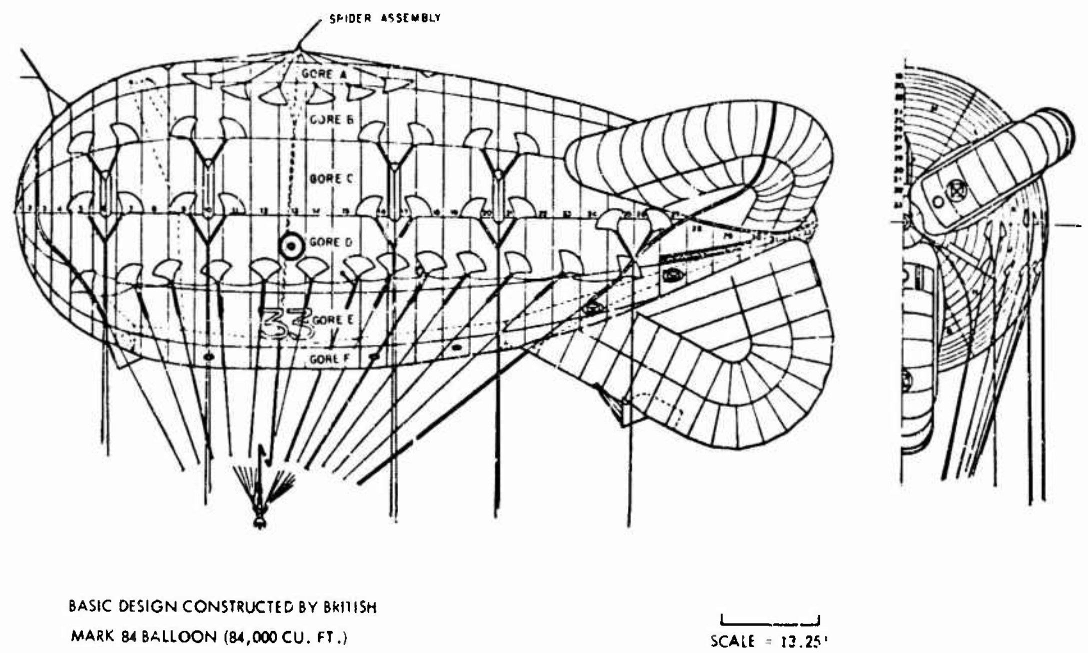

Figure 1. General Arrangement of Balloon

2.2 The Tether

Selection of a tether line for the balloon involved consideration of trade-offs among such factors as strength of lines, total lift capacity of balloon, and cost of line. A complicating factor in tether selection resulted, in that there was some question as to the actual volume (and hence lift capacity) of the balloon. Estimates of volume ranged from 70,000 to 84,000 cu ft.

Two tethering line materials were considered -- steel and Glastran (R) each in two sizes, 1/4 and 5/16-in. diam and 5/16 and 3/8-in. diam, respectively. For the estimated fixed weight of the balloon, rigging and payload (2525 lb), calculations were made for different balloon volumes and the several candidate tether lines to determine the most suitable material.

It was apparent that if the original performance requirements (payload, weight, and altitude) of the system were to be met, the only tether material with a chance for success was the 5/16-in. Glastran it alone provided the system with an adequate free lift for all conditions considered. Even with this choice of tether material, it appeared chancy whether a successful flight could be obtained with a 70,000 cu ft balloon, since the excess lift available would be only 175 lb.

On the other hand, if the most optimistic volume guess were correct, an 84,000 cu ft balloon would support a 1/4-in. steel tether with an excess lift of 465 lb at the start of the experiment and one could visualize that enough aerodynamic lift would be developed to compensate for relatively large helium losses during the 72-hour flight.

However, the selection of this cable configuration would underscore the importance of another area of uncertainty -- that of the maximum tension which would be developed in the cable during the flight. Hence, the lack of accurate knowledge of the vehicle and its aerodynamic lift capabilities under wind conditions made it prudent to select a tether material with a factor of safety greater than the minimum of 1.4:1.

To complete the discussion, two additional modes of comparison need be mentioned -- one technical and the other economic in nature. The technical point concerns the state-of-the-art in the development and utilization of the two materials. The many years of experience in the design and fabrication of steel cables have yielded a product which is very near the ultimate in its physical properties and highly predictable in its response to applied stresses. In addition, the design of handling equipment has been improved over the years to the point where maximum utilization of the cable is realized. In comparison, the use of fiberglas as the basic material for rope or cable construction is a relatively new concept. While the potential is very high, fabrication techniques are in the infancy of development and usage experience leading to the generation of acceptable handling techniques is negligible.

The economic factor is an important one for this low budget experiment. The cost of fiberglas cable is very nearly ten times the cost of steel cable of the same rated breaking strength.

The choice of tether material was made for an assumed volume of 75,000 cu ft. Table 1 shows the comparison between steel and Glastran cables for this balloon volume. By comparison of the figures on free lift available and the relative strengths of the two cables, the reasons for the selection of the Glastran cable are obvious.

Table 1. Comparison of Steel and Fiberglas Tethers for an Assumed Balloon Volume of 75,000 cu ft

Cable Type	1/4" Diam Steel	5/16" Diam Glastran
Maximum lift available for tether (lb)	1125	1125
Total weight of tether (lb)	1100	700
Net free lift available (lb)	25	425
Rated breaking strength (lb)	7000	10,000
Factor of safety	1.4:1	2.0:1

2.3 The Payload

In the interest of minimizing payload weight, it is most economical to use the balloon tether as a structural member to support the payload in an operation of this nature. Since the aerodynamic drag on the payload and the tether and the nonlinear weight distribution of the payload along the tether would have a major effect on the shape of the catenary the tether assumed, an accurate simulation of the payload with respect to its drag and weight properties has been made. The payload consisted of two major assemblies -- the gage stations and the electrical cable through which would be transmitted the signal to turn the gages on and the signals from the gages to a tape recorder on the surface. The total weight of the payload was 610 lb.

2.4 Test Site

The field test was conducted at the Army airport at Camp Atterbury, Indiana, where there are excellent ground facilities plus restricted air space up to 45,000 ft.

3. THE TEST

3.1 Test Procedure

The test was to be conducted in two phases. The first would consist in inflating and launching the balloon under somewhat ideal surface wind conditions (say winds of from 0 to 5 mph); raising the balloon to altitude, while attaching the payload; and flying the balloon at altitude for 72 hours. It was hoped that for some period during this phase the balloon might experience winds of magnitudes as great as 40 knots. During this flight, position data would be acquired on the balloon and the five gage stations and correlated with available concurrent wind data and lift reduction due to helium loss. From these data, we could then determine the variation in line of sight distance to each gage station from a fixed event point on the surface. The second phase was designed to determine the limitations imposed

on the system when the inflation and launching operations were attempted under adverse surface wind conditions. The experimental plan was to stand by until the surface winds reached a velocity of the order of 20 knots and attempt inflation and launching to an altitude of 500 ft in the presence of this high wind environment.

3.2 The Phase I Test

The Phase I test was conducted during the period 2 to 5 December. The first day was expended in laying out the balloon, inspecting for damage, repairing damaged areas, laying on the rigging, inflating and weigh-off. The complete process took 6 hours, 2 hours of which were devoted to inflation. During the morning of the second day, tail ballast was added to increase the angle of attack, and remotely controlled destruct equipment was installed. A second weigh-off was made prior to haul-out to determine the helium leakage rate. The loss was 30 lb for an 18-hour period. Haul-out began at noon, with the payload being added during the process. The total time of the haul-out to 8600 ft msl was 4.5 hours. The tension in the cable (with the balloon at altitude) varied between 1450 and 1600 lb. Since the calculated gross free lift was approximately 900 lb, the aerodynamic lift varied from 450 to 700 lb. The weather forecast for the night of 4 December called for increasing winds and severe icing at the 6000 to 7000-ft level. We decided to pull the balloon down to 4000 ft and moor it at that altitude overnight. At mooring, the tension had reached 2800 lb. At 0500 on 5 December, the tension in the cables had reached 3625 lb. Two hours later, the cable parted due to a sheave failure on the winch. The balloon rose rapidly and burst. While there is no record of the tension which had developed in the cable at the time the winch failed, it is felt that it must have exceeded 4000 lb, since the system had been tested at this tension prior to the launch.

4. DISCUSSION OF RESULTS

4.1 Payload Versus Altitude

The original requirement that the balloon system be capable of suspending a 750-lb distributed payload to an altitude of 10,000 ft was not achieved in the experiment. However, extension of the data acquired allows us to demonstrate the feasibility of achieving such a goal with some minor design changes (see Table 2). The gross weight of the system as it now stands is 3617 lb. If the rigging were redesigned to change the angle of attack, the necessity for the tail ballast would vanish and if one could accept the inherent self-destruction characteristic of the balloon as the only destruct mechanism, the drop weight and remote destruct instrumentation could be removed. Existing heavy steel hardware could be replaced with

aluminum hardware and the diffusers could be removed after inflation and prior to haul-out. Thus there would be a net savings of 317 lb, giving a new gross weight of 3280 lb, and, if the gross lift at 10,000 ft is 3900 lb, the free lift available would be 620 lb.

Table 2. Design Comparison of System Gross Weight
(in pounds)

System Gross Weight as Now Designed	
Existing balloon and equipment weight	2097
Proposed payload weight	750
Tether weight for 10,000-ft altitude	770
Gross weight	3617
System Gross Weight Savings by Redesign	
Removal of tail ballast	170
Removal of drop weight	40
Removal of destruct instrumentation	85
Substituting aluminum for steel hardware	30
Removal of diffusers	12
Net savings	337
Existing gross weight	3617
Less weight saved by redesign	337
New gross weight	3280
Gross lift at 10,000 ft msl	3900
Gross weight	3280
Free lift (fully pressurized balloon)	620

Thus, we see that even in the absence of aerodynamic lifting forces (a highly improbable situation) and with a very conservative prediction of helium losses (say 100 lb per day) the system could support the projected payload at the 10,000-ft altitude for several days.

4.2 Position Stability

An extremely important consideration for end-item use is the ability of the system to restrain the migration of the sensing stations to relatively small excursions with respect to an event on the surface under the influence of varying environmental conditions. The premature termination of the test prevented the acquisition of data over the complete wind velocity spectrum desired. However, sufficient information was gathered to establish the feasibility of the technique. Measurements of flying cable catenary, with the attached gage stations, were made

using two theodolites. One (theodolite A) was located at 324° -- 6600 ft from the mooring point; and the other (theodolite B) was located at 54° -- 2500 ft from the mooring point. Figures 2 and 3 represent the plots of two typical sets of measurements. Each of these figures is a composite showing two elevations and one plan view. The left-hand elevation is that seen by theodolite A, and the right-hand elevation is that seen by theodolite B. Figure 2 shows the shape of the catenary in a light wind situation and Figure 3 shows the shape of the catenary in a high wind environment. Comparison of these two figures clearly demonstrates the stability of the system relative to the mooring point. In spite of the contrast between wind conditions on 3 and 4 December, the change in line-of-sight distance and the vertical angle from the mooring point to each station is remarkably small. The maximum distance change was one percent and the maximum angular change 2.7°. The balloon stayed well within the 20° vertical angle stipulated in the original requirements.

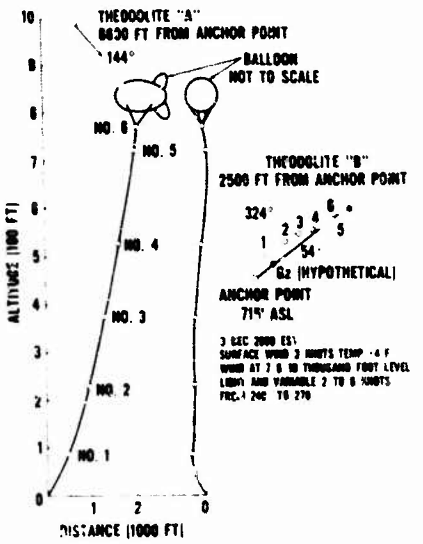

Figure 2. Catenary Shape at 2000 hr, 3 December 1966

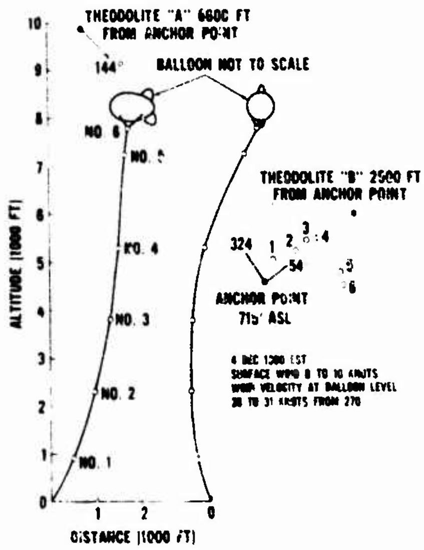

Figure 3. Catenary Shape at 1300 hr, 4 December 1966

This small influence of wind velocity on the off-set of the gage station array from the vertical, that is, from directly over the mooring point, can be used to advantage. For the experiment which we have in mind, it is desirable to make measurements in a small volume of space directly above surface zero, and yet field operational conditions discourage the placing of extraneous material at surface zero. Analysis of the test results show that gage stations can be positioned

in a 40° cone above surface zero by placing the mooring point of the balloon line about 500 ft from surface zero in the predicted up-wind direction (see Figure 2). In this way, with reasonable wind predictions and resulting tether line catenary, gages can be positioned with acceptable accuracy in a zone directly above surface zero without compromising the surface zero ambient conditions.

4.3 Launch Under Adverse Wind Conditions

The loss of the balloon during the Phase 1 test precluded the acquisition of data designed to demonstrate that the system could be launched in the open in winds up to 20 knots. On the basis of experience gained during the Phase I launch where the winds were of the order of 6 knots maximum, it would be impracticable to launch the system as it is now designed, using the same techniques, in a 20-knot wind. However, by modifying the balloon so as to make available points of attachment for the restraining lines which are better suited to controlling the balloon under high wind conditions, redesigning the rigging procedures so as to achieve more localized control of specific balloon areas and, by increasing the rate of fill to reduce the length of the period during which the balloon is most susceptible to destruction, we believe that launches in winds approaching 20 knots would be possible.

4.4 Launch at Sea

While the feasibility of launching the Mark 84 system at sea has not been demonstrated, the experience acquired during the test at Camp Atterbury does lend credence to the practicability of the concept. The small amount of real estate required by the launch crew and the fact that the ship can head with the wind indicate that the system could be launched successfully from an LST. One potential source of trouble peculiar to using the system at sea is the effect of wave action. It is not known if there is sufficient flexibility in all components of the system to absorb the effects resulting in sudden changes in tether tension due to the action of a heavy sea.

4.5 Electrical Charge Buildup

One problem area which was vividly demonstrated in the Atterbury experiment was that of the balloon system acquiring electrical charge resulting in a large potential gradient relative to the ground. Since the tether was a nonconductor, the only conductive path to ground was through the instrument cable which started 500 ft below the balloon at the fifth gage station. The magnitude of the potential was so great by the time haul-out had proceeded to the third gage station (4,000 ft below the balloon) that it was impossible to connect the gages to the instrument cable. While the magnitude of the potential buildup is not known, it was sufficiently large to be hazardous to launch personnel and at the same time create problems in the instrumentation system itself.

4.6 The Winch Failure

As stated earlier, the experiment was brought to a premature conclusion when the tether parted, resulting in the loss of the balloon. The parting of the Glastran tether was the direct result of the failure of one of the two tension sheaves of the winch shock absorbing system. The sheave flange broke off allowing the tether cable to slip off the sheave. When this happened the cable was stressed over a radius much smaller than the 6-in. minimum bending radius prescribed and as a result the cable parted.

5. CONCLUSIONS

5.1 Feasibility Established

From the results of this study we conclude: (a) that it is entirely feasible to use a balloon system of the type investigated in this experiment to deploy an instrument array vertically above and in the vicinity of a large explosion to altitudes up to 10,000 ft msl; (b) that such a system can be launched and maintained aloft under fairly adverse conditions for reasonable periods of time (say 2 to 3 days); (c) that provided with a suitable platform the system can be launched at sea as well as on land; (d) that the system when aloft will maintain the positions of the various gage stations such that there is a high probability of acquiring acceptable data from a large percentage of the stations.

5.2 Experimental Dividends

A much better understanding has been acquired of areas where little or no information was available prior to the study. For example: it has been demonstrated (a) that if the handling equipment is properly designed and careful handling techniques are observed, fiberglas with its attractive strength-to-weight ratio is a suitable tethering material; (b) that properly trained, a crew of 8 to 10 men can inflate and launch the system from an area as small as 70 × 130 ft in 8 to 10 hr; (c) that the stability of the system is much better than originally hoped; and (d) that if one desires to launch the balloon under more adverse surface conditions than those experienced, the balloon hold-down system will have to be modified.

XII. Aerostrand

J.L. Kane
Owens-Corning Fiberglas Corporation
Granville, Ohio

Abstract

Aerostrand is a glass fiber-epoxy resin tension member. It has been made in monostrand form having breaking loads up to 3,000 lb. The breaking length of Aerostrand is approximately 340,000 ft as compared to approximately 153,000 ft for the nearest competitive material. The physical and mechanical properties of Aerostrand, which have been determined, are given. A method of terminating and splicing the material is explained.

What is Aerostrand? It is a glass fiber - epoxy resin strand with a density of approximately 1.8 and 2.0 gm/cc, approximately two-thirds that of aluminum and one-quarter that of steel. It is made by collimating glass fibers, coating with a resin sizing, and curing the resin to form an integral strand. The material has a tensile strength between 250,000 and 325,000 psi; therefore it has a strength-to-diameter ratio equivalent to the higher strength material. It has a modulus of elasticity of 7×10^6 psi. These are the general mechanical properties of the materials. What do these figures mean with respect to balloon tethering? Table 1, taken from a contract performed for the Air Force Cambridge Research Laboratories, is a

comparison of various tether materials showing their breaking lengths. It can be seen that the GRP tension member, which we identify by the Aerostrand trademark name, has a breaking length over twice that of any of the other materials shown.

Table 1. Comparison of Tether Materials

Material	Diameter (in.)	Weight (lb/ft)	Breaking Strength (lb)	Breaking Length (ft)
Steel 1 × 19 cross lay rocket case strand*	0.086 0.219	0.0155 0.1082	1,675 10,185	108,000 94,000
Nolaro†, parallel strand, plastic jacketed, fiber				
Dacron ‡	0.25 0.50	0.0201 0.0828	1,650 8,250	82,000 100,000
Nylon ‡	0.25 0.50	0.0180 0.0720	2,400 11,000	133,000 153,000
Mylar rope	1/4 1/2	0.020 0.077	1,400 5,200	70,000 68,000
Rocket wire, Type 355 stainless steel – 7 × 10 × 0.010 construction	0.138	0.0394	2,038	52,000
Nylon rope	1/4 7/16	0.016 0.050	1,800 5,500	112,000 110,000
GRP tension member ¶	0.090	0.0047	1,600 (min)	340,000

* Data, American Chain and Cable Company, Inc., Detroit, Michigan
† Registered, Columbian Rope Company, Auburn, New York
‡ Polyethylene jacket
¶ Owens-Corning Fiberglas Corporation

Now, what can we make? Table 2 gives the monostrands we have produced.

Table 2. Monostrands Produced

Breaking Strength* (lb)	Approximate Diameter (in.)	Weight (lb/1000 ft)
440 (min)	0.043	1.21
1100 (min)	0.075	3.60
1500 min not established	0.086	4.60
3000 min not established	0.122	9.16

*0.05 in./in./min - 10 inch gauge length.

The breaking strength is dependent on glass control rather than strand size.

Gripping is one of the major problems associated with evaluation of this material. Unless you can grip a material to test it, you cannot measure its strength. We have fully characterized the 440-lb breaking strength material and have had relatively few problems with grips once we had developed the technique. Figure 1 shows the technique used for gripping the material. In this case, we are using a clevis fitting but any other type could be used. We had to modify the fitting by placing an Allen set screw in the back and an Allen head cap screw with a hole in it at the front. A hole is drilled in the fitting to allow application of the resin and two small holes drilled on each end to allow entrapped air to escape. The strand is split into 4 quadrants and inserted into the fitting. Without splitting the material, it slips out of the grips.

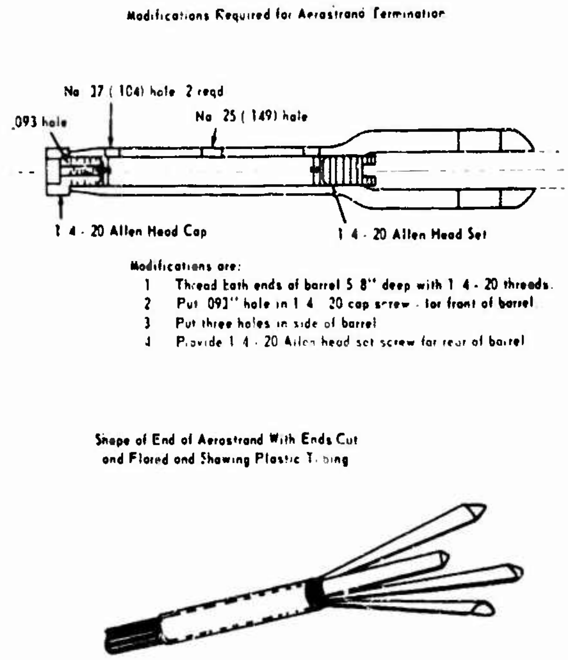

Figure 1. Gripping Technique

Although this system works reasonably well with the smaller size strands, as the strand size becomes larger, the gripping problem is greater because the strength increases greatly with a relatively small increase in surface area. Work is continuing on the grips for the larger diameter Aerostrand. Figure 2 shows some of the grips we have used.

While on the subject of gripping, we will discuss splicing. A splice developed by the American Chain & Cable Company for target towline has been used successfully for the 440-lb breaking material achieving 95 percent of the strength of the monostrand. Figure 3 shows the splice on the 440-lb material. The only other test of the splice was made on the 3,000-lb material and a considerably lower percentage of the breaking strength was achieved, 80 percent. NOTS China Lake (Technical Progress Report 389 NOTS TP 3830) has done some work in splicing this material to itself - (1) using beveled material, and (2) interlacing the material. Braided nylon has also been used successfully by NOTS China Lake for splicing.

As mentioned before, the 440-lb material has been more fully characterized than any of the others. Figure 4 shows the static fatigue properties of the 440-lb

Figure 2. Various Types of End Fittings

breaking load material. We used 7 specimens for determining breaking load. The first specimen to break gave 90 percent probability of survival with 50 percent confidence, and the fourth or medium specimen gave 50 percent probability of survival with 50 percent confidence. For applications such as balloon tethering, the duration of these tests is much too great and a tether of over 100 hours would probably be rather long. These data were obtained on a test machine placed outside in the weather as shown in Figure 5. We have test specimens in 98 percent RH and 78 °F which have been running for over 5,400 hours with 56.8 percent of minimum ultimate breaking strength.

I mentioned before that gripping was a problem with the larger size monostrands in determining the ultimate tensile strength. Since no tension member is ever used to its ultimate strength, this is not a major problem in use, but it is important to have the grip strength as close as possible to the material strength. Results of static fatigue tests on 3,000-lb breaking load material indicate that the ultimate strengths obtained are low. Figure 6 shows a comparison of the time to rupture versus percent ultimate for some 480-lb average breaking load and 3,000-lb material showing that larger diameter material is actually lasting longer at a given percentage of ultimate strength. The 3,000-lb material at 65 percent ultimate tensile strength is still running after 1,000 hours. The ultimate strength of the 3,000-lb material calculated on the basis of 480-lb material is 200 lb higher than that obtained in short term tensile tests.

We have run into a problem in determining dynamic fatigue properties of the material. By means of a Wiedemann Dynamic Fatigue Tester with a frequency of 1800 cycles/min, the material heats up in the grips because of its high damping characteristics and causes grip failure. Cooling the grip with air helps. Normally dynamic fatigue specimens have much larger gripped areas than the gage area, facilitating breaks at the gage area. This cannot be done with Aerostrand testing. This testing was done during grip development and no further work has been done.

Figure 3. Splice Package RAA-7066 (American Chain & Cable) Applied to Aerostrand

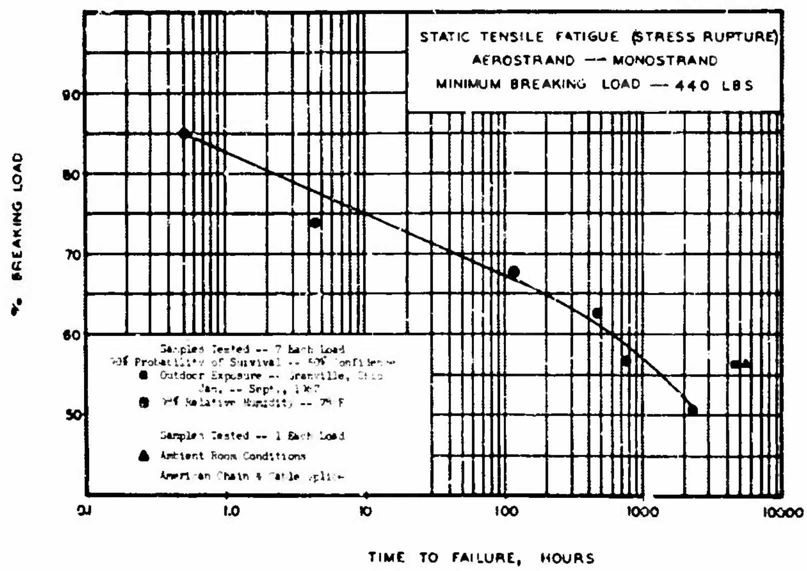

Figure 4. Static Tensile Fatigue (Stress Rupture) Aerostrand-Monostrand

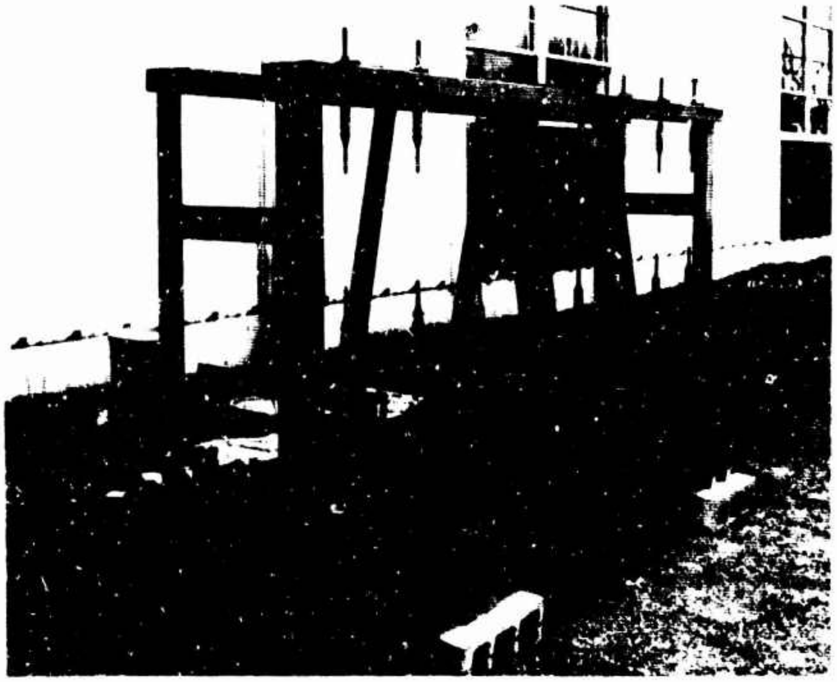

Figure 5. Stress Rupture Apparatus

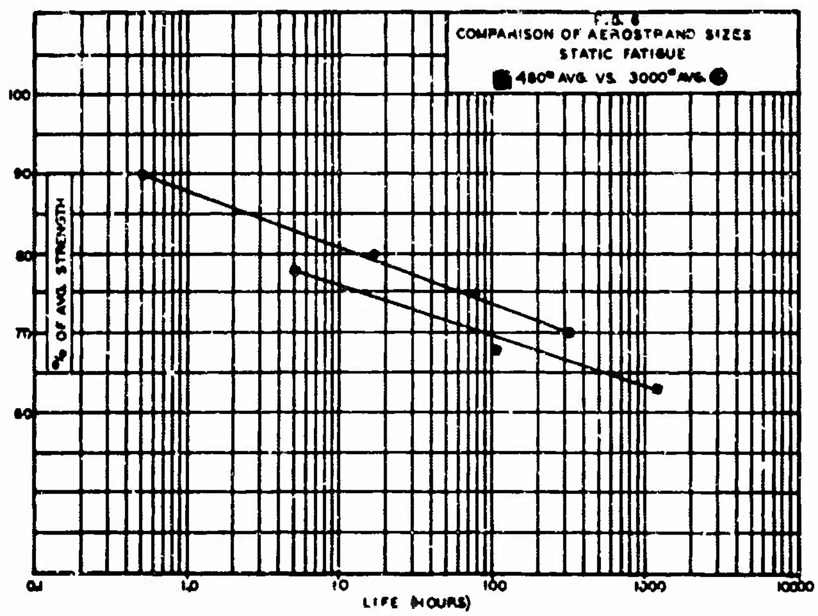

Figure 6. Comparison of Aerostrand Sizes – Static Fatigue

Another test which we have performed on the Aerostrand is an endurance test. Performed on the equipment shown in Figure 7, this test is used to qualify steel towlines for target towing. The large sheaves on the machine ar for testing large diameter material. Normally, 3.5-in. or 5.75-in. sheaves are used. In the towing of targets from airplanes, it is necessary to package the towline as small as possible and to run it over small sheaves to exit from the plane. The endurance tester attempts to simulate the treatment received by a line being run over sheaves in and out of the reel system. Table 3 gives results of 440-lb breaking load material of 3.5-in. diam sheaves. Since it is an empirical test, the results are hard to interpret. If these data are plotted on semilog paper, a curved line typical of abrasion failure of glass, rather than a straight fatigue curve, is found. We believe that part of the problem may be abrasion over steel sheaves. Experiments with PVC or Teflon coated sheaves are planned.

Figure 7. Endurance Tester

Table 3. Endurance Tests - 3.5-Inch Sheave
Tow Cables - 440 lb BL
Mil. Spec. T-23439A (WEP)

Load	Reversals		Number Trials
	Average	Minimum	
300	...	74	1
200	3,810	1,215	3
175	1,605	1,060	3
150	2,205	1,875	6
125	5,430	3,230	2
100	15,500	8,390	2

We have performed a limited effort on cabling material, determining the type of machine which can be used to produce cable, the effect of lay length, and the method of gripping the material. We have obtained over 100 percent of the minimum breaking strength of the 440-lb breaking load material in 1 × 7 cables over 3000 lb. Only several 1 × 19 cables have been broken and the grip problems have not yet been solved.

In conclusion, the strength-to-weight ratio of glass fiber impregnated with resin makes it very attractive for use in balloon tethering. Testing done to date reveals no reason why this material cannot be employed in this application.

XIII. Instrumentation for High-Altitude Tethered Ballooning

Edward C. Mangold
Oklahoma State University
Stillwater, Oklahoma

Abstract

Details are presented on instrumentation chosen for the monitoring of the aerodynamic performance of a high-altitude tethered balloon system. Modern aerospace transducers have been chosen for compatibility with an FM/FM telemetry system as well as low weight and power consumption and the ability to withstand the rigors of the high altitude environment. Particularly troublesome instrumentation problems are encountered in measuring the angle which the tether makes with the vertical at the base of the balloon in the presence of horizontal accelerations of the instrumentation package, and in the measurement of low wind velocities at high altitudes. Instrumentation requirements have been considered primarily for spherical or natural shaped balloons with some consideration given to the additional measurements necessary for monitoring the performance of aerodynamically shaped balloons.

Oklahoma State University has conducted an inquiry into the instrumentation requirements necessary to monitor the aerodynamic performance of tethered balloon systems operating in the altitude region of 50,000 to 100,000 ft. In addition to providing the engineering information necessary for the construction of packages for high altitude experiments, the system will also be required to furnish the flight

director information in real-time relating to the performance of the balloon system over a period of time up to seven days.

Telemetry system selection was influenced by the need for real-time readout of critical instrumentation parameters and the desire to utilize as few channels as possible for the instrumentation requirements, leaving the majority of the telemetry system information capacity for use by a prime experiment carried on the balloon. These considerations led to the selection of an FM/FM telemetry system using a 2-pole data commutator for the majority of the instrumentation parameters with critical elements necessary for the monitoring of balloon performance, such as the cable tension, also presented on individual subcarrier channels for real-time monitoring.

In addition to cable tension, the airborne data to be monitored consists of the atmospheric pressure and temperature, the balloon gas temperature and differential pressure of the balloon gas with respect to the atmosphere, the wind velocity, the cable angle measured with respect to vertical (which is required for calculating the drag force on the balloon) and information concerning the changing of the package and balloon orientation in time. Supplementation of the airborne data with additional information measured from the ground should enable the aerodynamic performance of the tethered balloon system to be determined. These parameters will include the cable tension and angle with vertical measured at the winch, total length of extended tether, the position of the balloon with respect to the winch which will be monitored by means of theodolite or radar, and radio and measurements of the horizontal wind profile.

Measurements of ambient air pressure and balloon differential gas pressure will be made using modern aerospace transducers selected for minimum weight and size, low power consumption, and outputs directly compatible with the airborne telemetry system. Temperatures of the ambient air and balloon gas will be measured using the miniature bead thermistor technique. Because of the difficulty of rigging thermistors throughout the balloon volume during the launch process, only one measurement of temperature will be made of balloon gas at a position near the base. Balloon gas temperature and differential pressure measurements will indicate the effects of solar radiation on balloon superheat and enable detection of balloon failure as indicated by loss of superpressure. Temperature measurements will also be made of critical components, such as the batteries inside of the instrumentation package, and critical transducers, such as the load cell for the cable tension measurement which requires a correction to be made in the data to adjust for the temperature of the transducer. Through the use of stable bridge voltage power supplies, correction of the data for the temperature of the strain gage load cell and inflight calibration of the telemetry system, it is expected that the measurement of the critical cable tension parameter can be made with an error of less than one percent.

Measurement of the angle which the tether makes with respect to the vertical by means of a pendulum type sensor is complicated by the fact that such sensors also respond to horizontal accelerations which the balloon may experience. Since the predicted tether angles are at most only a few degrees and less than one degree under some circumstances, very small horizontal accelerations will cause serious errors in the measurement of this parameter since a horizontal acceleration of 0.1 g will give the same deflection to a pendulous mass sensor as will a tilt angle of six degrees. Attempts to correct the output of the pendulous mass sensor with a horizontal accelerometer are frustrated by the fact that the output of a horizontal accelerometer is itself influenced by the tilt of the instrumentation package. The outputs of the two transducers are so close that, within instrumental errors, it is impossible to determine whether the output of the pendulum is due to a tilt of the instrumentation package, due to the tension on the tether, or a horizontal acceleration due to wind forces on the balloon and tether.

Although optical horizon sensors can give accuracies of small fractions of a degree when mounted in satellites, the optical horizon is defined only to an accuracy of two or three degrees when observed from a station situated within the atmosphere so the required accuracy cannot be achieved. Other possible techniques considered for determination of tether angle include measurements of the orientation of the package with respect to the earth's magnetic field or optically made measurements of the angle to a solar, lunar, or stellar reference object. To obtain aspect information to an accuracy of less than one degree is difficult to achieve with a magnetic aspect sensing system unless a servo-driven nulling technique is used. Measuring attitude with respect to an astronomical object for flights of several days duration would lead to a formidable data reduction problem. Although the information could be obtained from an inertial platform similar to that used on guided missiles, the increase in complexity, weight of the airborne system, and cost are so large that this approach does not seem warranted.

Balloon and package rotation about the vertical axis can be monitored by two magnetic aspect sensors mounted orthogonally in the horizontal plane. Package accelerations along the vertical axis can be monitored with a vertical accelerometer, but horizontal acceleration measurements are complicated by the influence of the earth's gravitational field due to tilt of the instrumentation package as mentioned in the discussion of the measurement of tether angle.

The measurement of wind velocity or wind direction by means of devices such as pitot probes is complicated by the low values of dynamic pressure at high altitude. The response of mechanically rotating anemometers has not been investigated under high altitude conditions, but it is predicted that the output will be adequate once wind velocity is raised above a critical low velocity region where the drag forces on the rotating elements are only marginally greater than those required to overcome bearing friction. Calibration runs on mechanical anemometers

will be made in the near future by rotating the devices on the end of an arm in a large environmental test chamber.

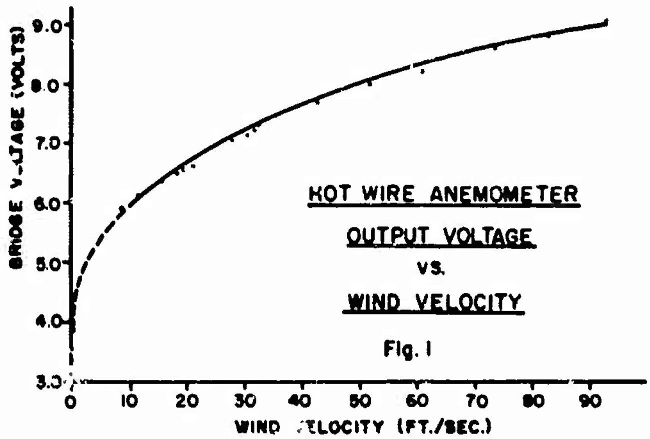

Figure 1. Hot Wire Anemometer Output Voltage vs Wind Velocity

The unique output response of a hot wire anemometer as a function of air density and velocity in which the output voltage varies as the fourth root of the wind velocity (King's law) seems favorable for the measurement of low wind velocities under high altitude conditions (Figure 1). Unfortunately, the output of a hot wire anemometer is also a function of the temperature difference between the wires and and the air, as well as wind velocity and air density. Due to the fragility of the thin hot wire probes commonly used, investigation was made into the use of the substantially more rugged deposited thin film probes. However, due to the wide temperature range over which the probes are expected to work at high altitudes, (-30°C to -90°C) it has not been possible to compensate adequately the probes for changes in air temperature. Calibration runs have been attempted on the hot film probes at the University of Minnesota Aero-Hypersonic Laboratory but problems of wind tunnel readout in the low velocity, low density region, restricted the data which were obtained to a velocity range of 75 ft/sec to 350 ft/sec which is considerably higher than that expected at tethered balloon altitudes. Test data taken with a rms error of two percent at a simulated altitude of 50,000 ft increased to nine percent at a simulated altitude of 100,000 ft. The hot film anemometer has also been calibrated by the rotating arm technique in an environmental simulation chamber which could produce both the air pressure and temperature at balloon altitudes. The rotating arm technique permits accurate generation of low relative velocities between air and probe but has the disadvantage of a higher turbulence level since the probe is traversing its own wake.

The monitoring of the rotation of an aerodynamically shaped balloon on the pitch, yaw, and roll axis may be conveniently accomplished with miniature rate gyros which can be caged at the beginning of a data gathering cycle to reference directions with respect to the balloon axes. The detection of the angle of attack and side slip of the balloon with respect to the wind direction can be monitored by two hot wire probes orthogonally mounted in the shape of the letter X. Since the

output of the wire is also a function of the direction which the wind velocity makes with the axis to the wire, the relative direction of the wind with respect to the probe will cause proportional changes in the outputs of the two wires so that the wind direction over a 90 degree span can be determined. Care must be taken, however, to mount the probe in an appropriate position with respect to the aerodynamically shaped balloon so that the flow is undisturbed by the presence of the balloon. Since this may require the rigging of long booms, wind tunnel testing may be required in order to determine the proper location for such probes.

The monitoring of high-altitude tethered balloon systems represents the extension of aeronautical engineering measurement techniques into a range of parameters which are in some cases considerably different from those encountered in aircraft practice and which are different from those used in low altitude lighter-than-air vehicles. The extension of these techniques offers considerable challenge to the instrumentation engineer.

Acknowledgments

The author wishes to acknowledge the support of the Advanced Research Projects Agency which funded this study under Contract ARPA F19628-67-C-0163 and Mr. Robert M. Bogart of the Air Force Cambridge Research Laboratories, who served as Contract Monitor. Gratitude is also due to Mr. Richard F. Buck, Projects Director of the Oklahoma State University Research Foundation Electronics Laboratory, Mr. Roy Larson of the North Star Research Institute, and many other individuals too numerous to mention, who have provided many of the ideas presented in this paper.

XIV. Glass-Epoxy Composite Cables for Tethered Balloons*

G.L. Hanna
Monsanto Research Corporation
Dayton, Ohio

Abstract

The 3/16-in. diam Glastran (a glass-epoxy composite) and steel cables were tensile tested to determine the breaking load and strength-to-weight ratio for each material. The absolute breaking load for the Glastran (4040 lb) was comparable to that of the steel (4270 lb). However, the strength-to-weight ratio of the Glastran was approximately three times that of the steel. Both materials were endurance tested over pulley-to-cable diameter ratios of 40:1 and 30:1. Subsequent tensile tests which indicated a degradation in strength resulted only in the Glastran when flexed over the 30:1 pulley-to-cable diameter ratio. Stress rupture (sustained load) testing of the cables at 50, 60, and 70 percent of their respective tensile strengths for 30-day periods revealed the Glastran to have superior resistance to creep and equal or longer times to failure than the steel. Both cables failed within 30 days (720 hours) when loaded at 60 and 70 percent of their tensile strength and neither cable failed at 50 percent of break strength. The higher strength-to-weight ratio and creep resistance of the glass-epoxy composite cable indicate that it should receive increased attention for use in tethering balloons.

---

*This work was conducted under Contract Nr. F33615-67-C-1315 under the direction of Mr. William Rooney, Materials Application Division, Air Force Materials Laboratory, Wright-Patterson Air Force Base, Ohio, and Captain E.F. Young, Air Force Cambridge Research Laboratories, L.G. Hanscom Field, Bedford, Massachusetts.

1. INTRODUCTION

The tethering of balloons requires a material possessing a strength-to-weight ratio significantly higher than that of the commonly employed zinc-coated steel aircraft cable. A prime candidate for this application is a glass-epoxy composite that exhibits a 300 percent improvement in strength-to-weight ratio over the same diameter steel cable. The purpose of this program was to determine and compare the endurance and stress rupture characteristics of 3/16-in. diam glass-epoxy and steel cables.

2. MATERIALS

The cable currently employed in tether programs is a zinc-coated steel aircraft cable supplied by U.S. Steel Corporation. It is 3/16 in. in diameter, excelloy preformed, and of a 7 × 19 construction. The minimum tensile break strength is 4200 lb. This type cable was tested along with a glass-epoxy composite cable in order to obtain a comparison of the two materials. The composite cable, Glastran, is manufactured by the Packard Electric Division of General Motors Corporation. Glastran is a glass fiber cable made of continuous filaments of high-strength glass impregnated with epoxy resin. Many filaments are assembled into strands that are then cabled together similar to conventional rope. The 3/16-in. diam cable tested consisted of a 1 × 19 construction and was protected from excessive abrasion by a 0.015-in. urethane jacket. The minimum break strength of this cable is 3800 lb.

3. TEST PROCEDURES

Tensile testing was conducted on a 15-ton capacity Riehle testing machine at strain rates of 0.010 and 0.0167 in./in./min. The gage length of all tensile specimens was between 27 and 28 in. The cables were splayed at both ends and potted in ferrules using an epoxy for the Glastran and solder for the steel. The Glastran cable specimens were potted by the Packard Electric Division of General Motors according to a standard procedure described in their catalogue, "Glastran Cable." The steel specimens were potted in steel ferrules, using Eutecrod 157. The end fittings and testing grips for each cable are shown in Figure 1.

The 30-day stress rupture (sustained load) tests employed the same specimen types used in tensile testing. As many as three samples of each material were dead weight loaded on Arcweld creep rupture machines to 50, 60, and 70 percent of the cable breaking strength. The creep of the cables was measured as a function of time at load for each material and load combination by placing a linear voltage differential transformer beneath the movable crosshead.

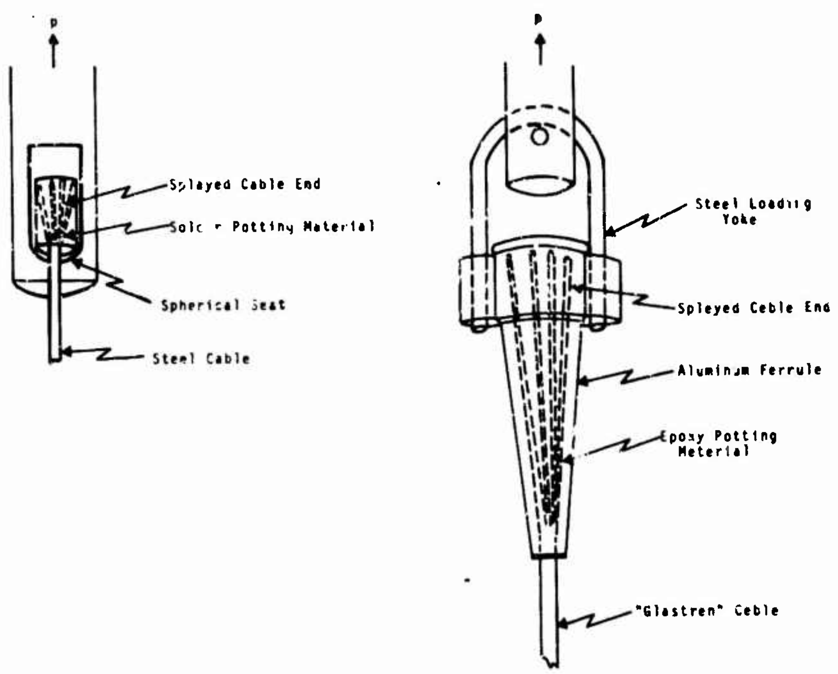

Figure 1. Schematic of End Fittings and Loading Fixtures Employed for Tensile and Stress Rupture Testing of Glastran and Steel Cables

Endurance testing was accomplished according to the proposed military specification for "Cable, Epoxy Impregnated Glass Fiber, Flexible," shown schematically in Figure 2. The 3/16-in. cables are tested employing pulley-to-cable diameter ratios of 40:1 and 30:1. In all cases the cable was flexed over the pulley for 130,000 complete cycles at a rate of approximately 60 cpm. Post-endurance tensile breaking strengths were then determined for the section of cable flexed over the pulley. In some instances the unflexed end of the sample was also tensile tested to better define the degradation due to the flexing action.

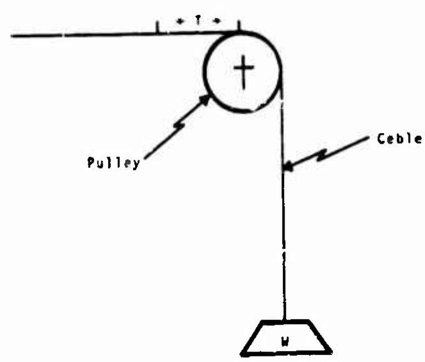

T = Travel distence shall be 12 inches at 60 cycles or 120 reversels per minute.
W = Test weight of 45 pounds.

Figure 2. Schematic of Endurance Test Method

4. RESULTS AND DISCUSSION

Tensile tests were conducted on the steel and Glastran 3/16-in. diam cables at two strain rates. As shown in Table 1, the anticipated strain rate dependence of the glass-epoxy composite cable was revealed. Average breaking loads of 3545 and 4040 lb resulted at strain rates, $\dot{\epsilon}$, of 0.01 and 0.0167 in./in./min, respectively. The faster strain rate represents that employed by Packard Electric, and resulted in tensile strengths in excess of the minimum quoted by them (that is, 3800 lb). The strength of the steel cable appeared to be lowered slightly by increasing the strain rate (see Table 1), and two samples tested at 0.0167 in./in./min failed slightly below the minimum break strength of 4200 lb.

A strength-to-weight ratio was calculated for each material and testing speed combination. As shown in Table 1, the Glastran cable exhibited approximately three times the strength-to-weight ratio of the steel.

Table 1. Breaking Loads of 3/16-Inch Diameter Glastran and Steel Cables

Material	Construction	Manufacturer	Strain Rate, $\dot{\epsilon}$ (in./in./min)	Average Breaking Load (lb)	Strength-to-Weight Ratio* (lb/lb/100 ft)
Glastran	1 × 19 with 0.015 in. urethane jacket	Packard Electric Division of General Motors	0.010	3545	1520
			0.0167	4040	1730
Steel	7 × 19 with zinc coating	U.S. Steel	0.010	4430	680
			0.0167	4270	605

*Strength-to-weight ratio equals breaking load weight per 100 ft of cable.

Samples from each cable material were endurance tested over pulley-to-cable diameter ratios of 40:1 and 30:1. This test is designed to simulate cyclic winding and unwinding on a winch, and to determine if a degradation in tensile strength results. As shown in Table 2, the Glastran that was flexed over the 30:1 ratio was the only material-test condition combination to result in a measurable degradation in properties. The low break strengths of two Glastran cables flexed over the 40:1 ratio were attributed either to damage during shipment or to an inhomogeneity in the material.

Stress rupture (sustained load) tests were conducted on both cables at 50, 60, and 70 percent of their respective breaking loads (determined at $\dot{\epsilon}$ = 0.01 in./in./min).

Table 2. Break Strength of Endurance Tested 3/16-Inch Diameter Cables
($\dot{\epsilon}$ = 0.0167 in./in./min)

Cable Type	Pulley-to-Cable Diameter Ratio	Breaking Load (lb) Flexed End	Unflexed End
Glastran	40:1	3420	3275
		3515	3500
		3800	4200
	30:1	2515*	4600
		3750	4225
		3630	4400
Steel	40:1	4270	....
		4220	....
		4270	4270
	30:1	4565	....
		4520	....
		4270	....

*Cable damaged in potting operation.

The cables were loaded for 30-day (720-hour) periods, and the creep (or elongation of the cable as a function of time under load) was measured for each cable and load combination. As shown in Table 3, the glass-epoxy composite cable was equal or superior to the steel cable when loaded at any given percentage of breaking load.

Table 3. Sustained Load Tests of 3/16-Inch Diameter Cables

Cable Type	Load (% of BL)	Failure Time (hr)	Total Percent Elongation (% in 28 inches)
Glastran	70	219.3	0.19
		68.4*	
		26.0*	
	60	568.1	0.18
		634	
		720 (NF)	
	50	737 (NF)	0.08
		1130 (NF)	
Steel	70	25.1	1.20
		16.2	
		2.1	
	60	555.1	1.25
		236	
		720 (NF)	
	50	720 (NF)	0.95

*Shear Failure
NF - No Failure

Both materials failed within relatively short times when loaded at 70 percent of breaking load, and two out of three of both cables loaded at 60 percent failed within 720 hours. Neither cable exhibited a failure within 30 days when loaded to 50 percent of its breaking load. In instances where failures occurred, the Glastran generally exhibited a longer time to failure than did the steel cable.

The Glastran was also superior to the steel under sustained load in its creep characteristics. The elongation per unit time under load was approximately 10 times smaller for the glass-epoxy composite than for the steel, as shown in Table 3 and Figures 3 and 4. Elongations in excess of 1 percent were observed in the steel cables under all loading conditions, and a maximum of 0.18 percent elongation was measured on the Glastran cable.

5. CONCLUSIONS

1. The glass-epoxy composite cable Glastran possesses three times the strength-to-weight ratio of steel cable of a similar diameter, and in addition has an absolute strength nearly equal to that of steel.

2. The Glastran can be degraded by approximately 10 percent in tensile strength by endurance testing over a 30:1 pulley-to-cable diameter ratio. Therefore, Glastran probably should not be wound on a winch with a spool diameter less than 40 times the cable diameter.

3. The stress rupture characteristics of the two cables are similar from a time to failure standpoint. However, the Glastran cable undergoes significantly less creep than the steel at any given load.

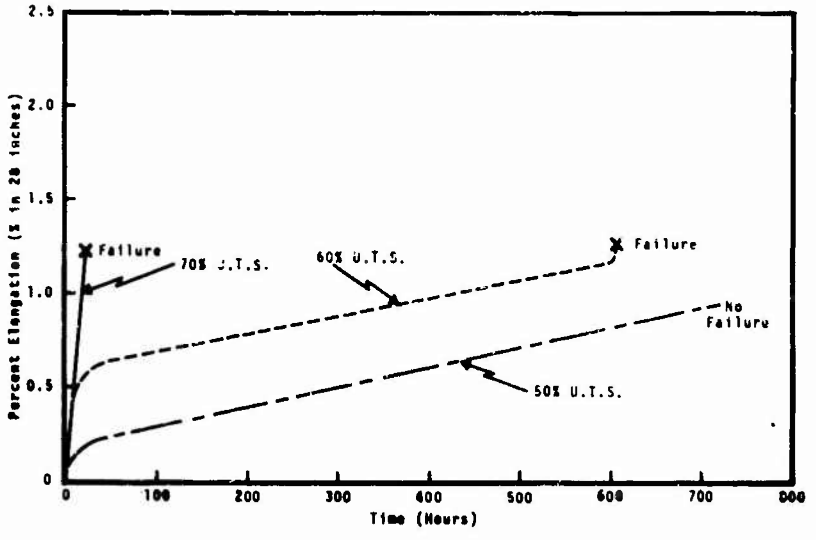

Figure 3. Creep Rupture Curves of 3/16-in. Diam Steel Cable Loaded to Various Percentages of Ultimate Tensile Strength

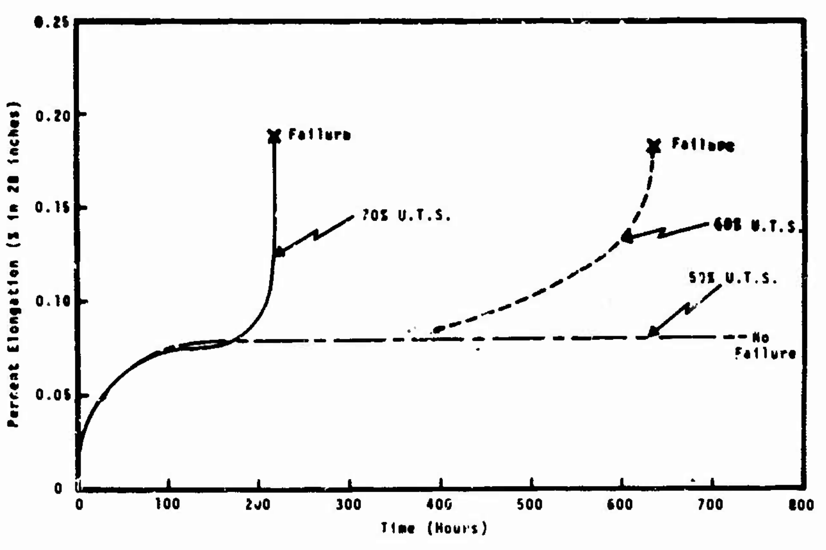

Figure 4. Creep Rupture Curves of 3/16-in. Diam Glastran Cable Loaded to Various Percentages of Ultimate Tensile Strength

XV. General Purpose Balloon Tethering Winch

Lewis A. Grass
Air Force Cambridge Research Laboratories
Bedford, Massachusetts

Abstract

This paper describes a traction drive winch system capable of handling 1/8- through 3/8-in. cable with loads up to 12,000 lb. A 110-hp Ford industrial engine powers a unique hydraulic system. This system can operate with stepless control between 0 and 1000 ft/min and provides controlled tension to the storage drum. Traction drive, level wind, and fairlead assembly have been coated with PVC to minimize abrasion of the cable.

For the past three years, AFCRL has been involved with low-altitude tethered balloon flights. Many of these flights have employed a three-line tethered concept to deploy the balloon and instrumentation over a specified position on the ground. Other flights have been made with a single line tether system using the Vee, Class C, and natural shape balloon. Generally speaking, the flights have been successful. Of course, we have had our share of problems.

During this time we have recognized certain deficiencies and have tried to correct them. One thing was certain, the need for a flight test facility where balloon systems could be evaluated was paramount.

I should like to take a brief moment to discuss a tethered flight facility now under construction on the White Sands Missile Range, New Mexico, where we intend to use the General Purpose Winch, the subject of my talk today. Here we can tether to unlimited altitudes where our only restrictions will be range scheduling and adverse meteorological conditions. This area has been investigated; and it does not appear to be a serious threat to an all year capability. Site selection was based upon availability of restricted air space and availability of a fully instrumented range. The site is located within 70 miles of AFCRL's R & D Balloon Flight Facilities, Holloman AFB, New Mexico.

Figure 1 depicts the general layout. The main winch assembly which is mounted on a flatbed trailer has been moved from its normal location at ground zero to a position 20 ft beyond a 40 ft high wind screen. The distance from ground zero to a side of a proposed octagonal shaped wind screen is 80 ft. A sheave assembly mounted on an adjustable steel framework is positioned at the winch. This assembly will serve two purposes: (1) to transfer the tethered cable from the winch level to ground level, and (2) to measure cable parameters. The mechanism has been designed to record cable tension, speed and footage; it can be used with either

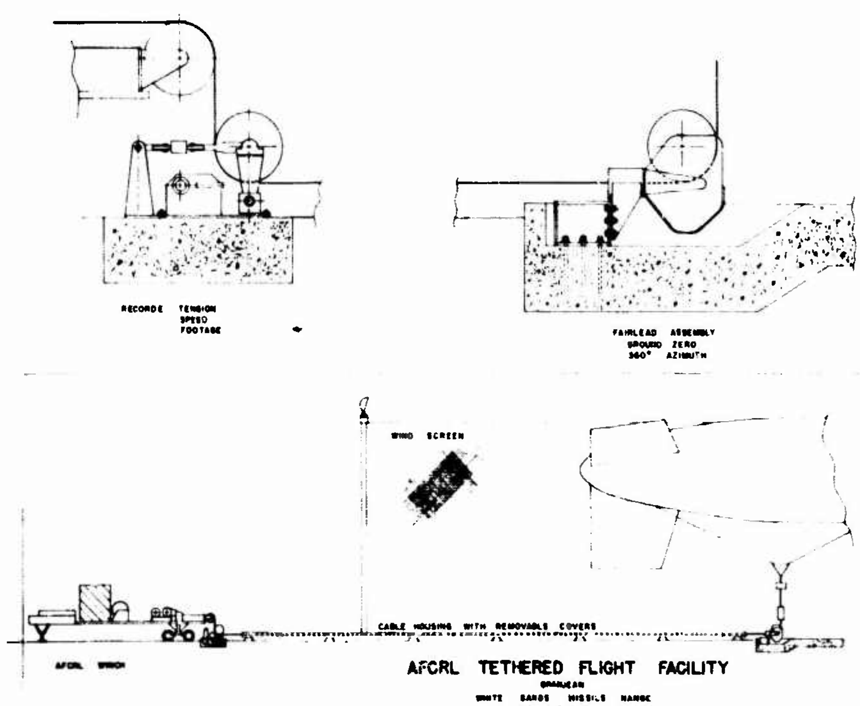

Figure 1. Tethered Site Layout

steel or fiberglas cable. The work on this site consists in emplacement of concrete pads for fairlead assembly, sheave assembly and protective housing for the tethered cable. The installation of a wind screen and additional ground handling equipment is planned for a later date.

A procurement was initiated to obtain a general purpose balloon tethering winch which is the heart of the tethered site. Specifications were prepared based upon our experience. In order to enhance the versatility of the winch, we included special features such as inhaul and outhaul speeds up to 1000 ft/min with stepless control, constant cable tension control for very low altitude applications, traction drives with adapters (that can be changed in the field) to accommodate various size cables, a suitable plastic coating in the sheave grooves to minimize abrasion of the cable, and specially designed storage drum assemblies to accommodate various size cables. Selection of a hydraulic system for power transmission offers smooth control, mobility, and is self contained. A contract was signed with Smith-Berger located in Seattle, Washington, for the manufacture of the winch.

The winch is capable of handling inhaul and outhaul speeds up to 1000 ft/min (including stepless control) with a 1200-lb line tension. Increasing the cable tension to 4000 lb decreases the inhaul speed to 300 ft/min. The winch is capable of handling up to 12,000 lb at approximately 100 ft/min. Limited speeds of 1000 ft/min are due to the maximum revolutions per minute restrictions of the hydraulic motors and pumps. At this speed the traction drives are rotating at the respectable rate of 180 rpm.

It is possible to accommodate cable sizes ranging from 45 to 400 mils by selection of traction sheave adapters and fairlead assemblies. Both the storage drum and level wind can be easily modified to accommodate any required changes.

Theoretical power requirement for the traction drive is 46 hp. The storage drum and other components require an additional 20 hp. The power unit develops 76 hp at 1800 rpm. The main winch assembly can be installed in an 8 × 25 ft area. In our case, we plan to install the winch on a flatbed, making the winch somewhat mobile.

It is possible to adjust the cable tension between the storage drum and the traction drive by a valve located on the control panel. Tension range is between 50 and 200 lb.

Figure 2 shows the over-all side view of the winch which consists of two basic units, a power pack, and the main winch assembly.

Figure 3 depicts the main winch assembly which consists of traction drives and traction drive gear reduction unit (11.3/1), storage drum with gear reduction unit, level wind assembly, hydraulic motors and necessary hydraulic components. A removable tensiometer, which monitors and measures tension, speed, and footage of a moving line, is mounted between the fairlead assembly and traction drive.

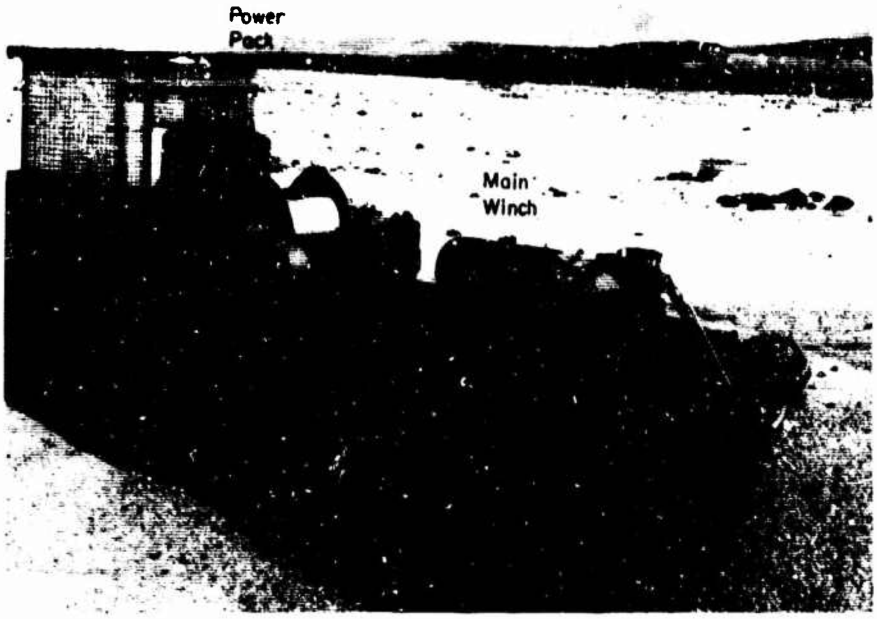

Figure 2. Over-all Side View of AFCRL Winch

This unit has been calibrated for use with 1/8, 3/16, 1/4, and 3/8-in. steel cable. The device is not suitable for fiberglas cable since it employs three steel sheaves of small diameters.

Four pairs of traction drive adapters are supplied with the winch. They have been designed to handle 1/8, 3/16, 1/4, and 3/8-in. cable. The sheave diameter is 20 in. Sheave grooves have been coated with polyvinyl chloride having a durometer of approximately 75. The forward sheave is directly coupled through a gear reducer which in turn is driven by two Vickers in-line piston type hydraulic motors. The aft sheave is coupled to the forward sheave by a chain drive. A disc brake to handle static loads when the winch is shut down has been mounted between the gear reducer and hydraulic motor located on the left-hand side of the winch looking forward toward the fairlead assembly. Mechanical braking is accomplished through the use of heavy duty compression springs. Braking is relieved by hydraulic pressure once the traction sheave motors experience pressure and are put into motion. Winch components have been mounted on a 5 × 14 ft frame.

The fairlead assembly has been designed to accommodate 1/8 through 3/8-in. cable and is also coated with polyvinyl chloride.

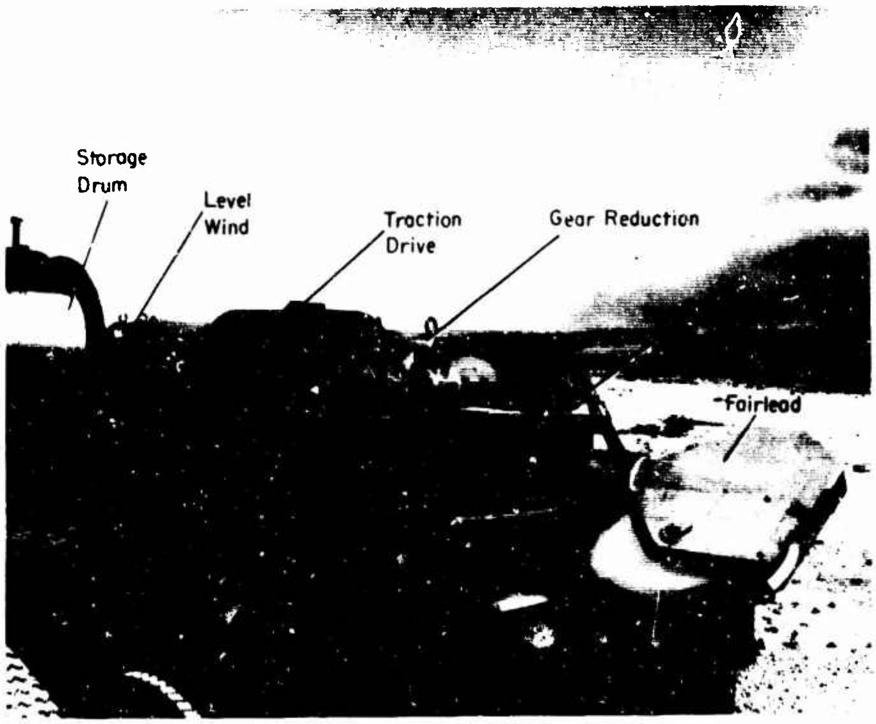

Figure 3. Side View of Main Winch Assembly

Figure 4 is a view of the storage drum and level wind assembly. Four storage drums will be provided with the winch. These drum assemblies, equipped with trunnions, can easily be changed in the field. The design is such that the alignment problems have been held to a minimum. The storage drum capacities are as follows:

Diameter Cable Capacity	Feet
1/8	104,600
3/16	47,600
1/4	26,250
3/8	11,650

For those who may be speculating, the storage drum has a potential capacity of 195,000 ft of 90 mil cable. The level wind assembly is mechanical and can be designed to accommodate any size cable. Vertical and horizontal guides associated with the level wind have been designed to a maximum possible diameter to minimize bending stresses. Total fleet angle is approximately 15° with an arc contact of approximately 3/4 of an inch for the 4-in. diam sheave guides, which have also been

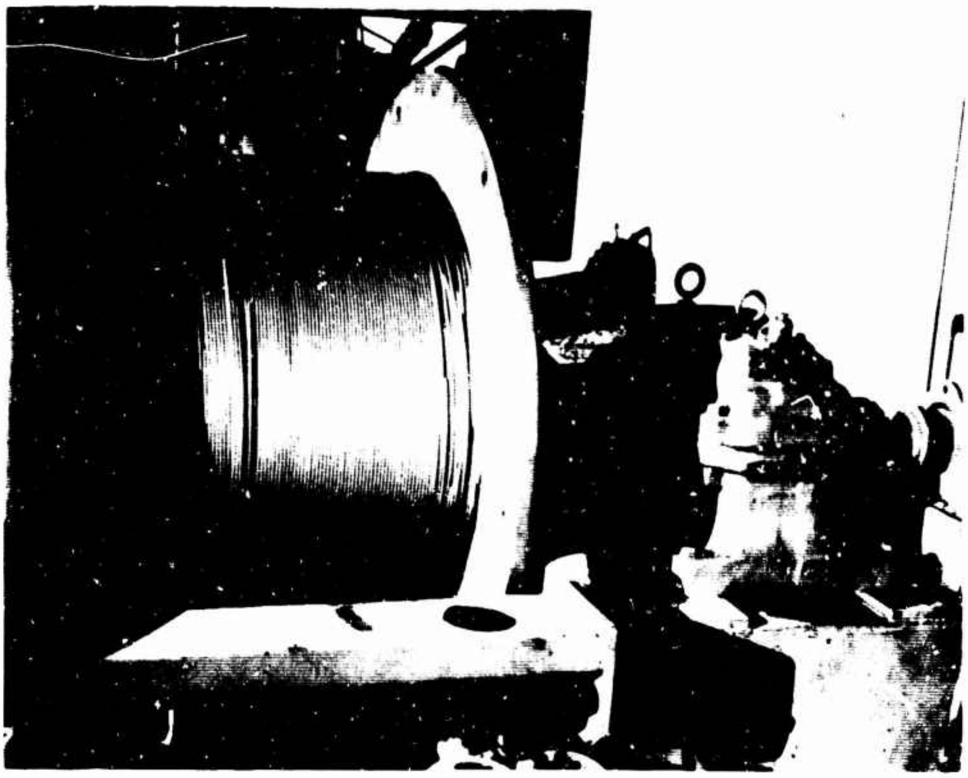

Figure 4. Storage Drum and Level Wind Assembly

coated with polyvinyl chloride. Four sets of sheave guides will be furnished with the winch. Each set has been grooved to accommodate 1/8, 3/16, 1/4, and 3/8-in. diam cable.

Adjustment of the level wind for the different cable sizes is accomplished by changing sprockets and chain combinations. These combinations have been properly marked for easy identification of each cable size. The storage drum and level wind assembly are driven by a piston type hydraulic motor through a 14 to 1 gear reducer.

The power pack is mounted on a subbase which incorporates a tank for the hydraulic system. The subbase is approximately 5 × 3-1/2 × [illegible] ft high. Hydraulic components include two main variable displacement piston pumps and one smaller variable displacement pump which provides power for the storage drum assembly and maintains initial supercharge pressure for the hydraulic system. These pumps are driven by a heavy duty Ford Industrial Power Unit capable of delivering 110 hp at 2800 rpm. Every available space on the subbase is occupied by various pressure relief valves, directional control valves, and necessary hydraulic plumbing.

The control panel is located on the right-hand side of the power pack assembly. Directly in front of the control panel are instruments which record cable tension, speed, and cable footage. In the upper right-hand corner of the control panel, full operating instructions are engraved on a brass plate.

A heavy duty protective cage mounted around the power pack and in the vicinity of the control panel provides protection for the winch operator.

It would be somewhat presumptuous to think that this winch would satisfy all tethered balloon requirements. We should like to think that it will meet a good many of our requirements and serve as a useful research tool for further development. This piece of equipment has passed preliminary acceptance tests and has been delivered to Holloman AFB where final acceptance tests are planned for the last week in October 1967.

XVI. Description and Performance Characteristics of a Captive Airfoil Balloon System Used in the Initial Phase of the Aeropalynologic Survey Project

Mendel N. Silbert
National Aeronautics and Space Administration
Wallops Island, Virginia

Abstract

The purpose of this paper is to present results of a system analysis and operational evaluation of a captive airfoil balloon system. The system was used operationally in support of an Aeropalynologic Survey Project at NASA Wallops Island, Virginia, during the summer of 1966.

I. BACKGROUND

The project requirements included the need for a system capable of lifting itself and a payload up to and including an altitude of 1,000 ft, remaining aloft for a one-week period, and capable of returning usable data to the ground. The short time increment between request and need for a lifting system did not permit specification, procurement, and evaluation of a new system. However, an available balloon system, operationally employed by the local Environmental Science Services Administration personnel, was used.

2. GENERAL DESCRIPTION

The subject system, referred to as a Kytoon, is an airfoil balloon which is sustained aloft by both aerostatic and aerodynamic forces. The Kytoon, which is manufactured by Dewey and Almy Company, is a four-finned airship consisting of a nylon casing, muslin tail fin assembly, nylon harness, rubberized shock cord, and a neoprene bladder, the latter serving as the gas envelope (Reference 4). The Kytoon is a symmetrical airfoil in the form of a body of revolution which is circular in cross section and elliptical along its longitudinal axis, the curve of which is given by

$$y = 0.6696 + 0.7132x - 0.0823x^2$$

where

y = the ordinate from the centerline and
x = the abscissa along the centerline.

The preceding equation was determined by the Method of Least Squares for Curve Fitting which was programmed into the GE-625 digital computer at Wallops Station, Virginia. The properties of the Kytoon are given in Table 1.

3. DETAILED DESCRIPTION AND PHYSICAL CHARACTERISTICS

The Kytoon, shown in Figures 1, 2, and 3, is 9.25 ft in length and has a maximum diameter of 4.350 ft, giving it a fineness ratio of 2.11. Its noninflatable fins, which are in a cruciform arrangement, have an area of 4.87 sq ft per fin. The bridle system consists of two sections of 170-lb test braided nylon line, one section of bungee shock cord and two brass harness couplings, one of which acts as the attach point for the tether line. Figures 1 and 3 show the arrangement of the bridle system in a tethered flight condition. It should be noted that by adjustments to the rigging of the bridle system, the point of attachment and conditions for equilibrium are changed.

Since the Kytoon is a nonrigid airship, its shape depends on the pressure of the lifting gas contained in the gas envelope. In addition to the loss of buoyancy, a decrease of the pressure inside the gas envelope will cause the Kytoon to become limp. Several gases which are lighter than air include coal gas, hydrogen, and helium. Due to the dangers involved and the nonavailability of the first two gases mentioned, helium was used to inflate the Kytoon. The properties of air and helium are given in Tables 2 and 3.

Table 1. Properties of Kytoon

Length	ft	9.25
Maximum diameter	ft	4.350
Fineness ratio		2.11
Volume	ft^3	87.791
F_B at 1A at sea level	lb	6.705
Weight	lb	3.1
Usable free lift	lb	2.134
Number of fins at 90° spacing		4
Area of each fin	ft^2	4.87
C_D		See Figure 6
C_L		See Figure 6
α	deg	7.5
β	deg	0
Permeability to helium per 24 hr	% usable free lift	15
Static efficiency $\frac{L_S}{F_B}$	%	32
Break strength	lb	160
Weight per 1,000 ft	lb	1.28
Spring constant at 95 lb tension and initial length of 10 ft	lb/ft	47.5
Stretch of 10-ft length after 95 lb tension is applied and released	%	1.58
Material	Nylon	
Type of construction	Braided	

Table 2. Properties of Air

Molecular weight		29
R	ft/°R	53.3
ρ at sea level	slugs/ft^3	$(2.377)10^{-3}$
ρ at 1,000 ft	slugs/ft^3	$(2.308)10^{-3}$
μ at sea level	lb/sec/ft^2	$(.38)10^{-6}$
μ at 1,000 ft	lb/sec/ft^2	$(.371)10^{-6}$
γ at sea level	lb/ft^3	0.07647
γ at 1,000 ft	lb/ft^3	0.07428
P at sea level	psi	14.69
P at 1,000 ft	psi	14.17
T at sea level	°R	519
T at 1,000 ft	°R	515.4

Table 3. Properties of Helium

Molecular weight		4
R	ft/°R	386
μ at 68°F	lb/sec/ft^2	0.0411
ρ at sea level	slug/ft^3	0.003276
γ at sea level*	lb/ft^3	01066
γ at 1,000 ft*	lb/ft^3	01036
P at sea level*	psi	14.834
P at 1,000 ft*	psi	14.314
T at sea level*	°R	519
T at 1,000 ft*	°R	515.4
He unit lift at 1A at sea level	lb/ft^3	0.062
He unit lift at 100°F at sea level	lb/ft^3	0.058

*Condition of He inside Kytoon.

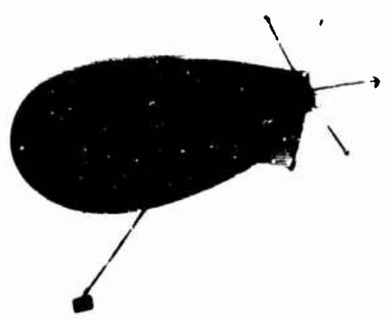

Figure 1. Kytoon in Tethered Flight

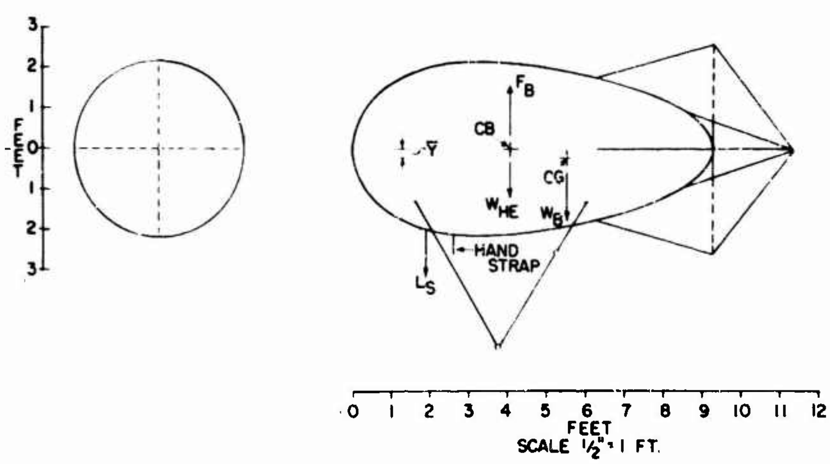

Figure 2. Free Body Diagram of the Kytoon on an Even Keel in Calm Air

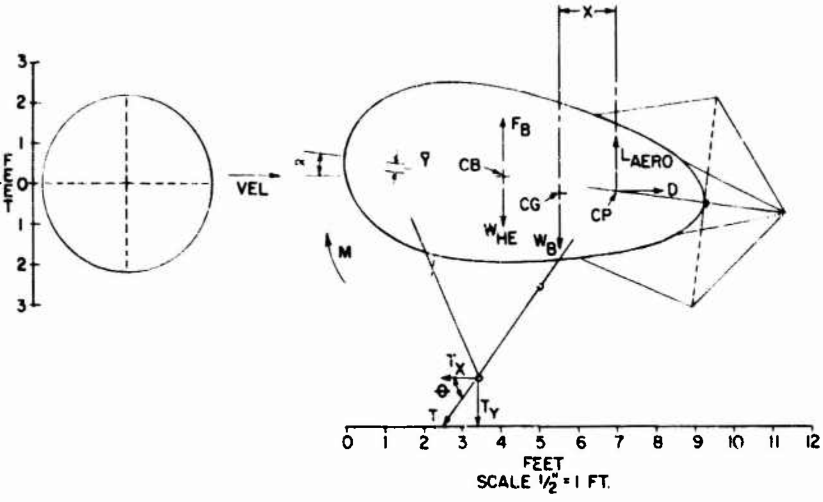

Figure 3. Free Body Diagram of the Kytoon in Tethered Flight

In order to determine the design strength of the tether line, loads on the Kytoon were investigated for the worst possible flight condition in a maximum wind of 30 mph. Since the optimum months for obtaining usable scientific data appeared to be April, May, and June, a statistical analysis was conducted for the winds on Wallops Island for these months (References 6, 7, and 8). From this statistical analysis, it was concluded that the probability was greater than 90 percent that these winds would be less than the design wind of 30 mph. It was found that the worst flight condition was that of a cylinder in cross flow, or that the Kytoon would have an angle of attack of 90°. For the cross-flow condition, the drag force was determined to be 93 lb for the design wind speed. A safety factor of 1.5 was incorporated, giving a minimum design break strength of the tether line of 140 lb.

Since a high strength-to-weight ratio was desired, wire rope, steel wire, and other types of line were eliminated owing to their low strength-to-weight ratio. Two types of line found to have the desired strength-to-weight ratio include twisted and braided nylon. For a given break strength, the twisted nylon was found to be 14 percent lighter than the braided nylon. However, experience has shown the following characteristics of the two types of line:

a. Braided nylon remains straight instead of knotting up in itself as does twisted nylon line when tension is continuously applied and released.

b. Twisted nylon will "friction wear" quicker than braided nylon ("friction wear" - rubbing against itself).

c. Braided nylon acts as a better shock absorber than does twisted nylon due to the variations of their respective spring constants. These spring constants

were determined at Wallops Station, utilizing a spring scale and tape rule to measure the force and elongation, respectively.

Based on this experience, 160-lb braided nylon bow string was used as tether line. The tether line was attached to the Kytoon by means of an attach swivel. A modified slip knot, which was experimentally determined to have a knot efficiency factor of greater than 95 (Reference 1), was used to connect the attach swivel to the tether line. The tether line was connected to a 3.5 to 1 hand-operated cable winch assembly, which was used to raise and lower the Kytoon. This winch was modified to be a 1 to 1 hand-operated cable winch in addition to the original 3.5 to 1 hand-operated cable winch. This modification was put into effect in order to reduce the possibility of contamination to the payloads during the raising and lowering of the Kytoon, which takes 10 to 13 min, respectively. The payload consisted of a microscope slide mounted in a pollen trap. The slide has an adhesive area capable of capturing and retaining any airborne particle which may come in contact with it. The pollen trap, as shown in Figure 4, designed and fabricated at Wallops Station, provides a means of suspension for the slide, protecting it from coming in contact with any undesirable airborne particles. Due to weight considerations and possible corrosive reactions, the pollen trap is nonmetallic and covered with a nonmetallic screen of 250 US Standard mesh (Reference 1). The pollen traps weigh approximately 100 grams each.

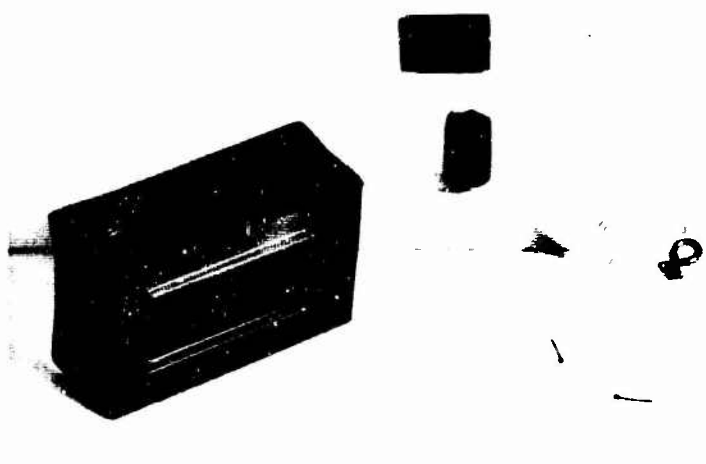

Figure 4. Pollen Trap

In order to prevent the payloads from fraying the tether line, a length of Teflon tubing was added to the tether line at the payload attach points. The Teflon tubing, flared on both ends, was attached directly to the Kytoon attach swivel. When more than one payload was employed, a separate line was attached to the Teflon tubing and followed the tether line until the desired increment of altitude was attained. This payload line was then connected to another section of Teflon tubing, where the additional payload was attached.

The pollen trap was connected to the payload line by a brass 2/0 snap swivel. The snap swivel was used because it provided both a means of attaching the payload and a swivel allowing the payload a limited freedom of movement. Brass hardware was utilized as much as possible owing to its resistance to corrosion.

The project requirements specify maintaining a total of seven pollen traps in 100-ft intervals from altitudes of 400 to 1,000 ft. In order to achieve an altitude of 1,000 ft, a tether line of 1,320 ft is required (Figure 9). From Table 1, the tether line weight was found to be 1.70 lb. Since the total weight of the seven pollen traps is 1.57 lb, the total weight to be sent aloft is 3.27 lb. Table 1 shows that the Kytoon can lift a maximum of 2.134 lb in the absence of any winds. Therefore, it is not feasible for the Kytoon to lift the required weight of 3.27 lb in a calm wind condition. Since one Kytoon would not meet the project requirements, two alternatives were investigated: (1) to put two or more Kytoons in tandem, and (2) to utilize several independent single Kytoon systems. The tandem arrangement was found to be impractical because of the following:

a. As the distance between two cylinders decreases less than 0.9, the maximum diameter of one of the bodies, the drag force increases. When these two bodies are in contact with each other, as is the case of two Kytoons being flown in tandem, the drag force for the two Kytoons would be approximately three times greater than the drag force on a single Kytoon (Reference 3).

b. When two Kytoons are in a tandem arrangement, the necessary tether line weight is increased, owing to greater tensile strength requirement, by a factor of 2.4 times greater than that required for the single Kytoon system. This tether line weight, when added to the weight of the pollen traps, is 1.4 lb greater than static lift of the two Kytoons in a tandem arrangement.

However, three independent single Kytoon systems will meet the project requirements, as shown in Table 4:

Table 4. Three Independent Single Kytoon Systems

System No.	No. of Pollen Traps	Total Amount of Weight Sent Aloft Per System (lb)	Percent of Additional Free Lift	Altitude of Kytoon (ft)
1	1	1.98	16	1,000
2	2	1.91	16	900
3	4	1.87	19	700

These three systems were arranged so that there would be a minimum chance of their respective tether lines becoming entangled with each other (see Figure 5). The south end of Wallops Island was chosen as the tether site because there were no buildings, power and telephone lines, or other obstacles with which the tether line might become entangled.

Figure 5. South End of Wallops Island Looking North

4. PERFORMANCE (STATIC AND DYNAMIC ANALYSIS)

4.1 Static Analysis

The volume of helium used to inflate the Kytoon to have a calm air usable free lift of 964 grams was found in two ways, both of which were in close agreement. The method of slicing, which is an approximate method to determine the volume of a body is given by

$$V = \sum_{0}^{\ell} A(x) \, \Delta x$$

and was found to be 87.791 cu ft. As $|\Delta x|$ becomes smaller, the approximation of the volume approaches the exact volume. The second method was to find the

volume of a solid generated by rotating a plane area about an axis; this is called a solid of revolution. To find the volume of a solid $A(x)$ of a circle whose radius $r = y = f(x) = 0.6696 + 0.7132x - 0.0823x^2$ so that

$$\begin{aligned} A(x) &= \pi r^2 \\ &= \pi [f(x)]^2 \\ &= \pi y^2 \\ V &= \int_0^{l} A(x)\, dx \\ &= 86.044 \text{ cu ft} \end{aligned}$$

The center of gravity (c.g.) of the Kytoon was found (see Figures 2 and 3). The buoyancy due to the helium has a resultant force F_B which acts vertically upward at the center of volume of the enclosed gas or the center of buoyancy (c.b.). According to Archimedes' principle, the buoyant force F_B for a body submerged in a fluid is equal to the weight of the fluid displaced by the body. Since the Kytoon is submerged in air, and it was assumed that the displaced volume of air is not compressed, the buoyant force is given by

$$F_B = \gamma_A V_A$$

where

$$\gamma = \frac{P_A}{R_A T_A}$$

The weight of helium was found in a similar manner, and since the weight of the uninflated Kytoon is known, the usable free lift, L_s, is determined by

$$\uparrow \Sigma F_Y = 0$$

and is shown in Figure 2. The usable free lift was computed to be 2.677 lb. However, for the measured volume of helium, the usable free lift was measured to be 2.13 lb. This difference is attributed to the fact that the actual pressure and temperature of air were slightly higher than standard sea level pressure and temperature and the internal pressure of the helium was somewhat different from the value which was assumed. The usable free lift is defined as the force necessary to hold the inflated airship in an equilibrium condition in calm air. The weight of the payload and attached hardware must be subtracted from the usable free lift.

4.2 Dynamic Analysis

When the Kytoon is exposed to a wind velocity, aerodynamic forces, such as aerodynamic lift and drag, must be considered. The resultant force exerted by the moving air on the tethered Kytoon due to the normal (pressure) and tangential (frictional) stresses will have a horizontal component D and a vertical component L_{Aero}. These are parallel and perpendicular to the direction of the wind velocity vector, v, respectively, and are assumed to act at the center of pressure (c.p.). These are shown in Figure 3 with the Kytoon assuming an angle of attack, α.

Tests conducted at Wallops Island showed that the Kytoon, when tethered in a wind velocity of 12 mph, has a pitch angle of attack $\alpha = 7.5°$ and a yaw angle of attack $\beta = 0°$. The pitch angle of attack was measured using a modified Model K-110-1 clinometer, whereas the yaw angle of attack was measured with a specially constructed beta gage.

As shown in Figure 3, the components of the tether line tension, T, are related to the total lift and drag forces of the Kytoon. The tension of the tether line is given by

$$\vec{T} = \vec{L_T} + \vec{D}.$$

When the Kytoon is in an equilibrium condition, the horizontal and vertical components of the tether line tension may be found by

$$\rightarrow \Sigma F_X = 0 = D - T_x$$

$$\uparrow \Sigma F_y = 0 = F_B - W_{He} + L_{Aero} - W_B - T_y$$

The aerodynamic drag on the tether line was computed and found to be negligible. The aerodynamic pitching moment, M, is found by

$$M_{c.g.} = \left(F_B - W_{He}\right)(1.49) - L_{Aero}\, x + T_x(4.6) - T_y(1.82) - D\left(x \tan^{\alpha} - \frac{\bar{y}}{\cos^{\alpha}}\right)$$

This resultant moment must be equal to zero when the tethered Kytoon is in a condition of equilibrium. The tether line tension and tether angle were measured on Wallops Station and the aerodynamic lift and drag forces were computed. From the aerodynamic lift and drag forces, the lift and drag coefficients were determined (see Figure 6). It is noted from the lift coefficient data that this system realizes a total lifting capability of 4.5 lb in a steady 15 mph wind. The tether line tension and tether angle were measured using a spring scale and a Model K-110-1 clinometer, respectively. The wind velocity, experienced by the Kytoon, was measured using a hand-held anemometer. Prior to these tests, the anemometer was checked

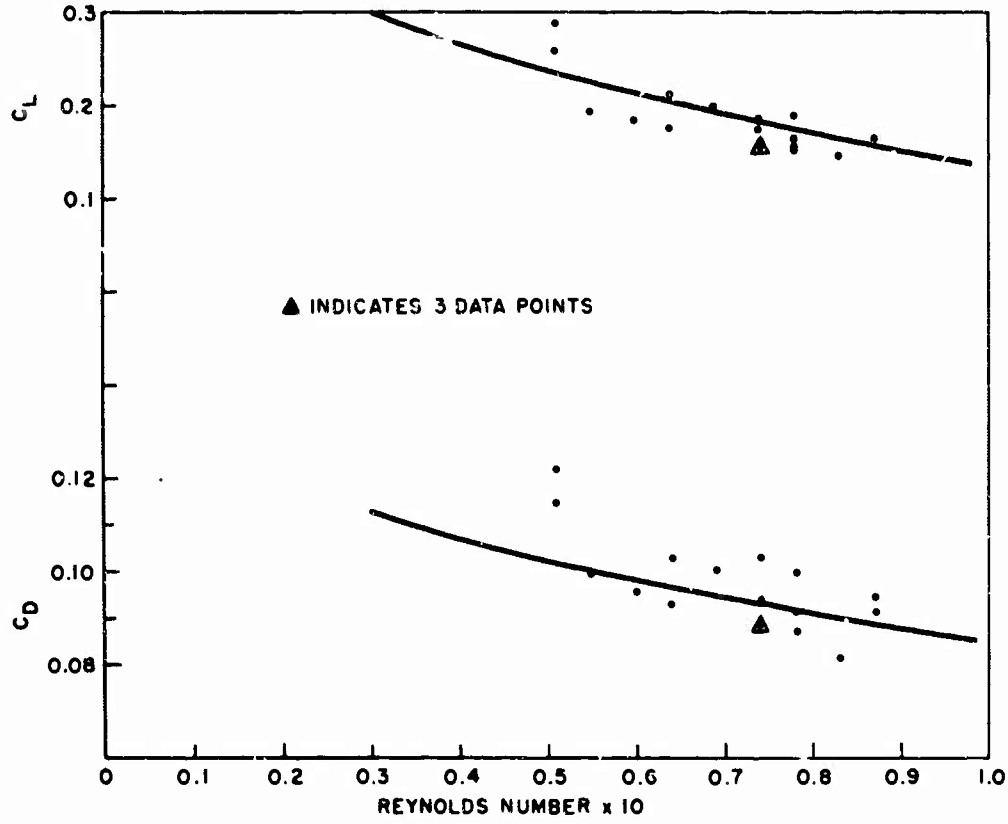

Figure 6. C_D and C_L vs Reynolds Number for the Kytoon. $R_N = \frac{\rho \, d_{max} \, v}{\mu}$

for accuracy and found to be in a calibrated condition. The tether angle, θ, versus wind speed is shown in Figure 7. The Reynolds number for the Kytoon was computed and is shown versus wind velocity in Figure 8. Figure 9 is a plot of measured tether line length versus Kytoon altitude for an average wind velocity of 12 mph. This test was conducted on Wallops Island and the data were acquired by the FPS-16 radar. Figure 10 presents smoothed radar data (FPQ-6) showing typical variations of altitude for a period of 200 sec, chosen at random, for the Kytoon in tethered flight. It is noted from this figure that the maximum change in altitude over this time period is approximately 8 percent. There was no instrumentation available to measure the local wind conditions during this period of flight.

Flight testing of this system revealed that when the Kytoon senses a steady wind velocity of 21 mph, it begins to undulate. As the steady wind velocity increases past 21 mph, this undulation becomes more violent. This dynamic behavior was experienced in repeated tests. A quantitative explanation for this behavior is not offered.

It is noted that this motion begins at a Reynolds number of approximately 1×10^6 and that this is a region of transition for similar bodies of revolution.

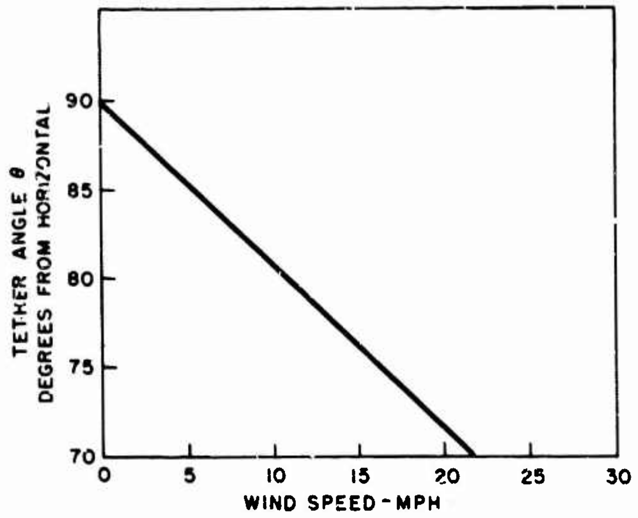

Figure 7. Tether Angle vs Wind Velocity for the Kytoon

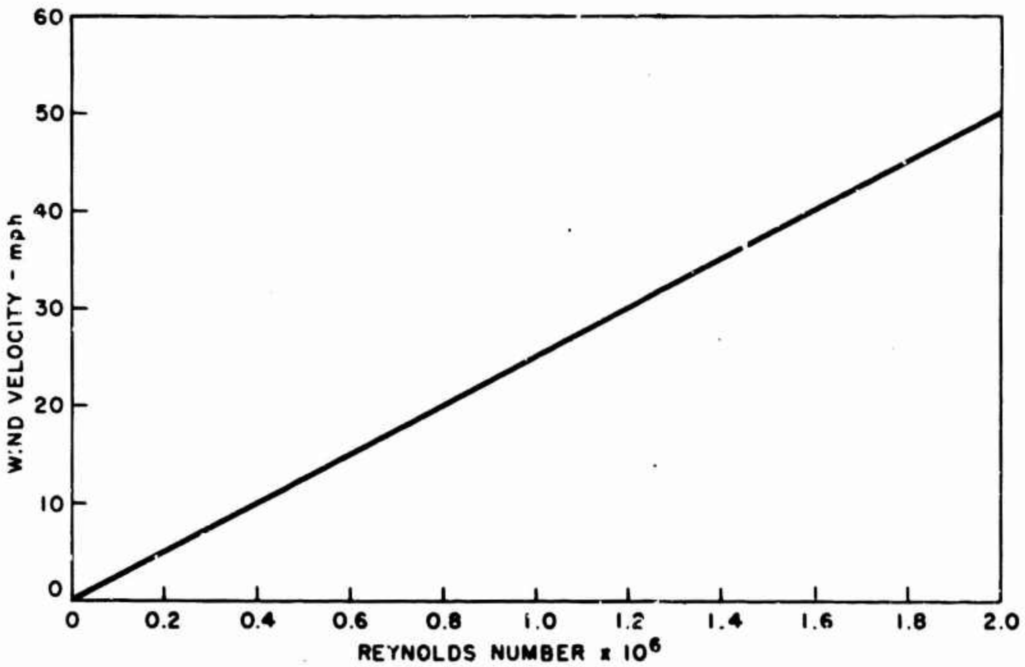

Figure 8. Wind Velocity vs Reynolds Number for the Kytoon. $R_N = \frac{\rho \, d_{max} \, v}{\mu}$

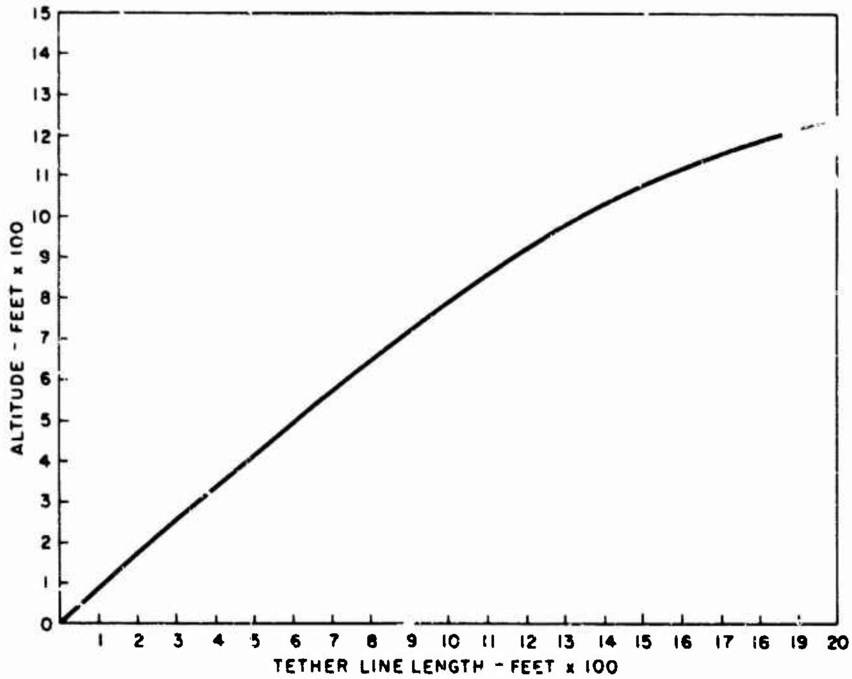

Figure 9. Altitude vs Kytoon Tether Line Length. Average wind velocity = 12 mph

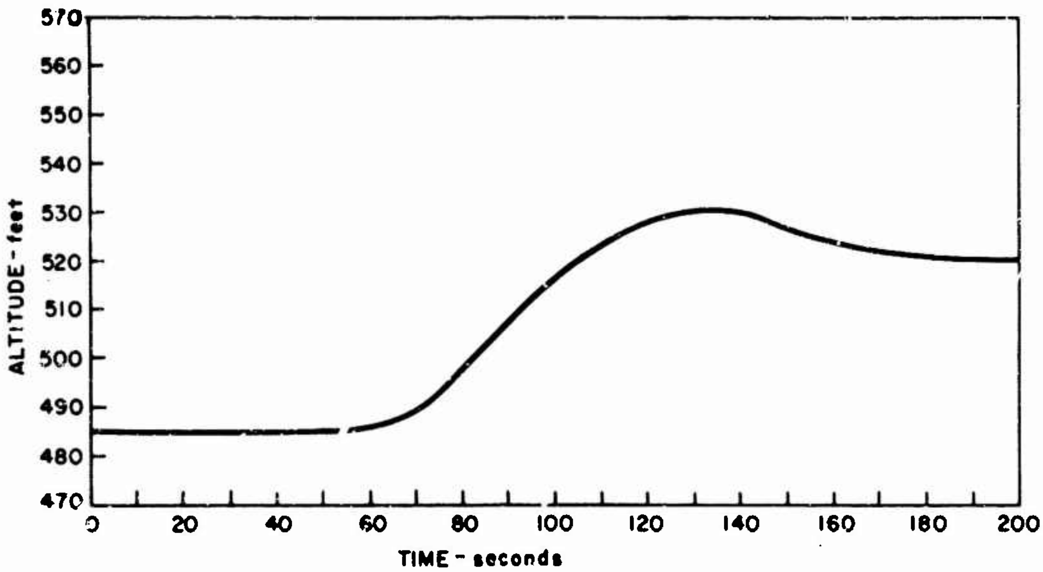

Figure 10. Altitude vs Time - Kytoon in Tethered Flight

5. OPERATIONAL EVALUATION

The Kytoon, as initially received from the manufacturer, did not prove satisfactory for prolonged tethered flight. It appeared that the nylon casing at the rear of the Kytoon would pull itself through the rear assembly tail plate, transmitting the fin loads directly to the neoprene bladder, causing it to become ruptured at its weakest point. Because of this basic design problem, the Kytoon was modified by attaching four tabs to the rear section of the nylon casing. When the tail assembly struts were placed through these tabs, the nylon casing was retained in its original position, causing the fin loads to be transmitted to the nylon casing rather than to the bladder. Since the Kytoon is not steady when totally restrained at the surface in gusty winds or winds greater than 10 to 12 knots, it is required that Kytoon inflation take place in a sheltered area. Due to its vulnerability in these winds, it was ascertained that the optimum time to send the Kytoon aloft is when winds are at their minimum speed, which usually occurs at dawn and dusk. Because there was not a sheltered area available at the tether site, the Kytoon was inflated in the Weather Bureau balloon inflation area and transported to the tether point. It takes two men approximately one hour to transport an inflated Kytoon from the inflation area to the tether point, attach the payload, send it aloft, and return to the inflation area. Approximately one hour is required by one man to change the bladder in the Kytoon and put it in a flight-ready condition provided that it is done in a sheltered area. Since the life expectancy of the neoprene bladder was found to be 12 hours of constant exposure to sunlight, the bladder should be changed after a 24-hour period of tethered flight, of which no more than 12 hours should be during the daylight hours. This condition was for a Kytoon with a high degree of thermal reflectivity. It was not determined what the life expectancy of the bladder would be if the Kytoon were to act as a "black body."

Due to the permeability of the gas envelope to helium, approximately 15 percent of the usable free lift is lost in a 24-hour period. In view of this loss of free lift, it was determined that, by over-inflating the Kytoon at dusk, it could remain aloft for a 24-hour period (the amount of overinflation being the amount necessary to compensate for the loss of usable free lift during the first 12-hour period of tethered flight). It is felt, however, that the Kytoon, which has remained aloft overnight, be inspected after 12 hours of flight in the event that maintenance may be required.

Prior to sending the Kytoon aloft, certain requirements of the Federal Aviation Agency (FAA) had to be met and special meteorological data and forecasts had to be obtained and evaluated. The FAA requirements were imposed in order to minimize the potential hazard to aircraft in the event that the flight condition of the Kytoon should change from tethered to free flight. Since the volume of the Kytoon is less than 115 cu ft and its maximum diameter is less than 6 ft, the FAA regulations did

not apply to the Kytoon itself, but to the payload which it carried (Reference 5). These requirements imposed by the FAA include the following:

a. Notification prior to sending the Kytoon aloft, expected time and position of flight, and a general description of the system.

b. Verification of position at least once every 2 hours on a continuous basis.

c. Notification of the nearest FAA Air Traffic Control facility in the event that the Kytoon was to achieve a free flight condition.

During the times of operation of the Wallops range, the time and position of flight were recorded by the Island Radar Section. The data obtained from radar were later reduced and used for data correlation. During the times that the radar facility was not available, the Wallops Damage Control Section would visually ascertain that the Kytoon was still in a tethered flight condition. A procedure was inaugurated to notify the FAA if it were deemed necessary.

The meteorological data and forecasts involved included the following:

a. The probability that thundershower activity would interfere with normal flight conditions.

b. Special forecasts for winds in the realm of flight.

During the times of operation of the Wallops range, these data were obtained from the Wallops Station forecast office. When the forecast office was not in operation, provisions were made to obtain the necessary meteorological data from another forecast office, which was evaluated by the writer when coupled with local conditions. If the probability was [illegible] percent or greater that undesirable weather conditions would occur, the Kytoon was grounded and placed in a shelter for the forecast period. In the event that these undesirable weather conditions occurred without any prior forecast, the writer was notified so that the tethered Kytoons could be grounded and placed in a shelter as soon as possible. For the period beginning at 1700Q, 3 June 1966, and ending at 0800Q, 22 June 1966, there were 37 12-hour periods of possible flight for the Kytoon systems. Of these 37 12-hour periods, 25 were cancelled owing to either a forecast of adverse weather conditions or actual adverse weather conditions that were not predicted. This represents 67 percent of the total possible time of operation.

6. CONCLUSION

The Kytoon system as configured and operationally deployed in this initial phase of the Aeropalynological Survey is capable of obtaining useful scientific data. However, the performance capabilities and operational characteristics of the Kytoon system have been demonstrated and found to be limited and not suitable as an operational tool for the Aeropalynologic Survey Project.

References

1. Baumeister, Theodore (1958) Marks' Mechanical Engineers Handbook, 6th ed., McGraw-Hill, New York.
2. Brown, Aubrey I., and Marco, Salvatore M. (1958) Introduction to Heat Transfer, 3d ed., McGraw-Hill, New York.
3. Hoerner, Sighard F. (1958) Fluid Dynamic Drag, published by the author, Midland Park, New Jersey.
4. How to Assemble and Fly Dewey and Almy Kytoon, Dewey and Almy brochure.
5. Moored Balloons, Kites, and Unmanned Rockets and Unmanned Free Balloons (1964) Federal Aviation Regulation, Part 101, Government Printing Office, Washington, D.C.
6. U.S. Dept. of Commerce, Winds Aloft and Summary Parameter Wallops Island, Virginia, April 1965, Weather Bureau, National Weather Records Center, Asheville, North Carolina.
7. U.S. Dept. of Commerce, Winds Aloft and Summary Parameter Wallops Island, Virginia, May 1965, Weather Bureau, National Weather Records Center, Asheville, North Carolina.
8. U.S. Dept. of Commerce, Winds Aloft and Summary Parameter Wallops Island, Virginia, June 1965, Weather Bureau, National Weather Records Center, Asheville, North Carolina.

Symbols

d	diameter	ft
d_{max}	maximum diameter	ft
ℓ	length	ft
f	fineness ratio $\frac{\ell}{d_{max}}$	
V	volume $\int_0^{\ell} A(x)\,dx$	ft^3
R_N	Reynolds number $\frac{\rho\, d_{max}\, v}{\mu}$	
v	velocity	fps
ρ	density	slugs/ft^3
μ	viscosity	# sec/ft^2
F_B	total buoyant force $\gamma_A V_A$	lb
γ	specific weight $\frac{P}{RT}$	#/ft^3
R	universal gas constant	ft/°R
°T	temperature	°R

P	pressure	psf
L_s	static or usable free lift	lb
L_{Aero}	aerodynamic lift $C_L qS$	lb
L_T	total lift $L_s + L_{Aero}$	lb
D	aerodynamic drag $C_D qS$	lb
S	aerodynamic reference area $V^{2/3}$	ft^2
α	pitch angle of attack	deg
β	yaw angle of attack	deg
C_L	aerodynamic lift coefficient	
C_D	aerodynamic drag coefficient	
q	dynamic pressure $1/2\ \rho\ V^2$	psf
T	tether line tension	lb
W	weight	lb
M	aerodynamic pitching moment	ft-lb
c.b.	center of buoyancy	
c.g.	center of gravity	
c.p.	center of pressure	
A (subscript)	air	
B (subscript)	balloon	
He (subscript)	helium	

XVII. Reinforced Fiberglas as a Balloon Tether

Robert B. McKee
University of Nevada
Reno, Nevada

Abstract

The Navy's Tethered Aerological Balloon System (TABS) program generated a requirement for a high strength-to-weight ratio tether cable. A brief summary of this program is presented and the design philosophy leading to reinforced fiberglas as the selected tether is discussed. Several problems that were encountered in production of the tether are discussed, as well as the problems associated with splicings and end fittings. The effect of tether length on strength is demonstrated and the difficulties of manufacturing glass tethers with greater strength are presented. It is concluded that reinforced glass tethers are feasible in long lengths and do possess the required tensile strength, flexibility, and resistance to environment and that larger size tethers can be made by combining smaller tethers into a flexible matrix.

I. INTRODUCTION

In June 1962 a proposal by Mr. Charles Smith of Aerological Laboratories, Encino, California, was brought to the attention of the U.S. Naval Ordnance Test Station (now Naval Weapons Laboratory) China Lake, California. The proposal

discussed the possibility of mooring a balloon at stratospheric altitudes for extended periods of time. The system was originally intended to support a vertical chain of sensors to monitor meteorological parameters continuously at a single location over a range of altitudes. Hence the acronym TABS (Tethered Aerological Balloon System). The utility of such a system was immediately evident and a contract was entered into between Aerological Laboratories and the Naval Weapons Center to prove the feasibility of the system. For the Navy, this activity was under the direction of Dr. Sheldon D. Elliott, Jr., of the Research Department. The author was attached to the Station at the time as an employed-when-needed (WAE) consultant to the Materials Engineering branch headed by Steve H. Herzog.

The feasibility of the proposed system rested upon the observation that temperate latitude profiles of wind velocity as a function of altitude almost invariably show a region of high winds and of consistent direction in the troposphere, followed by a region of light and variable winds in the stratosphere. Smith felt that a balloon could ascend through the troposphere, with tether pay-out minimized by use of a mobile launch vehicle (Figure 1), and achieve a stable configuration, if the tether were small and light enough. I believe that Chuck Smith is here, and if there are questions about the concept, he can defend himself.

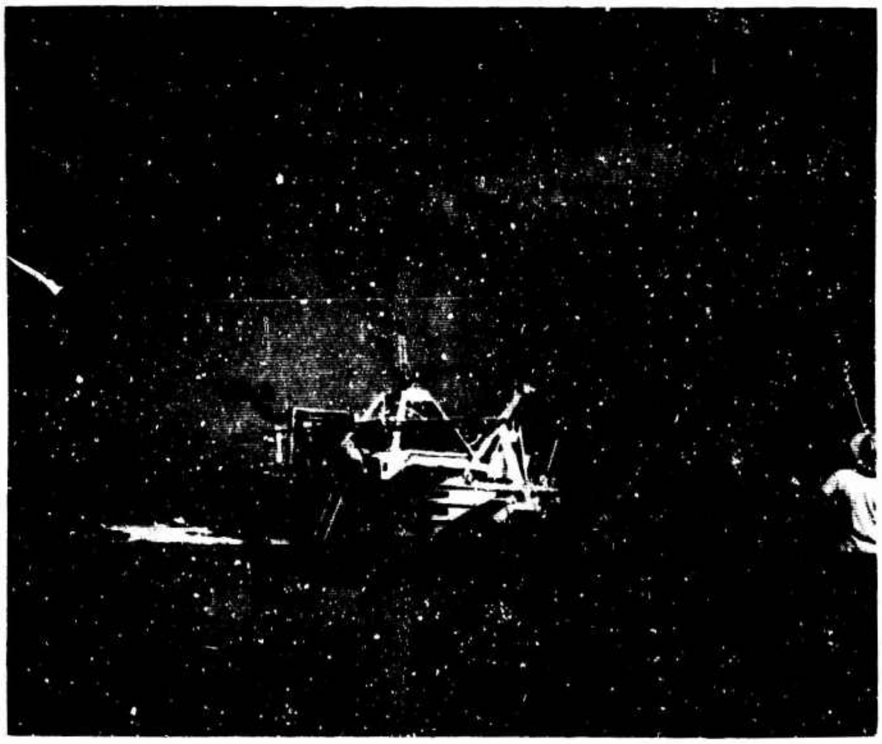

Figure 1. TABS Mobile Launch Vehicle

Configurations for stable moored balloon systems were developed by iterative calculations. They showed that a suitable tether would have to have a specific gravity of 1.5 to 2 and tensile strength of 150,000 to 200,000 psi. The corresponding strength-to-weight ratio, which is numerically equal to the length at which the tether would be broken by its own weight, is 240,000 ft. A typical configuration, for a hypothetical balloon flight at 60,000 ft, is shown in Figure 2.

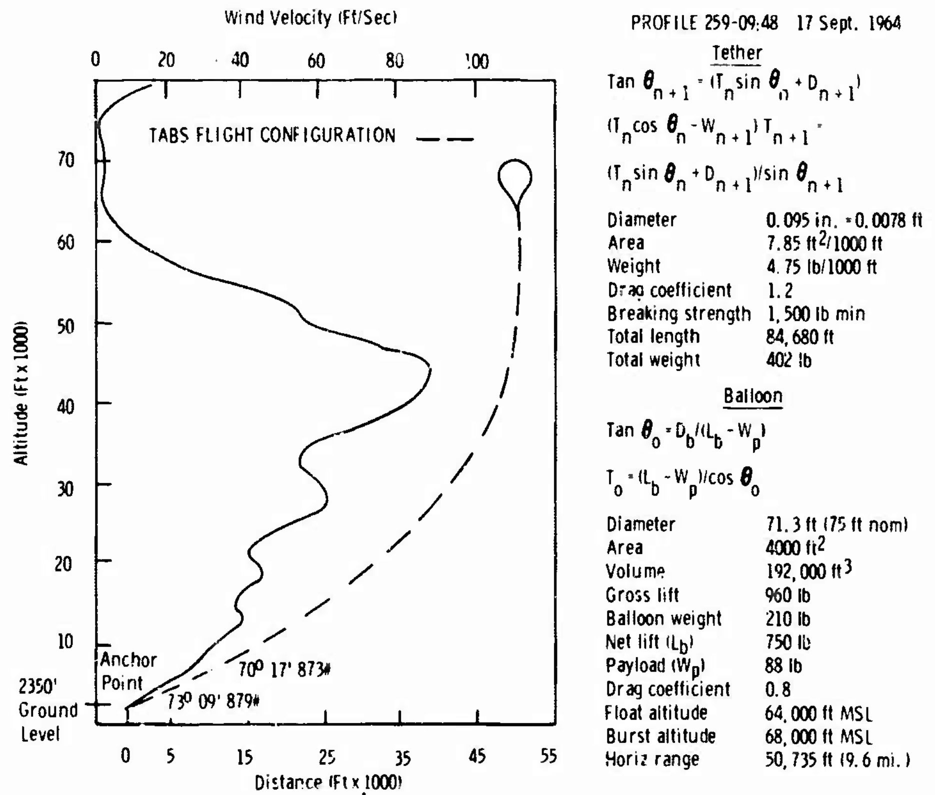

Figure 2. TABS Flight Configuration

Steel wire has the strength required for such a tether, but is much too heavy, with a strength-to-weight ratio of typically 117,000 ft. Other materials such as polyester and nylon were checked with similar results. Of the readily available fibers, only fiberglas had the requisite strength-to-weight ratio, well over 200,000 ft in commercial structures. A search for contractors to produce such a fiberglas tether was not successful, and it was decided to set up a production facility at the Naval Weapons Laboratory.

2. PRODUCTION OF THE TETHER

The information we possessed about the endurance of fiberglas articles indicated that to sustain a load of 800 lb for as long as a year would require a tether with a breaking strength of over 1,500 lb. A conservative estimate of fiberglas breaking strength in composite was 10 lb per "end." An "end" is a textile term which, in the case of the S994 fiberglas developed for the Polaris missile, refers to a bundle of 208 individual threads. Each thread has a diameter of about 0.0004 of an inch. The "end" when dry has a diameter of about 0.005 of an inch. Our original tether design, then, called for the use of 150 ends. These 150 ends, we calculated, would occupy about 60 percent of the volume of an epoxy resin matrix having an outside diameter of 0.090 in., the contemplated size of the tether. This proportion is generally regarded as good practice for optimum physical properties.

We established several design concepts for the production facility to attain the highest possible properties in the finished tether. Each strand of glass going into the production fixtures was separately tensioned and we determined that this tension should be applied by a brake upon the supply spool, rather than with a capstan or other friction device because the latter would involve a mechanical contact with the dry fibers. From the rack or creel, on which the fiber supply rolls are disposed in a roughly circular pattern, the fibers converge to the entrance of a resin holding tank which is surrounded by a circle of resin delivery ports. From the holding tank the rod passes through a preheating oven and through three successively smaller dies separated by two vacuum chambers (Figure 3). The tether matrix is cured in a 50 ft long oven held at 500°F and cooled in the air for another 60 ft or so before being wound on a converted Navy shipboard winch. The first facility, hastily constructed in an abandoned aeroballistics laboratory, was pretty crude and yet the tether produced there exhibited properties in excess of those required. For example, the breaking strength of tether, made with 140 ends of diameter of 0.075 in. instead of 0.090 in., consistently ran about 1400 lb, and occasionally above 1700 lb.

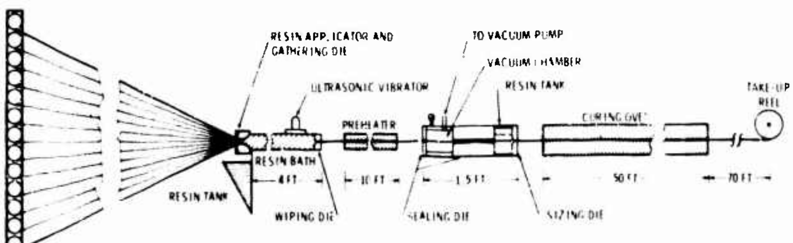

Figure 3. Manufacturing Process

Over a span of three years the production facility has been entirely rebuilt and nearly all of the individual units were replaced with more efficient, more reliable components. The original glass supply was "20 end"; that is, each spool contained a yarn made of 20 ends of glass. It wasn't possible to maintain the same tension on all 20 ends, and so we changed to "single end" supply in which each spool furnished only one end of glass. This solved the tensioning problem, but another problem arose because the textile machinery used to wind "single end" spools twists the bundle of glass about once per inch. This resulted in the finished tether having a pronounced tendency to untwist when placed under load. We finally made a special arrangement with the glass supplier to furnish single end fiberglas on the "cake," a light cardboard spool on which the glass is wound as it comes from the forming crucible. We have not attempted to put a skin of some other material on the tether because we have not found materials superior to glass and epoxy resin for exposure at high altitude. We made several attempts to apply a "gel coat" of epoxy resin to the outside of the tether without success. The gravity makes any excess resin run off our horizontal production line, and some mechanism, perhaps surface tension or residual kinkiness makes the tether tend to expand to the final die diameter as more liquid resin is furnished it. We found it possible to maintain a production rate of about 25 ft per min for long periods of time.

3. PHYSICAL PROPERTIES OF THE TETHER

The "out of roundness" of the finished tether was held within 0.001 to 0.002 in. by precise alignment of the dies and take-away equipment, and by use of the untwisted "cake" fiberglas supply. The tether emerged from the forming die almost water-clear, turning to a straw to amber color after cure. The surface of the finished tether was smooth to the touch, but the glass fibers do extend to the surface and the bare-handed handler was soon scratching. The finished tether in the 0.080 in. diam most commonly made can be flexed to a 9 in. radius repeatedly without damage; it must be bent to a radius of less than 2 in. before failure occurs by buckling on the compression side. We have found it advisable to add 10 percent of a much more flexible epoxy resin to the pure epoxy (DER 332) which serves as the basic resin system, in order to provide some "toughness" to the finished product.

The tensile breaking strength of the tether increases with an increase in the rate of loading, as shown by Figure 4. This behavior is characteristic of reinforced fiberglas articles, and of the fiberglas filaments themselves. The middle range of strain rate shown here corresponds to that which will bring a specimen 30 in. long to its breaking strength in one minute. The observation that lower tensile strengths are noticed when the load is more slowly applied leads to the expectation that lower tensile breaking stresses will also be associated with long load

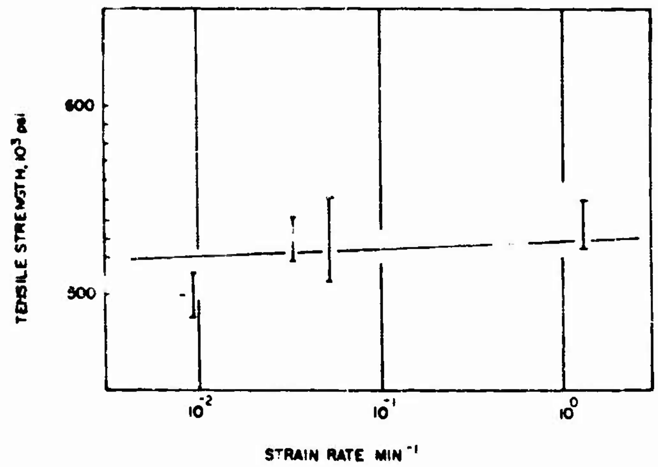

Figure 4. Tensile Strength as a Function of Rate of Loading (Strain Rate)

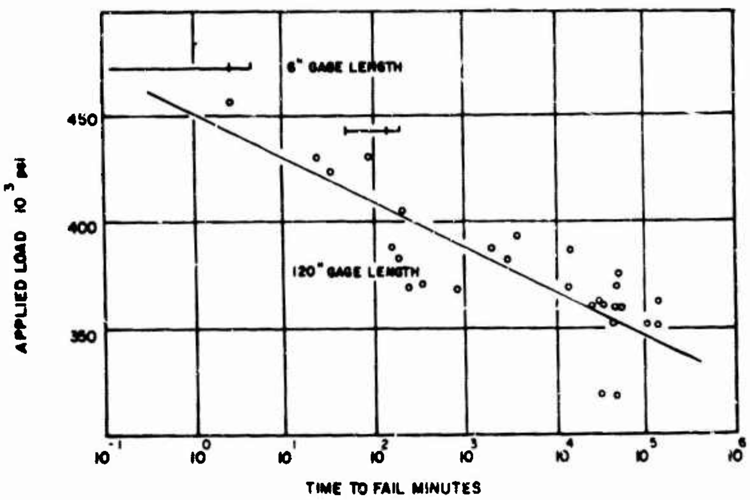

Figure 5. Tensile Strength as a Function of Time Under Load

duration, and this is the case (Figure 5). This behavior, usually known as "stress rupture," is also characteristic of other reinforced fiberglas articles and of the fiberglas itself. In fact, our original recommendation that design stresses be halved for a one-year service was based upon single fiber data. The effect of rate of loading and time under load on the breaking strength suggest that some sort of damage is occurring while the load is applied, and that the breaking strength in a conventional measurement would decrease as the time under load is increased. We sought to determine the effect of such damage by subjecting long samples of tether (120 in.) to live loads for periods of a month or more. Then these were cut into shorter samples and their strength measured by conventional tensile testing. Shorter samples were subjected to sustained loads in the testing machine and then immediately tested to failure. The results of these tests indicate that the effect of the applied loads, which ranged up to 90 percent of the breaking load in terms of the combination of load and time necessary to cause fracture, had no measurable effect on the final breaking load. In other words, the effects are either

not significant in relation to the experimental variables or can be explained by other observed effects, such as mechanical damage. This behavior also has been observed for single glass fibers. The breaking strength shown in these figures is the so-called glass stress; in other words, the load in pounds applied to the tether sample divided by the cross section area of glass. In this calculation the epoxy resin is not assumed to carry any tensile load. The tensile breaking strength referred to the total cross section area of the tether usually exceeds 280,000 psi. In one series of tests, the number of glass fibers fed into the production line was steadily decreased until the tether was only a little more than half of its original size. The proportion of glass and epoxy resin remained about the same, as did the composite breaking strength (the breaking stress referred to the entire cross section area of the composite).

The tensile breaking stress becomes smaller for larger or longer specimens, as may be inferred by the difference between the results shown in Figure. 5 for 6-in. and 120-in. specimens. I will have more to say about this later. A final interesting characteristic of the reinforced fiberglas tether is an almost complete absence of "creep." The long 10-ft specimens used for stress rupture studies were also instrumented to measure extension. We were able to measure some extension between the time the load was originally applied and the failure of the specimen, but these extensions were not related to the applied load. We have had to conclude that the creep strain, if any, was too small for us to measure. The breaking strength of any material, regardless of experimental variables, will exhibit a certain variation caused by natural variations in the composition of the materials being tested. Our balloon tether is no exception, exhibiting a fairly consistent coefficient of variation $\left(\frac{\text{standard deviation}}{\text{mean strength}}\right)$ for each type of test. This coefficient of variation was much larger than had been expected, and this difference helped to verify a new model for failure.

The balloon tether is usually thought of as a member "for tensile stress only." It may be interesting to note that, for a different application, we took some pains to measure the compressive stress for failure of the tether and achieved fracture stresses (and it is a fracture) from 180,000 to 230,000 psi. For such tests, it goes without saying that the specimen must be carefully restrained to prevent column buckling.

4. TETHER SPLICING AND END FITTING TECHNIQUE

The design of all handling facilities for the balloon tether was based on the capacity of the tether to be bent to an 18-in. diam without damage. The connection between the nylon rope used to fasten the payload to the balloon and the tether was an aluminum ring of this diameter around which the tether was wrapped several

times and its end fastened down with friction tape. This connector has performed quite well and is simple to implement. However, it should be cautioned that the act of bending any tension member around a drum induces extra stresses in the member, and inevitably reduces its capacity for external loads. This difficulty might be overcome by leading the tension member out along a modified volute so that the radius at the point of contact varies uniformly from infinity to the radius of the drum around which the tether is to be wrapped.

The capstan referred to here could not be used for tensile tests, not only because of the complicated stress pattern where the specimen meets the drum surface, but because the drums were too large to be accommodated in our testing machine. Therefore, metal fittings were developed (Figure 6) into which the tether specimens could be fastened with epoxy resin, permitting a test of the ultimate strength of the tether. The procedure for making this end fitting is as follows: The end of the tether specimen is split four ways for about 2 in. from the tip and reinforced with about half the number of ends of glass in the tether. This reinforcement is then overwrapped with a few extra ends of glass and the ends taped to the tether far enough from the tip so that it will stick out of the holder. Then the steel holder is capped on one end with a polyethylene plug and the other end wrapped with masking tape to form a tubular extension. The steel holder is stood upright on the polyethylene cap and filled with epoxy resin, and then the prepared end of the tether is inserted down through the hole in the holder and sloshed up and down until the air has been worked out of the cavity. It is quite essential that air be eliminated from the interior to get a good bond between the epoxy and the specimen. It is also essential that the hole through the specimen holder be large enough so that the very marked difference in elongation between the steel holder and the glass specimen will not cause destruction of the epoxy resin between the steel holder and the specimen. In the case of the 0.080 diam tether, this hole was drilled to a diameter of 3/16 in.

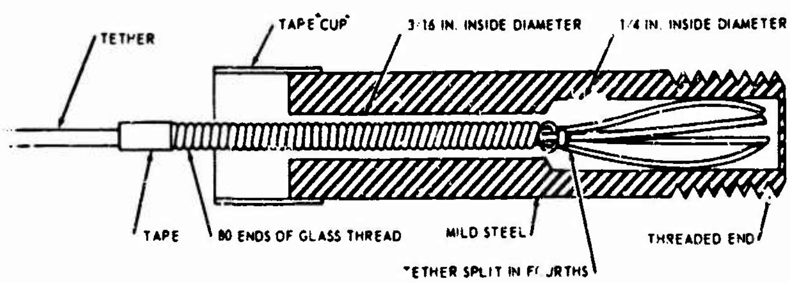

Figure 6. Metal End Fitting

An all-plastic end tab has been used for tensile testing at the University. The ends of the test specimen are split four ways and reinforced as before. Then, with up to a dozen other specimens, it is placed on a waxed aluminum sheet. Strips of 1/8-in. masonite serve to separate the holders. Chopped glass fiber is placed under and over the split ends and saturated with epoxy resin. Another aluminum sheet is placed over the specimens and weighted down. The resulting tab (Figure 7) is very reliable and simple to make and use.

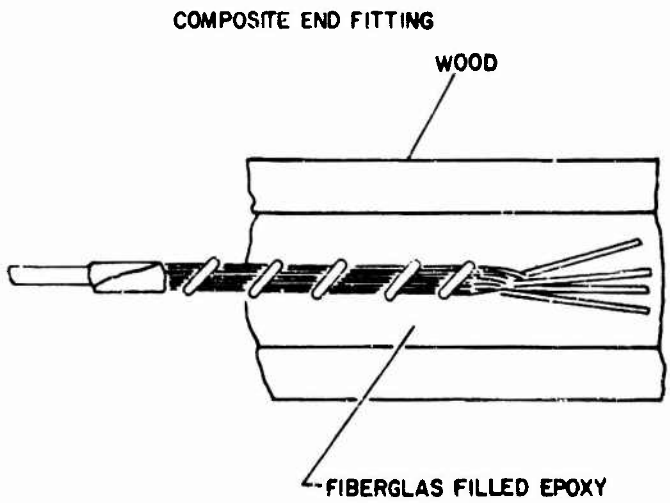

Figure 7. All-plastic End Tab

A fourth type of end fitting was a 1/4-in. braided nylon rope. When this rope is compressed slightly, a cavity appears in the center. The tether can be pushed into this cavity for a distance of about a foot and the rope impregnated with epoxy resin. We have not been able to make a convincing tensile test of this combination because the elongation of the nylon rope consistently exceeds the drawing capacity of our tensile testing machines, but it seems a safe conclusion that this method of holding will develop the full strength of the glass tether.

5. SPLICING TECHNIQUES

At the start of the project it seemed unlikely that we would be able to produce single lengths of balloon tether long enough for the flight contemplated (20 miles). Therefore, an effort was made to develop splices for the tether which would be usable with the handling equipment that was envisaged. Naturally, we wanted a splice that would be smooth and with a minimum of extra cross section area and stiffness so that it would run smoothly through our tether deployment equipment, causing a minimum of extra wind drag. The steel test holder had by this time reached a high degree of dependability; we knew that the full strength of the tether could be developed by providing enough shear stress area and a suitable distribution of strain. Three types of tether splices were developed by this program.

One might produce a joint having nearly the size and stiffness of the original tether by a beveled-lap splice long enough to transfer the load by shear stress. Theoretically, with fiberglas and epoxy resin, such a joint would have a bevel 75 diam long, or 6 in. in the case of the 0.080 diam tether. We found it impossible, however, to produce the required bevel on the end of the broken tether, because the tether is not stiff enough to stay flat in a jig. Therefore, the lap was changed to the design shown in Figure 8, in which the tether is first split in halves and then the ends of the split are beveled by hand, more to produce a smooth transition than to make a perfect beveled joint. This beveled joint (about 12 in. total length for the 0.080 tether) is reinforced with about the same number of ends as the original tether. These are held in place by a piece of polyolefin heat shrinkable tubing, which also serves to protect the joint from abrasion and hold it together while the epoxy cures.

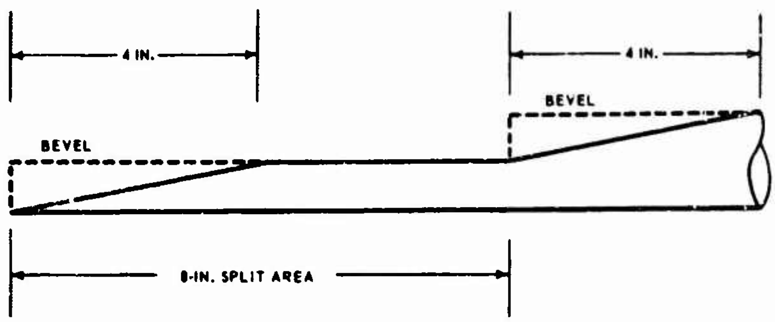

Figure 8. Beveled Lap Joint Splice

A splicing technique which relies upon mechanical interlocking has also been developed. This splice, with suitable reinforcing, is shorter than the lap splice and more reliable. It has exceeded the strength of the tether many times. However, it is much bulkier and stiffer than the lap splice, and more than twice the original tether diameter. In this technique the ends of the tether are cut into quarters for about 8 in. (100 diam). The split ends are interleaved and bound with glass thread; then the joint is reinforced with glass fiber and covered with shrink tubing as in the lap splice (Figure 9).

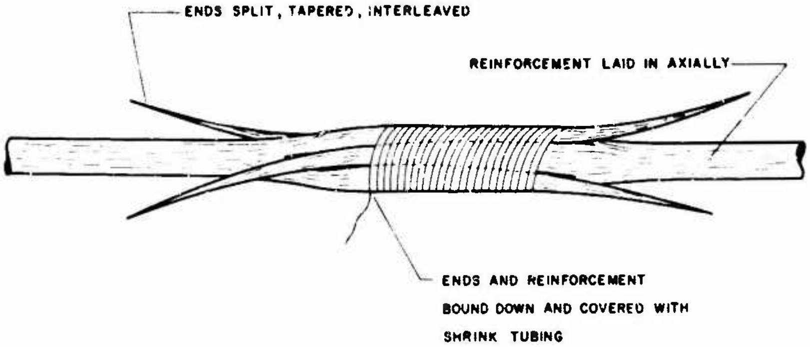

Figure 9. "Interlock" Tether Splice

6. POSSIBILITIES AND PREDICTIONS

We have shown that long fiberglas tethers can be produced that have the required strength-to-weight ratio and are handleable for use with moored high-altitude balloons. The Owens-Corning Corporation (Rhode Island plant) has produced a similar product with outer skins of epoxy resin and polyolefin (a tough thermoplastic).

We have been concerned, naturally, with the question of whether we could realize the sort of breaking strength in a 20 mile long tether that we have observed in a 30 in., or even a 10 ft tensile specimen. The data of Figure 5 indicate that some reduction in strength is to be expected with a longer specimen. It has been generally observed that structures of larger size break at lower tensile stresses. Kies, for example, produced the data shown in Figure 10.

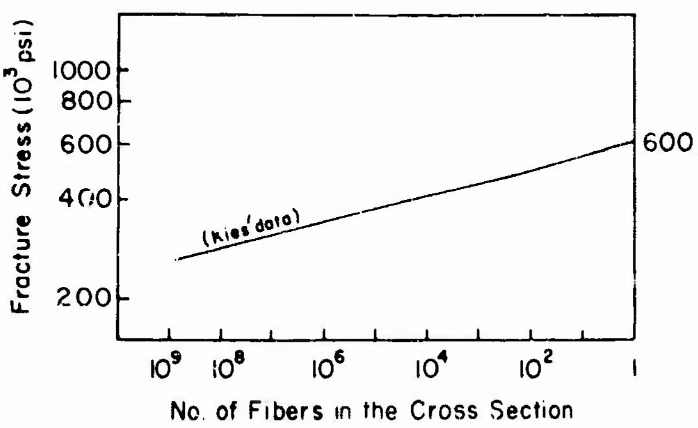

Figure 10. Effect of Structure Size on Fracture Stress

Much of this effect of specimen size on breaking stress can be explained by the natural expectation that larger structures are more likely to have flaws of any given large size. A theory for failure of composite structures has been based on this concept. Consider a bundle of rods under a steadily increasing tensile stress. If the rods are in fact identical, they will all break at the same instant; the over-all breaking stress will be equal to the breaking stress of any one rod, and because they are identical this will be equal to the average breaking stress of the rods. Real glass fibers are very smooth rods indeed, but they are not identical. If one were to keep a record of the results of applying this increasing tensile stress to a large collection of "statistically identical glass fibers" one at a time, he would find that the number broken at any given stress increases with the stress until, at some high stress, all of the collection have been broken. This relation between the number broken and the attained stress is pretty consistent. We can construct a mathematical function which will give the percentage which will have broken in any group placed under an increasing tensile stress, by the time that the stress has reached any given value. The most widely used mathematical function for this purpose is that proposed by Weibull in 1951. It looks like this:

$$G(\sigma) = 1 - e^{-N\left(\frac{\sigma-\sigma_u}{\sigma_o}\right)^m}$$

where σ is the stress, N the length of the fiber, and m, σ_o, and σ_u are parameters that describe the behavior of the particular fibers. The matrix that surrounds and infiltrates the bundle of glass rods serves little purpose as long as the rods are all unbroken; it carries no shear stress and little tensile stress. When a fiber is broken by the increasing tensile stress being placed onto the composite, the load is transferred to adjacent fibers by shear stress in the matrix. This results in a magnification of stress in these neighboring fibers. The likelihood of a break in the neighboring fibers at that location is consequently increased, and when the break occurs the "stress concentration" is worsened. Failure is predicted when the statistical expectation of another break in the fibers surrounding a typical break location is at least equal to one. In other words, at any given over-all tensile stress, we can predict that there will be a certain number of places where two fibers have broken next to one another; a smaller number of locations where three breaks are adjacent; and perhaps a yet smaller number of locations where four breaks are adjacent. We cannot say statistically that at any particular location there will be thus and such exact number of additional broken fibers. What we can say, statistically, is that over a large number of sites where three breaks are adjacent, there will be an average number of new broken fibers equal to, say, 1.25, and if the average number of new breaks is greater than one we expect that, since each additional break worsens the stress concentration, the number of breaks will increase exponentially

and a crack will propagate across the specimen, resulting in a tensile failure. Now, as the number of rods in a group is increased, it is more likely at any given stress that we will find, say, three breaks in a row and if three breaks in a row constitute the failure criterion for that stress then the large specimen will fail at a lower stress than the small one.

The same reasoning applies to length, since we must consider not only the number of flaw sites in a cross section, but also the number of such cross sections contained in the length of tether under test. This latter is determined by the characteristic fiber length required for the fiber stress. The characteristic length is that required for the fiber strain to be brought back to the value typical of the composite by shear strains in the matrix. Figure 11 shows the predictions of this failure theory applied to the data of Kies. The effect of specimen length on expected breaking stress is calculated by simply substituting the number of characteristic lengths for the number of rods in the cross section, with the result shown in Figure 12 for specimen lengths which we have tested, and a 100,000 ft balloon tether.

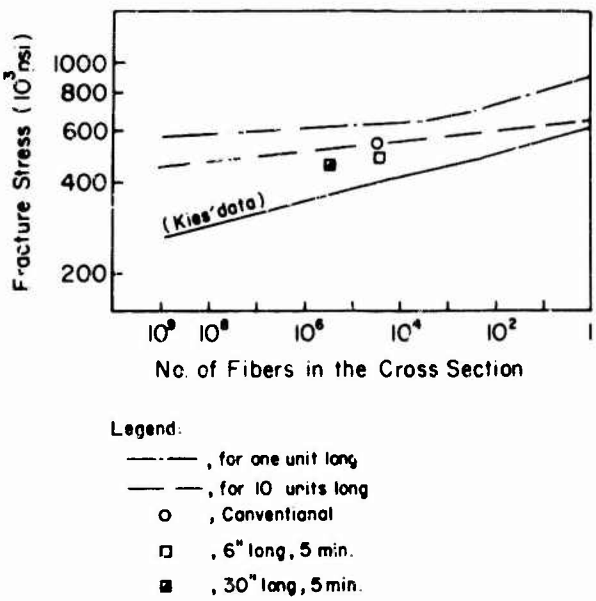

Figure 11. Predictions of Failure Theory Compared with Kies' Data

This theory also predicted that the tether would not exhibit any creep strain. The explanation of this is beyond the scope of this paper. I will just comment that our theoretical calculation of the stresses in the vicinity of a broken fiber are not sophisticated enough to represent the real state of stress. It is my feeling that when sufficiently accurate calculations of stress distribution are available, they will indicate that a small amount of creep strain, beyond that of the glass itself, is to be expected.

One more comment should be made in regard to the feasibility of tethers for higher gross tensions. The reduction in tensile breaking stress predicted by our theory is modest. For example, twice as many fibers in the cross section should yield a breaking strength which is greater by a factor of perhaps 1.98 in terms of gross load. However, the difficulty of manufacture will increase out of proportion

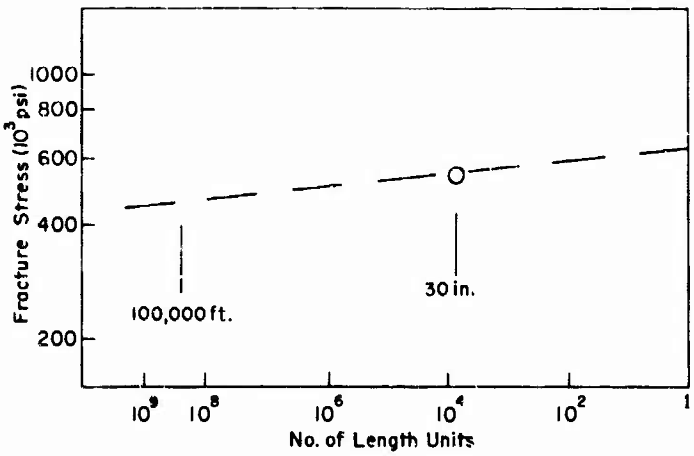

Figure 12. Effect of Length on Fracture Stress

to the size of the tether because of the difficulty of maintaining tension, of eliminating air and other volatiles, and of securing a good cure at the center without an over-cure at the outside surface. Therefore, members for higher loads are likely to be made of several smaller tethers fastened together by a matrix of lower stiffness. Such a structure should have a higher reliability, although its strength-to-weight ratio will be lower – a pretty familiar trade-off.

7. CONCLUSIONS

We can conclude that the reinforced fiberglas balloon tether is feasible to make in the lengths required for stratospheric tethered balloons, and does have the required tensile strength, flexibility, and resistance to environment. End fittings and splices can be made to develop the full strength of the tether without prohibitive bulk or stiffness. Perhaps most important, these fittings can be made in the field. The tether will support loads for long periods of time with little creep, and the imposition of relatively large loads for long periods of time has little effect on the breaking strength of the material. Larger size tethers to support heavier loads can be made most feasibly by combining smaller tethers into a large unit by means of a flexible matrix. These would have the added advantage of improved reliability, flexibility, and ease of handling. On the subject of handling it must be reported that although the tether made at China Lake from the untwisted cake fiberglas material was successfully wound on, and deployed from the large aluminum winch, deployment of glass tethers from a spinning drum winch can only be described as a 'pain in the neck.' Certainly, better deployment techniques can and should be developed.

XVIII. Skyhook Aerial Rescue System

John H. Gilchrist
Robert Fulton Company
Danbury, Connecticut

Abstract

A tethered balloon system developed as a land-to-air and sea-to-air system for inflight recovery of men and equipment is described. Balloon system and design parameters generated by operational requirements are included.

I. INTRODUCTION

Unlike most of the balloon systems about which we have heard in the context of this symposium, the balloons I wish to discuss are very small. They fly at a low altitude and support nothing but their own mass plus the mass of the tether line. In so doing, this tethered balloon system makes possible the saving of human life.

Fourteen years ago ONR asked Robert Fulton of Newtown, Connecticut, to develop a land-to-air and sea-to-air system for inflight recovery of men and equipment stranded in remote regions inaccessible to conventional modes of aerial retrieval. Several years later the feasibility of the Fulton Skyhook was demonstrated. Two years after that the first man-pickup took place. Since that time hundreds of

day and night line pickups have been accomplished from jungle clearings, open water, the Arctic ice cap and the decks of ships. Today the ARRS alone has sixty HC 130H aircraft fully equipped with the Fulton Skyhook, capable of retrieving single pickup loads up to 500 lb within a 5000-mile radius.

2. OPERATION OF SKYHOOK

The rescue aircraft, a fixed-wing propeller plane exhibiting a yoke mounted on the nose for guiding the tether line into "home" position at intercept, is also provided with: (1) permanently installed electromechanical ("Skyanchor") and hydraulic (winch) equipment for effecting lock-on and load retrieval after intercept, and (2) drop kits containing rescue software which are parachuted to the survivor.

Let us run through the sequence of events of a Skyhook pickup, emphasizing those that precede the moment the survivor is actually airborne, since this is the phase in which the tethered balloon subsystem does its job.

Figure 1 presents a condensation of the initial sequence whereby the survivor receives his software and performs the ground-sea operation that will enable the rescue aircraft to retrieve him. Upon donning the harness-suit and removing the balloon and helium modules from their containers, he inflates the balloon to the indicated pressure and launches it to 500-ft altitude, the "anchor" end of the tether line secured to his harness straps. From this point the survivor simply waits for the aircraft to intercept the tether line, approximately 20 to 25 min from the time he receives the drop kits.

Figures 2 and 3 show in detail the survivor inflating the balloon, featuring the helium supply, inflation gear, and harness-suit. A fully inflated balloon, ready for launching, appears in Figure 4. Observe the "anchor" end of the tether line hooked into the shoulder straps behind the survivor, lower left. The balloon is a nonextensible, equal-pressure aerodynamic design, aspect ratio about 3:1, exhibiting static lifts ranging from 40 to 65 lb, according to whether the balloon is for a one-man (680 ft^3) or two-man (1200 ft^3) pickup.

With the balloon flying at altitude, the survivor sits back to wind, facing the direction from which the aircraft will make its approach for intercept (Figure 5). We will leave our friend for a moment while we consider the tactical operation facing the pilot overhead.

Figure 6 presents a panorama of operations from a vantage point aloft. Observe in the center the man-tethered balloon system, the focus of both our attention and the pilot's. Notice too that the balloon serves three functions: (1) to hold aloft the tether line; (2) to present a visible target for the rescue aircraft; and (3) to enable the pilot to navigate a precise upwind approach for intercept by virtue of its directional properties.

Traveling at 125 knots, the aircraft flies its downward leg, losing altitude in such a way that upon circling into the final upwind leg the aircraft will intercept the tether line roughly 50 ft below the balloon.

This final maneuver calls for the exercise of judgment by the pilot in winds of sufficient intensity to cause the balloon-line system to "fall off" more than 20° from the vertical. He must adjust both his altitude and his angle of approach, in response to the severity of "fall-off," in order that upon intercept the initial portion of the survivor's trajectory will be as vertical as possible (see Figure 7).

Figure 8 features the configuration of the nose yoke on a twin-engine rescue aircraft, with a span of 25 ft and included angle of 105°. Less evident are the fending lines extending from wing tip to corresponding yoke, installed to prevent fouling of propellers in the event of a missed intercept. Figure 9 shows an HC-130H ARRS aircraft about to make an intercept; observe the relative positions of intercept point and balloon.

Let us now go back quickly to our survivor, who has been left waiting for his pickup (Figure 5). His line having been locked into the nose of the aircraft, he becomes instantaneously airborne as the line pulls vertically, the aircraft moving from left to right (Figure 10). The same moment of "lift-off" is recorded in the case of a dual pickup (Figure 11) in which the men are hooked together to minimize their relative motions as they ascend rapidly toward the aircraft (Figures 12 and 13). The shoulder straps are designed to compel the load to travel backwards once its trajectory develops an appreciable X-component of velocity.

In the final sequence of photographs (Figures 14, 15, and 16), the men are reeled into the aircraft by means of a hydraulic winch in the rear bay. The view offered by Figure 16 makes it possible to discuss the changing relationship of tether line to aircraft, from moment of lock-on at the nose until this same line is transferred to the winch in the rear. As the load reaches the level portion of its trajectory, the tether line under the aircraft also rises to the point where a crewman may engage it as the line passes directly under the rear bay. How the line appears from the bay, after engagement by the winch, is shown in Figure 17.

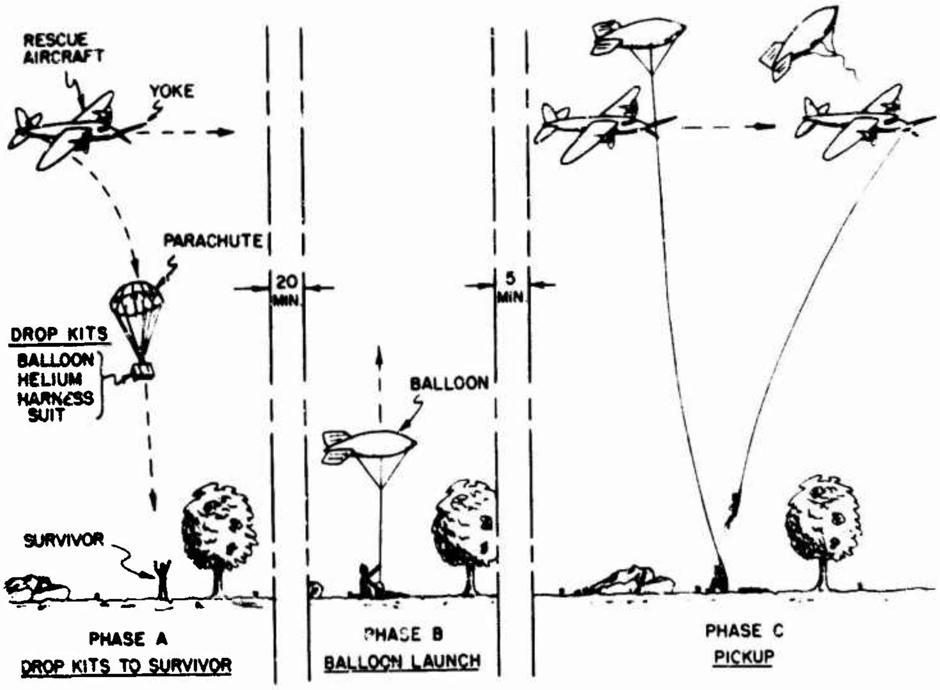

Figure 1. Fulton Skyhook Sequence of Events

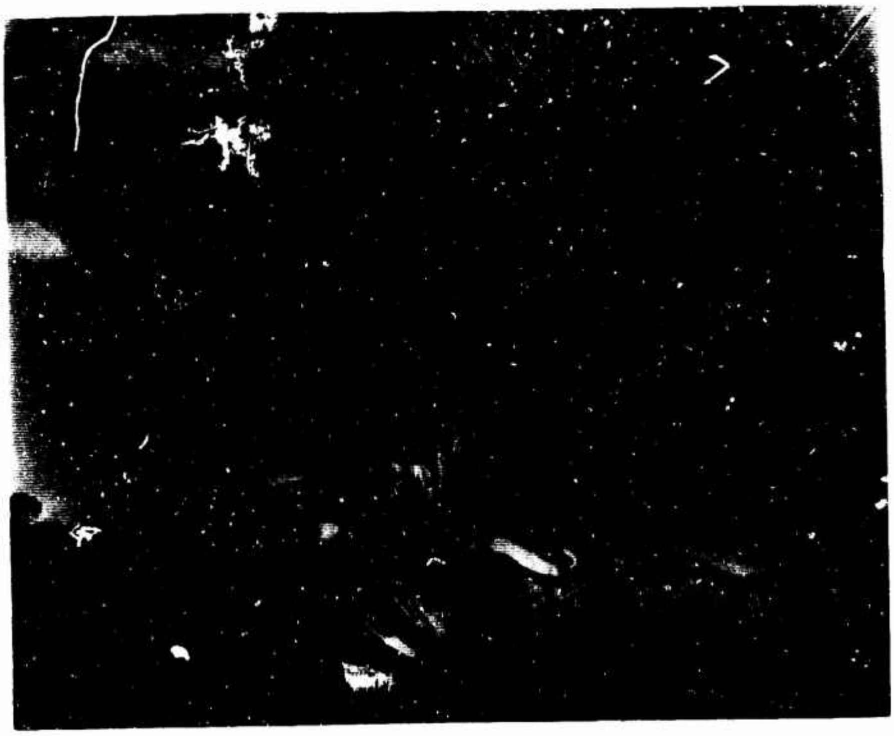

Figure 2. Balloon Inflation Showing Helium Supply, Inflation Gear, and Harness-suit

Figure 3. Balloon Inflated

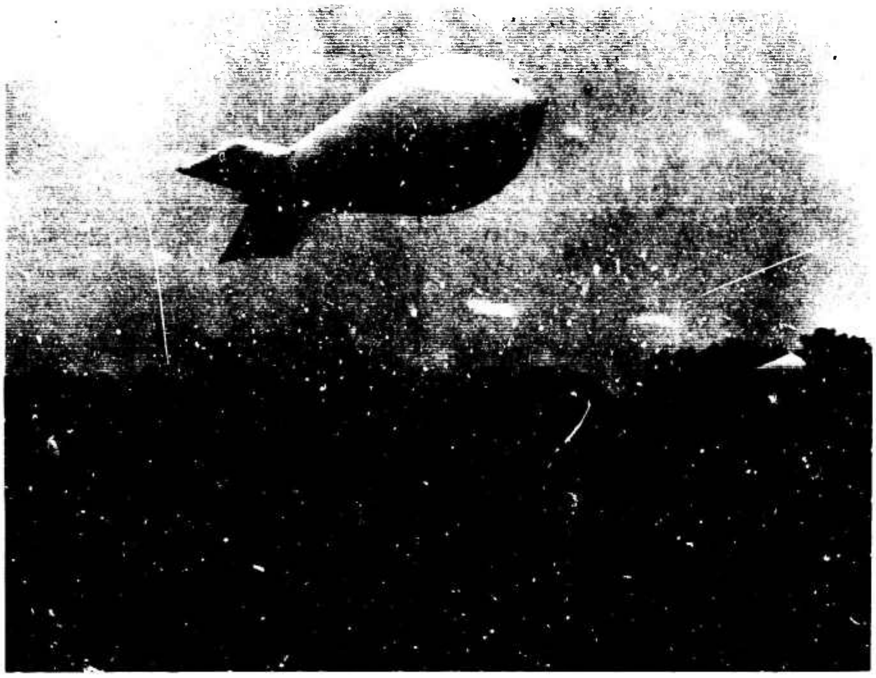

Figure 4. Fully Inflated Balloon Ready for Launching

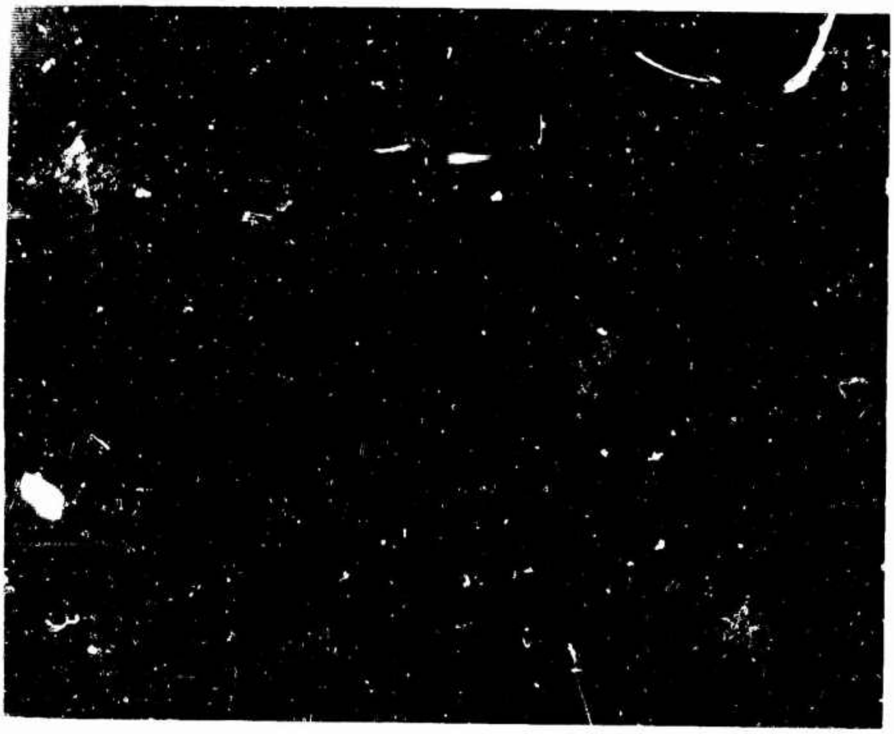

Figure 5. Survivor Ready for Pickup

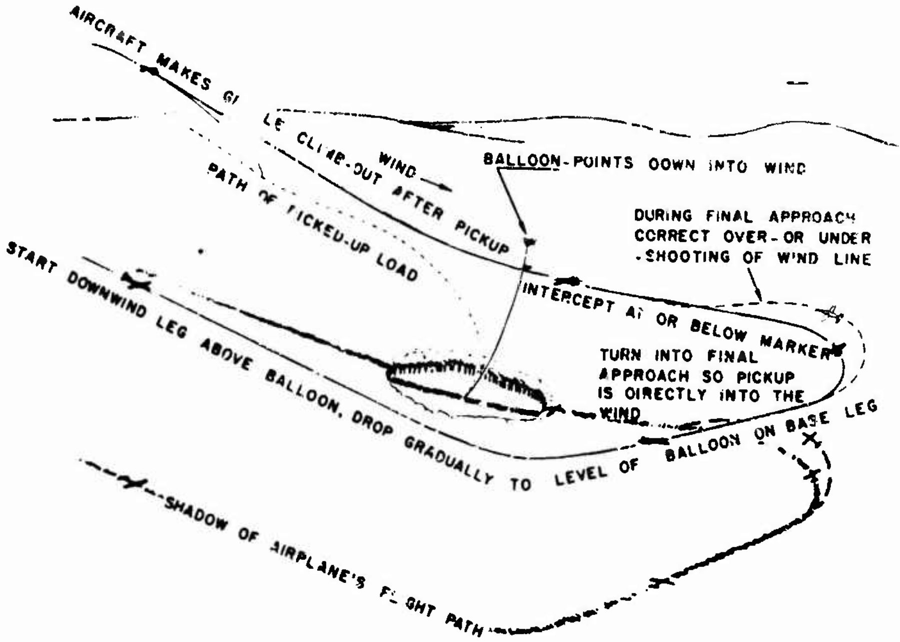

Figure 6. Fulton Skyhook Pilot Technique

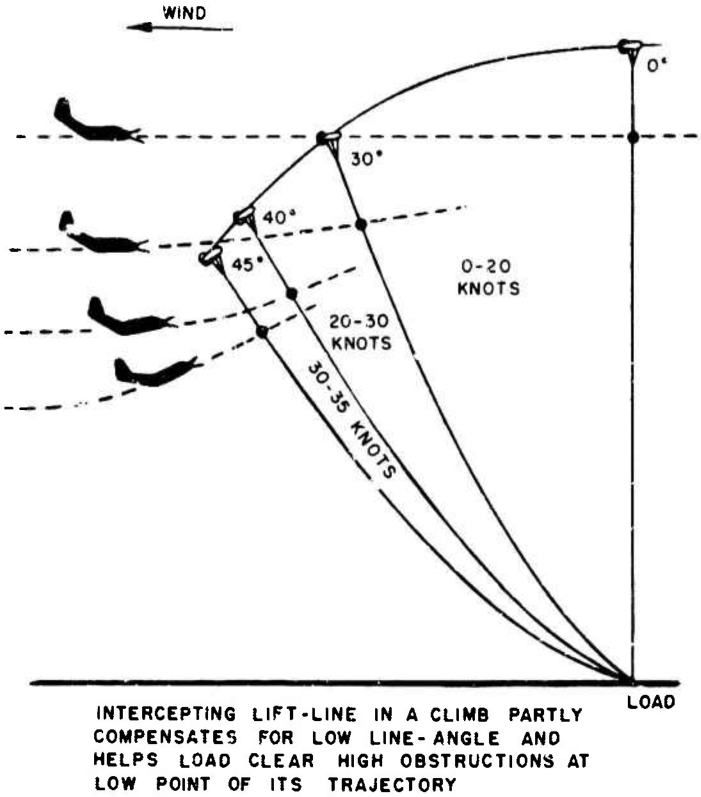

Figure 7. Line and Intercept Angles Versus Wind

Figure 8. Nose Yoke Configuration on a Twin-Engine Rescue Aircraft

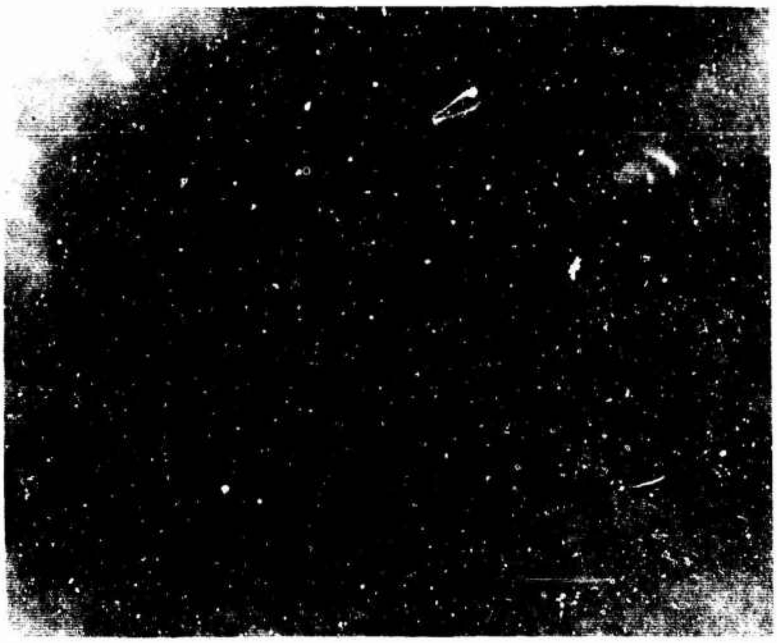

Figure 9. HC-130H ATRS Aircraft About to Make an Intercept

Figure 10. Survivor Becomes Airborne

Figure 11. Dual Pickup

Figure 12. Men Ascending Toward Aircraft

Figure 13. Men Ascending Toward Aircraft

Figure 14. Men Being Reeled into Aircraft

Figure 15. Men Approaching Aircraft

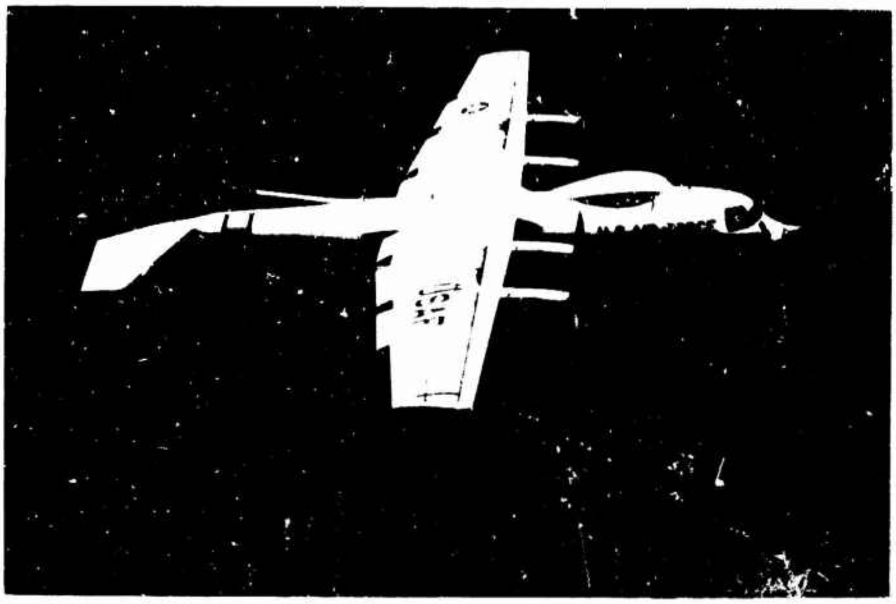

Figure 16. Full View of Men Approaching Aircraft

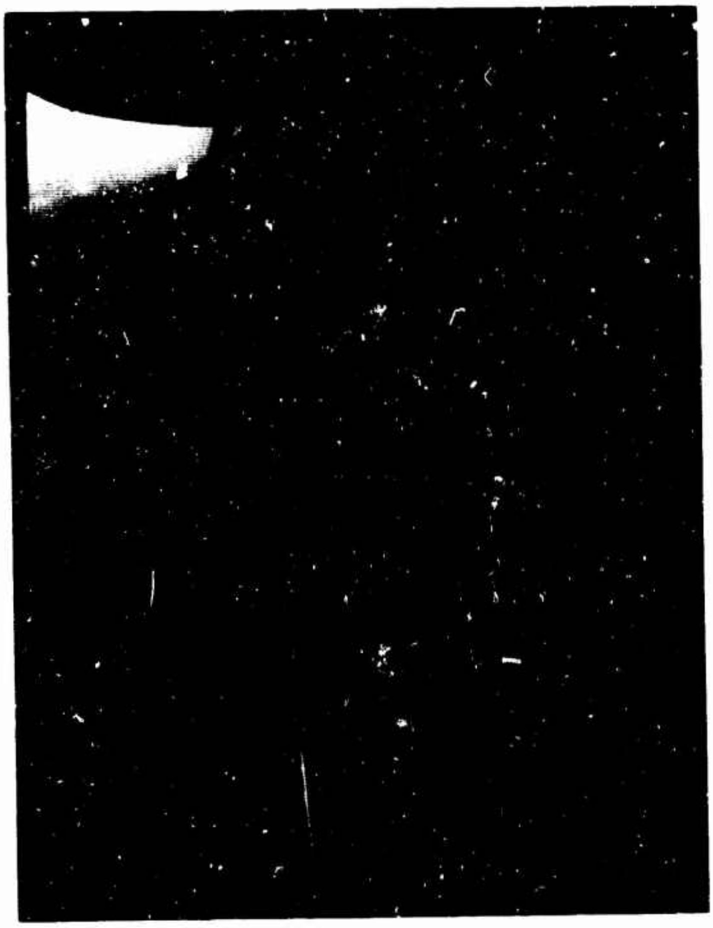

Figure 17. View of Line as Seen from Aircraft Bay

Appendix A

Mechanics of Load Trajectory

1. Cycloidal Theory

In Figure A1, if the ordinate of 0 horizontal distance is considered the Y-axis, that of 0 vertical distance the X-axis, and their point of intersection the origin "0," let us superimpose a linear time scale along the X-axis, negative to the left of the origin and positive to the right.

If time "0" coincides with the moment the aircraft intercepts the tether line, negative time corresponds with the existence of a simple, static man-tethered balloon system, positive time with the existence of a dynamic, free man-aircraft system experiencing translatory and rotational motion. More specifically, at "0" time interception of the tether line instantaneously converts the man-tethered balloon system into the kinematics of a generating "cycloid" whose "cycloidal" path is described by the man-load as the point on a circle rolling along the X-axis with center determined by the flight path of the aircraft, and generating radius defined by the tether line uniting man and aircraft.

The term "cycloid" is placed in quotation marks because there is no a priori reasoning to indicate that the actual trajectory is cycloidal, or even trochoidal, simply the existence of forces so related geometrically as to suggest the cycloid is a highly plausible result of their interaction for the initial part (180 ft) of the trajectory only; beyond this point, forces like gravity and wind resistance probably supervene to account for the rapid departure of the trajectory from the equivalent cycloid

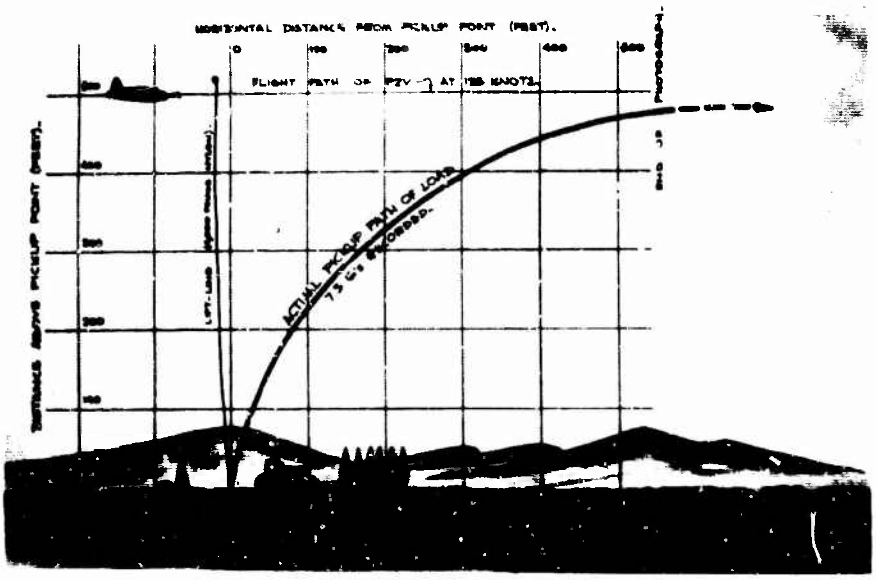

Figure A1. Skyhook Trajectory

on which it began. Thus one may think of the initial portion of the trajectory as reflecting the instantaneous kinematics (that is, at pickup or lift-off) of a cycloid that presently (2 sec later) merges into a curve increasingly responsive to the <u>dynamics</u> of a mass particle obeying the three forces whose equilibration ultimately establishes the steady-state condition of motion – gravity, wind drag, and tether line tension. Except for the fact that line elasticity will undoubtedly introduce a time delay in the initial lift-off velocity and acceleration, there is evidence that the initial trajectory both kinematically and graphically approximates the equivalent cycloid, with these parametric equations of motion:

Load velocity:

$$\frac{ds}{dt} = \omega \sqrt{\rho a} \sin \tfrac{1}{2} \phi \tag{A1}$$

Tangential acceleration:

$$\frac{d^2s}{dt^2} = \omega^2 a \cos \tfrac{1}{2} \phi \tag{A2}$$

Normal acceleration:

$$\frac{1}{\rho}\left(\frac{ds}{dt}\right)^2 = \omega^2 a \sin \tfrac{1}{2}\,\phi \qquad \text{(A 3)}$$

where

ϕ = generating angle at time t

$\omega = \frac{d\phi}{dt}$ = angular velocity of generating circle

ρ = radius of curvature of cycloid at time t

a = aircraft altitude (tether length)

Support for the cycloidal theory is found in tracings from photographs showing the changing relationship of load trajectory to intercept altitudes. In Figure A2 we see as aircraft altitude diminishes, the corresponding peak is relatively higher, which follows from Eq. (A2) in which acceleration in the direction of motion is a function of ω^2, but of a (intercept altitude) to the first power only. That the absolute peaks are progressively lower as intercept altitude diminishes follows from Eq. (A3) where $\sin \frac{1}{2}\,\phi$ predominates over $\cos \frac{1}{2}\,\phi$ sooner at time t, the smaller generating circle.

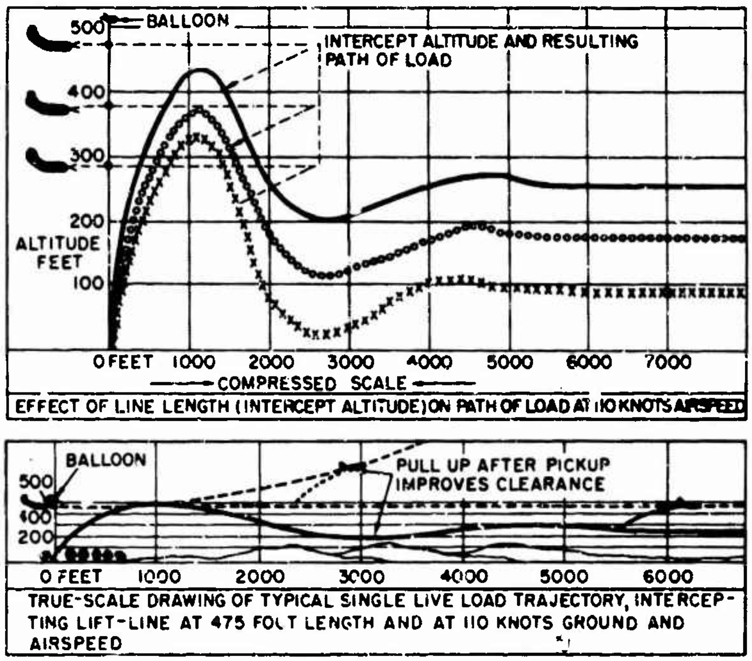

Figure A2. Effect of Intercept Altitude on Load Trajectory

2. Balloon Drag – Correlation Study

I should like to conclude with a note about drag on which some of you may be able to shed light.

We have attempted to correlate field measurements of balloon drag with drag values predicted by empirical friction formulations developed by German investigators in the past. The graph (Davidson, 1936) in Figure A3 exhibits the classical relationship of the coefficient of frictional resistance (C_f, or drag) to Reynolds number for any totally submerged body in the Reynolds number range relevant to our balloon work.* In physical terms, since a body submerged in a moving fluid experiences resistance (drag) essentially frictional in nature, the relationship shown is actually a plot of the trend of the ratio of normal to shearing stresses in fluid particles within the boundary layer, as a function of Reynolds number.

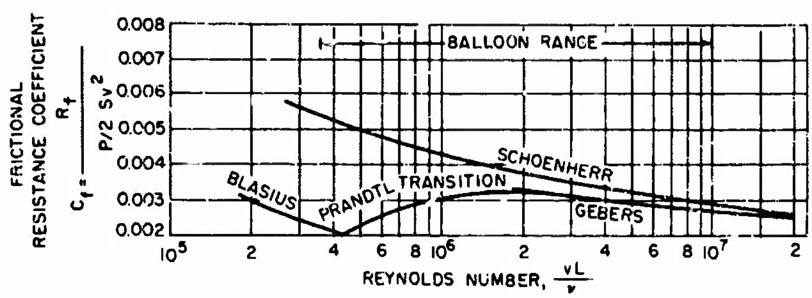

SEMILOG CHART OF C_f VS REYNOLDS NUMBER – EMPIRICAL FRICTION FORMULATIONS

$R_e = 1.08\ VL \times 10^4$

$R_f = 0.107\ C_f S V^2$

BALLOON LENGTH (L) FT	BALLOON AREA (S) FT²	WIND SPEED (v) KNOTS	R_e $\times 10^6$	C_f B	C_f P	C_f G	R_f LBS
16	190	2	.34	.0022			1.8
		30	5.1			.0030	5.4
19	250	2	.42	.0020			2.2
		30	6.3			.0028	67
26	480	2	.56		.0024		5.0
		30	8.5			.0026	120
31	680	2	.65		.0026		7.6
		30	9.7			.0026	170

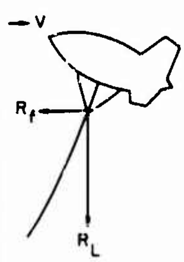

Figure A3. Balloon Drag (R_f) and Classical Fluid Friction Data

---

*Of particular interest is the fact that this range encompasses the whole of the "transition" region, between laminar and turbulent flow.

The table of Figure A3 indicates the derivation of "classical" predicted drag (R_f) values applied to our balloons, using the expressions appearing to the left of the table. These values of R_f are two to threefold R_f drag values observed in the field, obtained by solving the right triangle defined by measured tether line tension and observed angle of tether line with the vertical where it meets the shroud lines.

Two possible explanations present themselves:

1. Is it credible that measured field values of R_f are low because they actually represent "residual" drag, that is, absolute drag* minus a forward-directed drive such as exists in yacht sails going to windward (Davidson, 1936)? Positive evidence for this "drive-force" in balloons appears in their capacity to fly at the zenith, or slightly upwind of it, in light winds of 5 to 8 knots.

2. Is boundary layer flow actually laminar in the R_e balloon range, despite theory and empirical evidence suggesting it should be transitional-to-turbulent?

In any case, these very tentative answers point to a need for exhaustive field and wind-tunnel studies to illuminate this area of balloon aerodynamics.

References

Davidson, K.S.M. (1936) Some experimental studies of the sailing yacht, Proc. Soc. Nav. Architects and Marine Engrs 44:301.

Op. cit., 294-295.

*Drag plus induced drag (due to a finite angle of attack)

XIX. A Tethered Heavier-Than-Air Vehicle for Atmospheric Sounding

Robert D. [illegible]
Ohio State University
Columbus, Ohio

Abstract

This paper describes the instrument carrying system developed by the Atmospheric Science Department of Colorado State University under the direction of Professor Lewis O. Grant. The author participated in this project both as a member of the Mechanical Engineering Department faculty of Colorado State University and during summers since his affiliation with Ohio State University.

I. BASIC PROJECT OBJECTIVES

One of the many research projects being carried out by the Atmospheric Science Department of Colorado State University is the study of orographic clouds which form over the Colorado Rockies. The main objectives of these studies are to explore and define the physical properties of the cloud systems and to develop means by which they may be modified to produce additional water supplies for the region. Various ground stations, including radar, in and near the field study area were the major data acquisition sources for the project. While the information obtained from

these sources proved to be a valuable contribution as far as knowledge of cloud processes and their modifications were concerned, it was indirect information. It was felt that observations taken directly within the cloud system should be made.

2. SELECTION OF A SUITABLE SYSTEM

Methods of carrying instrumentation into the cloud systems which were considered in the early 1960's included aircraft, balloons, towers, rockets, and kite systems. The rugged terrain in and near the study area precluded the use of aircraft. Free balloons with telemetering equipment have and are being used and provide valuable, though limited, information. Tethered balloons can be useful under conditions when the wind velocity is low. It was felt that it would be rather difficult to maintain these vehicles on station during the periods of high wind velocity which would be encountered during a good portion of the observation. Rockets were eliminated from further consideration because the information provided from their instrumentation would even be more limited than that provided by the free balloon systems. Towers were rejected for various reasons including the difficulty, if not impossibility, of constructing them in the desired location.

Wind was one of the primary reasons for rejection of most of the systems considered. Since the tethered kite system requires wind in order for it to be able to function, it was decided to inaugurate a developmental study on this type of system. At this point, it should be indicated that since the primary objective of the research project was the study of the cloud systems, the developmental work on the kite system has been held to a minimum. There is much work that could and should be done in further development of this system.

The use of kites as carriers of meteorological instruments is not new. When the box kite was invented about 1892 by Lawrence Hargrave, an Australian engineer, its stability and lift characteristics were so outstanding that meteorologists in Europe and the United States began developing programs to use box kites as atmospheric sounding vehicles. In the United States, the program was carried on until the last kite station of the U.S. Weather Bureau was closed in 1933.

3. KITE DEVELOPMENT

In the early stages of the developmental program, it was thought that through use of materials currently available it would be possible to build a box kite which would have improved flight and structural characteristics as compared with the earlier Hargrave kites. Among the design objectives for the proposed vehicle were that it should be capable of being collapsed or disassembled into a small

package for storage purposes and that the transition from storage to flying conditions be a quick and easy one. While the Hargrave kite met the first of the design criteria, it was somewhat lacking as far as the second was concerned. Assembly was relatively easy under normal atmospheric conditions, but it was considerably more difficult during periods of high winds and low temperatures. This difficulty could have been overcome by the addition of a building to the fixed launch complex. However, this would not have been a convenient solution to the problem if a mobile launch facility had been used.

About this time the parawing (a vehicle developed by F.A. Rogallo of NASA Langley) was receiving considerable publicity. In its simplest form, the parawing consisted of a flexible membrane which, in flight, would assume the hape of portions of surfaces of two intersecting cones. It appeared that a vehicle of this type could be fabricated in such a manner as to have the portability desired. Several experimental models were built but all proved somewhat unstable. It is believed that this instability resulted from designing the prototypes with too rigid a structure. Work on this phase of the project was halted after the acquisition of several Jalbert Parafoils.

4. JALBERT PARAFOIL

The Parafoil has acquired many nicknames including that of "flying air mattress." Essentially, the Parafoil consists of a series of parallel tubes having rectangular lateral cross sections. Each pair of adjacent tubes shares a common wall or bulkhead. In outline, each bulkhead resembles a conventional aircraft wing rib. However, instead of a rounded leading edge, the front end of the Parafoil rib terminates in a straight edge slanting down and back, located at approximately 5 percent of the chord from where the leading edge would be in a conventional rib. In flight the Parafoil resembles a conventional aircraft wing which has been left open along the leading edge.

The entire vehicle is fabricated from a strong, nonporous fabric which is highly impervious to moisture. A small opening at the rear of each tube maintains a positive flow of air through the tube. As air passes through the tube the pressure rise accompanying the velocity decrease is sufficient to maintain inflation of the Parafoil. Alternate ribs are provided with triangular flaps extending below the lower surface of the Parafoil. The number of these flaps on each rib depends upon the length of the rib. Nylon cords extending from the triangular flaps are brought together at common points below the Parafoil. This conjunction of cords continues until they terminate at the main flying line. At this point, it should be emphasized that there is not a single compression member in this vehicle.

As far as has been determined, the performance of the Parafoil can be predicted through use of the conventional relationships of low speed aerodynamics. Lift and drag are functions of planform area, mass density of the air, air velocity, and of lift or drag coefficients which vary as the angle of attack changes. These coefficients are normally determined by experimental means.

Because the Parafoil flies tethered rather than free, an additional factor must be considered in determining the effective coefficient of lift under actual flight conditions. The ratio of lift to drag is the tangent of the slope angle of the kite line at its upper extremity. This angle will be defined as theta. For any specified angle of attack, there will be corresponding values of C_L and theta. The effective C_L for the tethered kite can be determined by multiplying the normal C_L by the term $(1 - \cos \Theta)/(\sin \Theta)$. As might be expected, the effective C_L is quite sharply reduced at low values of theta.

While most of the wings used have been rectangular in planform, some of the original models were shaped like the letter "t." This configuration was actually three wings. The center portion consisted of a wing having an extremely long chord but short width while two stub wings with relatively shorter chord were fixed to each side of the center wing. Models of this shape were naturally called "T-birds."

Aspect ratio is the ratio of the length of the wing from tip to tip to the length of the chord from leading edge to trailing edge. Early models of the rectangular wing had relatively low aspect ratios. It was found that increasing the aspect ratio would improve the over-all performance of the wing considerably, giving much better curves for the lift and drag coefficients and, of course, a correspondingly better L/D ratio. Kites having areas of up to 300 sq ft and aspect ratios of about five have been used. No icing of the wing has been observed, nor have lift and drag coefficients changed during flight due to distortion of the kite.

With one major exception, the subsystems needed to operate a tethered heavier than air vehicle are much the same as those required for a tethered lighter than air device. The exception is, of course, some vehicle or tanking system for handling a lifting media such as hydrogen or helium. These components include the instrument package (which will not be discussed in this paper), the cable or line by which the kite is tethered, and the winch system for managing the line.

5. LINE SELECTION

While cost is certainly an important factor in the selection of a line, the relative importance of this item may be considerably lower than that of certain physical properties of the line such as strength, weight, line diameter, and elasticity. A high strength-weight ratio is desirable, especially if flights to high altitude are being attempted. A line having high elasticity is needed whenever sudden increases

in load may be anticipated. Flying in gusty air is one example of this. Since the load is produced by an increase of wind pressure on the kite, an elastic line will permit some movement of the kite in the direction of the wind. Relative wind velocity past the kite is lowered resulting in a slower buildup of wind pressure on the kite. In flying in winds of high velocities, line diameter becomes a factor since line drag horizontal and vertical components act to decrease the maximum altitude the vehicle can reach.

Three types of line were used in the CSU kite operations. These included spring steel piano wire, braided nylon line, and a special titanium alloy wire. For current operations, nylon seems to be the best. Total height above launch sites in the present experiments is not extremely great and it is possible to select a kite of suitable area to reach the selected altitude and downwind location in spite of adverse effects from line drag. The nylon line being used has the same breaking strength as the piano wire and although both types of lines have been broken, the frequency of breakage has not been as great with the nylon. Another disadvantage of the wire is its electrical conductivity. If the line should break in such a manner as to leave a considerable length dragging from the still flying kite, considerable inconvenience and damage can be caused when there are electrical power lines along the flight path. It is quite probable that if flights to extremely high altitudes become a part of the program, a line will have to be selected which has a much smaller diameter than the nylon presently being used.

6. WINCH DEVELOPMENT

When the original kite program was begun, it was quite apparent that some means of handling the line would be ultimately needed. As a beginning, a rather crude winch was fabricated. This unit consisted of a reel manufactured from a relatively small diameter grease drum with circular end plates fabricated from mild steel. The reel shaft ran in bearings mounted on a heavy wooden frame. The unit was driven by a 5-hp industrial type engine and could be mounted in the rear of a pickup truck.

With the arrival and testing of the first Parafoil, it became obvious that the loads encountered were considerably greater than had originally been anticipated and that a much stronger winch unit would be required. The drum of the original winch collapsed while one of the kites was being reeled in. This was attributed not only to the extremely large loads encountered but also to the constrictive forces applied by the stretched nylon line which was being used.

Although several companies were contacted, bids submitted for the design and construction of a winch which met specifications far exceeded the budgetary limitations of the project. A design and fabrication group was organized including

individuals from the Atmospheric Science Department who had been assigned to the project, a faculty member of the Mechanical Engineering Department, and a local machine shop. This group ultimately produced a winch at a cost of approximately 10 percent of the average of bids submitted.

A surplus radar van was remodeled to house the winch system. A guide arm, or boom, which was free to rotate through 360° about a vertical axis was installed on the roof of the van. This device provided a means of keeping the line free of the van roof which would permit flight operations to be conducted during winds from any direction.

The reel on this winch was extremely rugged. It was fabricated from 16-in. outside diameter steel tubing, having a wall thickness of 3/4 of an inch. Discs of 3/4-in. steel plate were welded inside the tube to provide additional bracing while the end plates were 2-ft diam discs also fabricated from 3/4-in. steel plate. The reel was supported in a frame fabricated from heavy steel plate. Braking system consisted of a standard automotive type brake drum with a hydraulically operated shoe plus a pawl and ratchet locking device.

The 60 hp air-cooled industrial type engine used to drive the winch was mounted outside the van. This was connected to the torque converter of a Chrysler Corporation automatic transmission. The axis of this transmission was parallel to the axis of the winch reel. In order to obtain the number of speed ratios desired, the gear box of a second automatic transmission was installed along side and parallel to the first transmission. The interconnection between the two transmissions was accomplished by means of a countershaft installed between them with a short chain drive extending from each end of the countershaft to the appropriate transmission. A considerable amount of effort was expended in interconnecting the two transmissions hydraulically so that they could be operated by push-button control from the operator's control console.

The distance from the point at which the line entered the van to the reel was relatively short. Thus the angle between the line and the level wind guide would, at times, decrease to a value where forces of considerable magnitude would be transmitted to the line guide. The magnitude of these forces was so great that the use of a typical diamond shaft level wind device seemed impractical. The line guide was mounted on a threaded shaft using ball-nuts. Since this shaft had only a single thread running in one direction, it became necessary to reverse the rotation of the shaft each time the line guide reached the end of the shaft. (A diamond shaft level wind has both a left- and a right-handed thread and is designed so that the line guide will transfer from one thread to the other automatically when the line guide reaches the end of the diamond shaft. Thus the diamond shaft can rotate continuously in one direction and provide the required level wind effect.) Since the rotation of the line guide shaft was relatively slow, it was possible to design a reverse mechanism

using two clutches. During the change of shaft rotation, both clutches are momentarily engaged at the same time. However, the time interval is so short that damaging action does not occur.

The level wind guide mechanism is driven by a chain drive extending from the end of the last transmission shaft. Several sets of sprockets are provided so that the speed of the level line device can be adjusted to compensate for changes in line diameters which may occur in the operation of the system

The operators console is provided with throttle, brake, and speed changing controls. In addition, line speed and line tension lead-outs are provided. The sensor for the line tension readout consists of a set of offset rollers mounted on the guide boom. Deflection of the frame in which these rollers are mounted is measured by a suitable strain gage arrangement and is proportional to the tension in the line.

While the kite van just described has proved highly satisfactory for most operations, it does have one big disadvantage. This, of course, is lack of mobility which is soon evident when the van is located in an area in which there are several feet of snow on the ground. Immobility of the first winch, together with the fact that additional experimentation was envisioned in which it would be necessary to fly two kites simultaneously, leads to the design and construction of a second winch. This winch can be mounted easily on the back of a flatbed truck, which provides mobility. The entire unit (including line guide system, reel, operator's cab, and power unit) can be rotated about a vertical axis through an arc of at least ±90° and can be tilted about a horizontal axis. This positioning flexibility, as well as the large glassed-in window area of the cab, provides the operator with the opportunity to keep the kite under visual observation unless flying in or beyond cloud cover.

7. FLIGHT OPERATIONS

For the present purposes of the research project, it has been possible to fly the kite and collect satisfactory data. However, it is not yet possible to predict a position vector (straight line distance from winch to kite, angle of this line with the horizontal and azimuth angle) of the kite before it is launched. Magnitudes of the position vector parameters are dependent upon the shape of the curve assumed by the line and direction of the wind. When a line having a considerable amount of flexibility is being used, the line curve shape will closely approximate that of a catenary curve. The term "catenary" as used in this paper refers to the mathematically defined catenary and not to a generic catch-all which would include any line curve shape. As wind velocities increase, however, line drag begins to enter the picture resulting in a lower elevation and greater downwind distance than would be predicted from the catenary equations.

Line drag will be a function of line diameter as well as of the dynamic pressure, q, of the air moving past the line. Dynamic pressure is defined as being one-half the product of the mass density of the air and the square of the wind velocity. Unit weight of the line is another factor which must be considered in determining the line shape curve. The complexity of the line shape curve may be seen when we consider that the dynamic pressure profile changes with altitude and that there is the tendency of the nylon line to stretch under load. Effective result of this line stretch is to give a line of non-uniform diameter and non-uniform unit weight.

There appear to be great possibilities of increasing the versatility of the kite system. At the present time, once an angle of attack has been established before launch, the position to which the kite can be flown is limited by the direction and magnitude of the dynamic pressure forces. The altitude to which a single kite can be flown is limited by line drag. When the slope angle of the line becomes zero at the winch, maximum elevation has been reached. However, it is possible to attach additional kites to the line once the kites in the air have reached their maximum altitude. This process can be repeated as often as necessary; it is apparently limited only by the supply of kites and line.

If it becomes necessary, additional work could be done to develop a system by which the aerodynamic characteristics of the kite and payload could be changed by the operator with the kite in flight. Initially a system could be developed which would permit the operator to change the angle of attack. This capability combined with reeling the kite in or out would give the operator considerably more control of the position of the kite directly down wind from the launch site. Additional flexibility of operation could be provided by developing a system which would permit flying the kite to either side of the down wind position.

8. PROBLEMS OF TESTING AND FLYING

Some mention should be made of the test program during the developmental period of this system. Unfortunately, winds of the required magnitude were not always available when it was desired to conduct a test. However, there were areas available within easy driving distance where roads unencumbered by power lines or fences along side and with little or no traffic could be found. A pickup truck was generally used as a towing vehicle during this phase of operation. The system was found to be, to a certain extent, fail-safe under testing conditions. This depends upon one's definition of safe. As the speed of the towing vehicle increased, a point was reached where the kite would lift the rear end of the truck off the ground, thereby limiting the speed that could be attained.

One of the greatest problems as far as the research program is concerned has been that of obtaining unrestricted clearance for flights in the research area. While it has been possible to obtain clearance for flights that have been made, lead times required for clearance requests result in considerable inconvenience. Eventually it is hoped that it will be possible to obtain a restricted air space above an area five or ten miles in diameter centered at the launch site. Once this space is obtained it should be possible to carry out operations on a much more flexible schedule.

Appendix

Publications of Proceedings of Past AFCRL Balloon Symposia and Workshops

Due to interest expressed in the proceedings of past AFCRL balloon symposia and workshops, and because the report series for these reports has been changed, a listing of the proceedings of all past AFCRL balloon symposia and workshops follows.

TITLE	AFCRL REPORT NO. AND DATE
Proceedings of the AFCRL Balloon Symposium	AFCRL-63-919 December 1963
Proceedings, 1964 AFCRL Scientific Balloon Symposium	AFCRL-65-486 July 1965
Proceedings, AFCRL Scientific Balloon Workshop, 1965	AFCRL-66-308 May 1966
Proceedings, Fourth AFCRL Scientific Balloon Symposium	AFCRL-67-0075 January 1967

Unclassified
Security Classification

DOCUMENT CONTROL DATA - R&D		
(Security classification of title, body of abstract and indexing annotation must be entered when the overall report is classified)		
1. ORIGINATING ACTIVITY *(Corporate author)* Air Force Cambridge Research Laboratories (CRE) L.G. Hanscom Field Bedford, Massachusetts 01730	2a. REPORT SECURITY CLASSIFICATION Unclassified 2b. GROUP -	
3. REPORT TITLE PROCEEDINGS, AFCRL TETHERED BALLOON WORKSHOP, 1967		
4. DESCRIPTIVE NOTES *(Type of report and inclusive dates)* Scientific. Interim.		
5. AUTHOR(S) *(First name, middle initial, last name)* Thomas W. Kelly (Editor)		
6. REPORT DATE March 1968	7a. TOTAL NO. OF PAGES 201	7b. NO. OF REFS 20
8a. CONTRACT OR GRANT NO. b. PROJECT, TASK, WORK UNIT NOS. 6665-01-01 c. DOD ELEMENT 65402l2F d. DOD SUBELEMENT 632800	9a. ORIGINATOR'S REPORT NUMBER(S) AFCRL-68-0097 9b. OTHER REPORT NO(S) *(Any other numbers that may be assigned this report)* Special Reports, No. 72	
10. DISTRIBUTION STATEMENT 1-Distribution of this document is unlimited. It may be released to the Clearinghouse, Department of Commerce, for sale to the general public.		
11. SUPPLEMENTARY NOTES TECH, OTHER	12. SPONSORING MILITARY ACTIVITY Air Force Cambridge Research Laboratories (CRE) L.G. Hanscom Field Bedford, Massachusetts 01730	

13. ABSTRACT

The AFCRL Tethered Balloon Workshop was held in October 1967 for the purpose of exchanging information on the current tethered ballooning. This was the first such meeting held exclusively for reporting on this rapidly expanding technology. In addition to informal meetings, nineteen prepared talks were presented, all of which are contained herein. Subjects include: tethered balloon motion, balloon design, fiberglas tether cables, tethered balloon instrumentation, a tethered balloon winch, and several operational programs that used tethered balloon systems.

DD FORM 1 NOV 65 1473

Unclassified
Security Classification

Unclassified
Security Classification

14. KEY WORDS	LINK A		LINK B		LINK C	
	ROLE	WT	ROLE	WT	ROLE	WT
Balloon Inflatables Instrumentation balloon systems Tethered balloons Winches Hot air balloons Fiberglas cable						

Unclassified
Security Classification